

The University of Sydney

# Epileptic Seizure Detection and Forecasting Ecosystems

by

Nhan Duy Truong

*Principal Supervisor*

Dr. Omid Kavehei

*Auxiliary Supervisor*

Dr. Luping Zhou

*A thesis submitted in fulfillment of the requirements  
for the degree of Doctor of Philosophy*

Faculty of Engineering

2020

## Statement of authentication

This is to certify that to the best of my knowledge, the content of this thesis is my own work. This thesis has not been submitted for any degree or other purposes.

I certify that the intellectual content of this thesis is the product of my own work and that all the assistance received in preparing this thesis and sources have been acknowledged.

Nhan Duy Truong

01 October 2019

# Abstract

Epilepsy affects almost 1% of the global population and considerably impacts the quality of life of those patients diagnosed with the disease. Ambulatory EEG monitoring devices that can detect or predict seizures could play an important role for people with intractable epilepsy. Many outstanding studies in detecting and forecasting epileptic seizures using EEG have been developed over the past three decades. Despite this success, their implementations as part of implantable or wearable devices are still limited. To achieve high performance, many of these studies relied on handcraft feature extraction. This approach is not generalizable and requires significant modifications for each new patient. This issue greatly limits the applicability of such methods to hardware implementation.

In this thesis, we propose a deep learning-based solution for generalized epileptic seizure detection and forecasting that does not require handcraft feature extraction. The method can be applied to any other patient without the need for manual feature extraction. Secondly, we optimize seizure detection and forecasting systems to reduce computational complexity and power consumption. The optimization is performed from two aspects: algorithm and input signal. In the first aspect, we propose two approaches: (1) automatic channel selection to reduce the number of necessary EEG electrodes; (2) Integer-Net, an integer convolutional neural network, to reduce computational complexity and required memory. In the second aspect, we investigate how sensitive seizure detection algorithms are regarding EEG's resolution. Another problem that we would like to address is the lack of labeled EEG data for epilepsy. Today the process of epileptic seizure identification and data labeling is done by neurologists, which is expensive and time-consuming. We propose an unsupervised learning approach to make use of unlabeled EEG data which is more accessible.

## Acknowledgements

Above all, I would like to thank my supervisors, Dr Omid Kavehei and Dr Luping Zhou. I thank my mentors, Dr Levin Kuhlmann and Dr Mohammad Reza Bonyadi.

I appreciate Prof Ping Koy Lam at Department of Quantum Science, the Australian National University for hosting my visit to Centre for Quantum Computation and Communication Technology to evaluate the predictability of their Quantum Random Number Generator with deep learning. I appreciate Prof David Reutens at Centre for Advanced Imaging (CAI), the University of Queensland for inviting me to CAI to establish a research collaboration on epilepsy. I also thank Dr Jing Yan Haw, Dr Syed Assad, and Dr Quang Tieng who have been working closely with me in different research collaborations. I thank Vivek Kumar and Steve Morris at Technology and Analysis - Big Data, Telstra, for allowing me to experience the professional and great place to work and to apply my deep learning knowledge to different practical problems in the industry during my four-month internship.

I would like to thank the financial support from Faculty of Engineering, The University of Sydney via the Engineering and Information Technologies Research Scholarship and acknowledge partial support provided via John Makepeace Bennett Gift Scholarship funded by the Australian Institute for Nanoscale Science and Technology (AINST) and administered by the University of Sydney Nano Institute. I acknowledge The Commonwealth Scientific and Industrial Research Organisation (CSIRO) partial financial support, PN 50041400. I also acknowledge the support from Sydney Informatics Hub, funded by the University of Sydney.

I would like to thank my friends who have kept encouraging and “insulting” me during my studies.

Most of all, I am grateful for the love and support from my parents, my wife, and my little son.

# Table of Contents

List of Tables	ix
List of Figures	xiii
<b>1 Introduction</b>	<b>1</b>
1.1 Research motivation . . . . .	1
1.2 Problem statements . . . . .	2
1.3 Research questions . . . . .	3
1.4 Thesis organization . . . . .	3
1.5 List of publications . . . . .	5
1.5.1 Journal publications . . . . .	5
1.5.2 Conference publications . . . . .	5
1.5.3 Other publications . . . . .	6
1.6 List of source codes . . . . .	7
<b>2 Literature review</b>	<b>8</b>
2.1 What is epilepsy? . . . . .	10
2.2 Treatment of drug-resistant epilepsy . . . . .	13
2.3 Seizure detection and prediction . . . . .	16
2.4 Hardware implementation of seizure detection . . . . .	20
2.5 Discussions . . . . .	21

<b>3</b>	<b>Seizure prediction with convolutional neural network</b>	<b>23</b>
3.1	Introduction . . . . .	25
3.2	Dataset . . . . .	27
3.3	Proposed method . . . . .	29
3.3.1	Preprocessing . . . . .	29
3.3.2	Convolutional neural network . . . . .	30
3.3.3	Postprocessing . . . . .	32
3.3.4	System evaluation . . . . .	32
3.4	Results . . . . .	35
3.5	Discussion . . . . .	40
3.6	Conclusion . . . . .	42
<b>4</b>	<b>Semi-supervised learning for seizure prediction</b>	<b>44</b>
4.1	Introduction . . . . .	46
4.2	Dataset . . . . .	48
4.3	Proposed Method . . . . .	49
4.3.1	Pre-processing . . . . .	49
4.3.2	Adversarial Neural Network . . . . .	50
4.3.3	Seizure forecasting with features extracted by DCGAN . . . . .	54
4.3.4	System evaluation . . . . .	54
4.4	Results . . . . .	55
4.5	Discussion . . . . .	57
4.6	Conclusion . . . . .	58
<b>5</b>	<b>Automatic channel selection for seizure detection</b>	<b>64</b>
5.1	Introduction . . . . .	66
5.2	Dataset . . . . .	69
5.3	Proposed method . . . . .	70

5.3.1	Automatic channels selection . . . . .	71
5.3.2	Feature extraction . . . . .	72
5.3.3	Classifier . . . . .	74
5.3.4	System evaluation . . . . .	75
5.4	Results . . . . .	76
5.5	Discussions . . . . .	79
5.6	Conclusion . . . . .	82
<b>6</b>	<b>Hardware-friendly deep learning for seizure detection</b>	<b>85</b>
6.1	Introduction . . . . .	87
6.2	Dataset . . . . .	89
6.3	Proposed method . . . . .	90
6.3.1	Pre-processing . . . . .	90
6.3.2	Integer-Net: An integer convolutional neural network . . . . .	90
6.3.3	Integet-Net for seizure detection . . . . .	94
6.3.4	System evaluation . . . . .	94
6.4	Results . . . . .	96
6.5	Discussion . . . . .	100
6.6	Conclusion . . . . .	103
<b>7</b>	<b>Low precision EEG signals for seizure detection</b>	<b>105</b>
7.1	Introduction . . . . .	107
7.2	Dataset . . . . .	109
7.3	Method . . . . .	110
7.4	Results . . . . .	111
7.5	Discussion . . . . .	112
7.6	Conclusion . . . . .	118

<b>8</b>	<b>Seizure prediction on portable hardware</b>	<b>120</b>
8.1	Introduction . . . . .	120
8.2	Dataset . . . . .	120
8.3	Proposed method . . . . .	121
8.3.1	System overview . . . . .	121
8.3.2	Adversarial neural network . . . . .	122
8.4	Results . . . . .	124
8.5	Discussion . . . . .	125
8.6	Conclusion . . . . .	126
<b>9</b>	<b>Concluding Remarks</b>	<b>127</b>
9.1	Thesis contribution . . . . .	127
9.2	Future research directions . . . . .	128
	<b>References</b>	<b>130</b>

# List of Tables

3.1	Summary of the three datasets used in this work. . . . .	28
3.2	The chosen $S$ value for each patient. . . . .	32
3.3	Seizure prediction results obtained with the Freiburg Hospital interictal EEG dataset. The model was executed twice, and average results with standard deviations were reported. The seizure occurrence period (SOP) was 30 min and the seizure prediction horizon (SPH) was 5 min. The $p$ value was calculated for the worst case for each patient; that is, with minimum sensitivity and maximum false prediction rate (FPR). Our seizure prediction approach achieves significantly better performance than an unspecific random predictor for all patients except Pat14, where the convolutional neural network results are only marginally better than the random predictor's. . . . .	36
3.4	Seizure prediction results obtained with the Boston Children's Hospital-MIT scalp EEG dataset. The model was executed twice, and average results with standard deviations were reported. The seizure occurrence period (SOP) was 30 min and the seizure prediction horizon (SPH) was 5 min. The $p$ value was calculated for the worst case for each patient; that is, with minimum sensitivity and maximum false prediction rate (FPR). Our seizure prediction approach achieves significantly better performance than an unspecific random predictor for all patients except Pat9, where the convolutional neural network results are only marginally better than the random predictor's. . . . .	37

3.5	Seizure prediction results obtained with the American Epilepsy Society Seizure Prediction Challenge dataset. The model was executed twice, and average results with standard deviations were reported. The seizure occurrence period (SOP) was 30 min and the seizure prediction horizon (SPH) was 5 min. The $p$ value was calculated for the worst case for each participant; that is, with minimum sensitivity and maximum false prediction rate (FPR). Our seizure prediction approach achieves significantly better performance than an unspecific random predictor for four of five dogs and for Pat1. . . . .	38
3.6	Benchmarking of recent seizure prediction approaches and this work . . .	39
4.1	Summary of the three datasets used in this work. . . . .	49
A1	Seizure forecasting performance for the CHB-MIT dataset. $p$ -values are from the single-tailed Hanley-McNeil AUC test to compare our seizure forecasting performance with the chance level (AUC= 0.5). Patients with $p$ -values not being highlighted in gray color have seizure forecasting performance significantly better than the chance level with the significance level of 0.05. . . . .	60
A2	Seizure forecasting performance for the Freiburg Hospital dataset. $p$ -values are from the single-tailed Hanley-McNeil AUC test to compare our seizure forecasting performance with the chance level (AUC= 0.5). Patients with $p$ -values not being highlighted in gray color have seizure forecasting performance significantly better than the chance level with the significance level of 0.05. . . . .	60
A3	Seizure forecasting performance for the EPILEPSIAE dataset. $p$ -values are from the single-tailed Hanley-McNeil AUC test to compare our seizure forecasting performance with the chance level (AUC= 0.5). Patients with $p$ -values not being highlighted in gray color have seizure forecasting performance significantly better than the chance level with the significance level of 0.05. . . . .	61
A4	The EPILEPSIAE scalp EEG dataset. . . . .	62
5.1	Summary of existing EEG-based seizure detection methods . . . . .	67
5.2	Summary of the dataset . . . . .	70
5.3	Comparison among three channel selection methods. . . . .	79

5.4	Comparison between state-of-the-art and proposed method on computational efficiency. . . . .	80
A1	Channels selected using the three channel selection methods. . . . .	83
A2	Comparison between state-of-the-art and proposed method on AUC, sensitivity (SEN), specificity (SPE) and F1-score for binary classification of seizure and non-seizure states for the modified leave-one-out cross-validation of the training set. Threshold values were chosen to achieve best SEN-SPE balance and similar specificity scores between the two methods. This helps the sensitivity and mean detection delay comparisons meaningful. . . . .	83
A3	Comparison between state-of-the-art and proposed method on AUC, sensitivity (SEN), specificity (SPE) and F1-score for binary classification of seizure and non-seizure states for the unlabeled dataset. The threshold values were kept the same as being used during cross-validation. The total AUC is the AUC estimated across all the subjects. . . . .	84
6.1	Seizure detection leave-one-out cross-validation results on Freiburg iEEG dataset. . . . .	96
6.2	Seizure detection leave-one-out cross-validation results on CHB-MIT sEEG dataset. . . . .	97
6.3	Seizure detection leave-one-out cross-validation results on UPenn and Mayo Clinic iEEG dataset. . . . .	99
6.4	Seizure detection test results on UPenn and Mayo Clinic iEEG unlabeled dataset. . . . .	99
6.5	Reduction rate of weight size achieved with 4-bit Integer-Net. . . . .	100
6.6	Energy consumption for various operations in 45nm 0.9V process (Horowitz, 2014). . . . .	101
7.1	Seizure detection performance (AUC in %) for the Freiburg Hospital dataset with convolutional neural network. Mean values and standard deviations of AUC for each patient over the course of four runs of leave-one-seizure-out cross-validation are reported. . . . .	112

7.2	Seizure detection performance (AUC in %) for the CHB-MIT dataset with convolutional neural network. Mean values and standard deviations of AUC for each patient over the course of four runs of leave-one-seizure-out cross-validation are reported. . . . .	113
7.3	Seizure detection performance (AUC in %for the Freiburg Hospital dataset with engineered feature-based approach. Mean values and standard deviations of AUC for each patient over the course of four runs of leave-one-seizure-out cross-validation are reported. . . . .	114
7.4	Seizure detection performance (AUC in %) for the CHB-MIT dataset with engineered feature-based approach. Mean values and standard deviations of AUC for each patient over the course of four runs of leave-one-seizure-out cross-validation are reported. . . . .	115
8.1	Summary of the CHB-MIT dataset. . . . .	121
8.2	Processing time for one 28-second EEG time-series data. . . . .	125

# List of Figures

1.1	The overall breakdown of the percentage of patients living with epilepsy (Litt and Echauz, 2002). . . . .	2
2.1	Proportions of disability-adjusted life years caused by neurological conditions in Australia. Adapted from (Australian Institute of Health Welfare, 2016). . . . .	11
2.2	Different seizure types. Adapted from (CURE, 2019). . . . .	12
2.3	A self-evaluation prediction system. High-performance seizure detection is required for this system to work properly. $t_d$ is the point of time when a seizure is detected. $t_p$ is the point of time when an incoming seizure is predicted. . . . .	22
3.1	(a) Example spectrogram of a 30-s window. (b) Same window after removal of power line noise. . . . .	30
3.2	Generate extra preictal segments to balance the training dataset by sliding a 30-s window along the time axis at every step $S$ over preictal signals. $S$ is chosen per subject so that there are a similar number of samples per class (preictal or interictal) in the training set. . . . .	31

3.3	Convolutional neural network architecture. This illustration is applied to the Freiburg Hospital and Boston Children’s Hospital–MIT datasets. For the American Epilepsy Society Seizure Prediction Challenge dataset, the feature sizes are different because of the different recording sampling rate. Short-time Fourier transforms of 30-s windows of raw EEG signals are input. There are three convolution blocks, named <i>C1</i> , <i>C2</i> , and <i>C3</i> . Each block consists of a batch normalization, a convolution layer with a rectified linear unit (ReLU) activation function, and a max-pooling layer. For simplicity, max-pooling layers are not shown and are noted as <i>MP</i> . For <i>C1</i> , there are 16 $n \times 5 \times 5$ kernels, where $n$ is the number of EEG channels, with stride of $1 \times 2 \times 2$ . ReLU activation is applied on convolution results before they are subsampled by a max-pooling over a $1 \times 2 \times 2$ region. The same steps are applied in <i>C2</i> and <i>C3</i> except the convolution kernel size is $3 \times 3$ , stride is $1 \times 1$ , and max-pooling size is $2 \times 2$ . Blocks <i>C2</i> and <i>C3</i> have 32 and 64 convolution kernels, respectively. Features extracted by the three convolution blocks are flattened and connected to two fully connected layers with output sizes of 256 and 2, respectively. The former fully connected layer uses a sigmoid activation function, while the latter uses a soft-max activation function. Both of the fully connected layers have a dropout rate of 0.5. . . . .	33
3.4	Practice to prevent the convolutional neural network from overfitting the data during training. Twenty-five percent of later samples (diagonal lines) from preictal and interictal recordings in the training dataset are used for monitoring and the rest are used for training. . . . .	34
3.5	Definition of the seizure occurrence period (SOP) and the seizure prediction horizon (SPH). For a correct prediction, a seizure onset must be after the SPH and within the SOP. . . . .	34
3.6	Comparison among our method, the preprocessing step using the continuous wavelet transform (CWT) (Khan et al., 2018), and cost-sensitive learning. AUC, area under the receiver operating characteristic curve; CHB, Boston Children’s Hospital. . . . .	41
3.7	Number of seizures versus time of day across patients for the Boston Children’s Hospital—MIT dataset. Most seizures occur in the early morning. Two lower peaks occur around 4 p.m. and 2 a.m. . . . .	42

4.1	(a) Example spectrogram of a 28-second window. (b) Spectrogram of the same window after removing power line noise. . . . .	50
4.2	The Generator takes a random sample of 100 data points from a uniform distribution $\mathcal{U}(-1, 1)$ as input. The input is fully-connected with a hidden layer with the output size of 6272 which is then reshaped to $64 \times 7 \times 14$ . The hidden layer is followed by three de-convolution layers with filter size $5 \times 5$ , stride $2 \times 2$ . The numbers of filters of the three de-convolution layers are 32, 16 and $n$ , respectively. The Discriminator consists of three convolution layers with filter size $5 \times 5$ , stride $2 \times 2$ . The numbers of filters of the three convolution layers are 16, 32 and 64, respectively. . . . .	51
4.3	Seizure forecasting with features extracted by DCGAN’s Discriminator. Inputs are short-time Fourier transform (STFT) of 28-s windows of raw electroencephalogram (EEG) signals. Features extracted by the three convolution blocks of the Discriminator are flattened and connected to a neural network consisting of 2 fully-connected layers with the output sizes 256 and 2, respectively. The former fully-connected layer uses a sigmoid activation function while the latter uses a soft-max activation function. Both of the two layers have drop-out rate of 0.5. Note that the two-layer neural network can be replaced with any other binary classifier. . . . .	52
4.4	The Discriminator’s and the Generator’s loss values in two scenarios: update the Generator (1) once (a-b) and (2) twice (c-d) every mini-batch using data of Patient 1 from the CHB-MIT dataset. . . . .	53
4.5	Definition of seizure occurrence period (SOP) and seizure prediction horizon (SPH). For a correct prediction, a seizure onset must be after the SPH and within the SOP. . . . .	54

4.6	Seizure forecasting performance for the CHB-MIT dataset, the Freiburg Hospital dataset, and the EPILEPSIAE dataset. Four methods are evaluated: (1) CNN: convolutional neural network (Truong, Nguyen, et al., 2018a) (global means: $83.89 \pm 1.28\%$ , $88.86 \pm 1.87\%$ , $71.65 \pm 2.44\%$ ), (2) GAN-NN: unsupervised feature extraction using generative adversarial network (GAN) and classification performed by a two-layer neural network (global means: $77.68 \pm 2.85\%$ , $75.35 \pm 3.62\%$ , $65.05 \pm 2.78\%$ ), (3) GAN-PS-NN: similar to (2) but GAN is done patient-specific (global means: $72.63 \pm 3.80\%$ , $60.91 \pm 1.62\%$ , $63.60 \pm 3.16\%$ ), (4) GAN-PS-USPL-NN: similar to (3) but $10\times$ over-sampling of samples is performed when training GAN (global means: $75.66 \pm 3.15\%$ , $74.33 \pm 2.54\%$ , $65.76 \pm 2.33\%$ ) . . . . .	56
4.7	Seizure forecasting performance (AUC) across different patient-specific characteristics for the EPILEPSIAE dataset: (a) - Seizure type, (b) - Gender, (c) - Age. Refer to Table A4 for the patients' details. Dots indicate outliers. Data points in red (*) are from the same patient. FA: focal aware, FIA: focal impaired awareness, FBTC: focal to bilateral tonic-clonic, UC: unclassified. . . . .	59
A1	Receiver operating characteristics (ROC) curves of seizure forecasting performance testing for different patients of the three datasets: (a) - the CHB-MIT sEEG dataset, (b) - the Freiburg Hospital iEEG dataset, and (c) - the EPILEPSIAE sEEG dataset. Each line corresponds to one patient. Above the green dash line: good performance; above the blue dash line: very good performance (adapted from (Kuhlmann, Lehnertz, et al., 2018)). . . . .	63
5.1	Flowchart of the proposed method. Raw iEEG data from all $N$ channels is fed to ACS to find $M$ channels which contribute the most to a seizure. The ACS engine is executed one time only for each subject at the beginning and indexes of the $M$ channels are stored on hard-disk. Feature extraction in both frequency and time domains is done on the $M$ channels. Extracted features are fed to a classifier using Random Forest algorithm to discriminate interictal, ictal and early ictal epochs. . . . .	71

5.2	Sample 1 s iEEG recordings. (a, b and c) interictal; (d, e and f) ictal at early state (within 15 s from seizure onset); (g, h and i): ictal after early state. iEEG signals presented in one column, (e.g. a, d and g) are recorded from the same channel. . . . .	73
5.3	Sample 1 s iEEG recordings power spectrum. (a, b and c) interictal; (d, e and f) ictal at early state; (g, h and i): ictal after early state. iEEG signals presented in one column, (e.g. a, d and g) are recorded from the same channel. Subplots in this figure are one-by-one associated with subplots in Fig. 5.2. . . . .	74
5.4	Covariance matrix: a) interictal; b) ictal at early state; c) ictal. Correlation between channels is very low in interictal period. The channels are more correlated after the seizure onset and highly correlated in ictal state. . . . .	74
5.5	iEEG recording of a seizure since its onset from Dog-1. Selected channels using focal, variance-based, and our methods are (9, 10, 13),(3, 8, 9). and (4, 10, 12) respectively. . . . .	77
5.6	Channel selection method comparison on overall AUC scores. The dots are for outliers. Focal: focal channel method; Variance: variance-based method; ACS: automatic channel selection (our method). . . . .	78
5.7	Comparison between the method reported by Hills (2014) and the proposed method in terms of detection delay, number of processed channels and processing time. . . . .	81
6.1	Generate extra ictal segments to balance the training dataset by sliding a 1 s window along time axis at every step $S$ over ictal signals. $S$ is chosen per each subject so that there are similar number of samples per each class (ictal or interictal) in training set. . . . .	90

6.2	Convolutional neural network architecture. This illustration is applied for Freiburg and CHB-MIT datasets. For UPenn and Mayo Clinic’s seizure detection dataset, feature sizes are different due to different recording sampling rate. Input are FFT transforms of 1 s windows of raw EEG signals. There are three convolution blocks naming C1, C2 and C3. Each block consists of a batch normalization, a convolution layer with ReLU activation function, and a max pooling layer. For the sake of simplicity, max pooling layers are not shown and are noted as MP. For C1, sixteen $n \times 5$ kernels, where $n$ is number of EEG channels, are used with $1 \times 2$ stride. ReLU activation is applied on convolution results before being sub-sampled by a max pooling layer over $1 \times 2$ region. The same steps are applied in C2 and C3 except convolution kernel size of $1 \times 3$ , stride $1 \times 1$ and max pooling over $1 \times 2$ region. Blocks C2 and C3 have 32 and 64 convolution kernels, respectively. Features extracted by the three convolution blocks are flatten and connected to 2 fully-connected layers with output sizes of 256 and 2, respectively. The former fully-connected layer uses sigmoid activation function while the latter uses soft-max activation function. Drop-out layers are placed before each of the two fully-connected layers with dropping rate of 0.5. . . . .	95
6.3	Validation approach during training to prevent the convolutional neural network from over-fitting. 25% later samples (diagonal lines) from preictal and interictal sets are used for validation and the rest for training. . . .	96
6.4	AUC scores of different seizure detection CNN models: full precision (32-bit floating-point), binary weights only (BW), XNOR-Net, and Integer-Net with 2- to 5-bit. Dots in the figure are outliers. Integer-Net with 2-bit (Int-2) has better AUC than XNOR-Net. Integer-Net with higher number of bits in use (Int-3, Int-4, Int-5) results in higher AUC. . .	98
6.5	Integer-Net implementation can reduce more than ten times in energy consumption. . . . .	102
6.6	AUC scores of different seizure detection CNN models with the use of automatic channel selection for channel reduction on a subset of patients with large number of electrodes (30 to 72). Dots in the figure are outliers. All models, except Int-2, has improvement in seizure detection using less than 1/3 of channels on average. . . . .	103
7.1	Seizure detection performance using convolutional neural network. . . .	109

7.2	Seizure detection performance using feature engineering and random forest classifier. . . . .	111
7.3	Waveform and power spectrum of a 1-second EEG segment from one channel using different numbers of ADC bits. . . . .	116
7.4	Power spectrum with DC removed of two thousand random 1-second EEG segments for patients with high (Patient 18) and low (Patient 21) seizure detection performance using different numbers of ADC bits during ictal (red) and interictal (blue) periods from the Freiburg Hospital dataset in three cases: (a) 16-bit ADC, (b) 8-bit ADC, and (c) 4-bit ADC. . . . .	117
7.5	Power spectrum with DC removed of two thousand random 1-second EEG segments for patients with high (Patient 10) and low (Patient 21) seizure detection performance using different numbers of ADC bits during ictal (red) and interictal (blue) periods from the CHBMIT dataset in three cases: (a) 16-bit ADC, (b) 8-bit ADC, and (c) 4-bit ADC. . . . .	118
8.1	(a) Block diagram: The seizure prediction system consists of a Raspberry Pi 3 and a Movidius Neural Computing Stick (NCS). Time-series EEG signals are sent from a recorder to the Raspberry board where they are pre-processed to be compatible with a CNN loaded in the NCS. (b) Full system dimension. The NCS can sit on top of Raspberry Pi 3. . . . .	122
8.2	(a) The Generator takes a random sample of 100 data points from a uniform distribution $\mathcal{U}(-1, 1)$ as input. The input is fully-connected with a hidden layer with the output size of 6272 which is then reshaped to $64 \times 7 \times 14$ . The hidden layer is followed by three de-convolution layers with filter size $5 \times 5$ , stride $2 \times 2$ . Numbers of filters of the three de-convolution layers are 32, 16 and $n$ , respectively. The Discriminator consists of three convolution layers with filter size $5 \times 5$ , stride $2 \times 2$ . Numbers of filters of the three convolution layers are 16, 32 and 64, respectively. (b) Seizure forecasting with features extracted by DCGAN's Discriminator. Features extracted by the three convolution blocks of the Discriminator are flattened and connected to a neural network consisting of 2 fully-connected layers with the output sizes 256 and 2, respectively. The former fully-connected layer uses sigmoid activation function while the latter uses soft-max activation function. . . . .	123
8.3	Seizure prediction AUC per patient. Prediction is within 35-5 minutes prior to seizure onset. Some patients do not have enough data. . . . .	125

8.4 Google Voice Kit: A Voice Bonnet board that has the same Myriad 2 processor as in NCS is placed on top of a Raspberry Pi Zero. . . . . 126



# Chapter 1

## Introduction

In this research, we focus on how to effectively and reliably detect and more importantly predict seizure onset based on electroencephalogram (EEG) patterns. Detection and prediction of seizure are of crucial importance for patients who cannot be treated by drugs or surgery. This chapter discusses the motivation, objectives, research questions, overall structure of the thesis, and related publications.

### 1.1 Research motivation

Epileptic seizure affects nearly 1% of the global population, but only two thirds can be treated by medicine, and approximately 7 – 8% can be cured by surgery (Litt and Echauz, 2002) (see Fig. 1.1). Therefore, seizure onset detection and subsequent seizure suppression become important for the patients that cannot be cured by either drug or surgery. Early detection can allow early electrical stimulation to suppress the seizure (Echauz et al., 2007). Precise seizure detection allows electrical stimulation to timely interrupt the alteration of consciousness and subsequent convulsions. Seizure prediction is useful to provide the patients with warning messages so they can take some precautions for their safety. Moreover, seizure prediction can be used in combination with seizure detection to improve the effectiveness of the electrical stimulation.

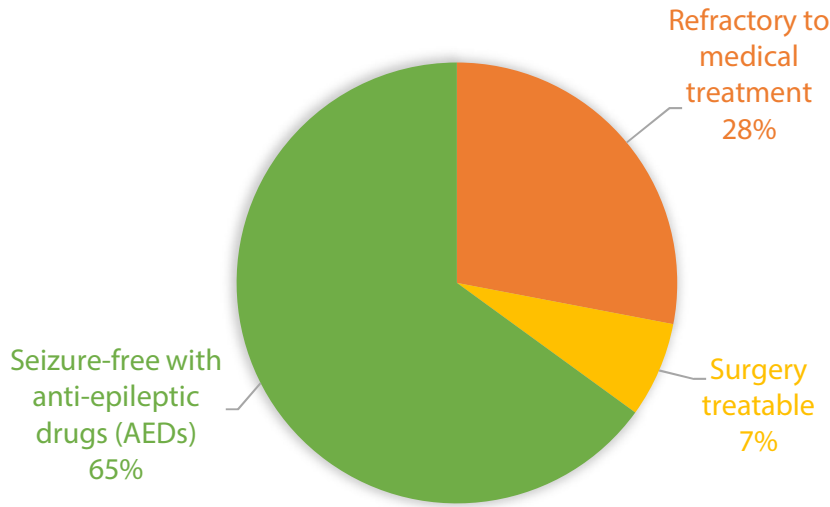


Figure 1.1: The overall breakdown of the percentage of patients living with epilepsy (Litt and Echauz, 2002).

## 1.2 Problem statements

Because of the unpredictability of epileptic seizure activities, epilepsy greatly decreases the quality of life of those patients living with the disease (Kuhlmann, Lehnertz, et al., 2018). The lack of effective treatment of drug-resistant or intractable epilepsy creates an urgency for research to develop reliable and accurate seizure detection and forecasting. Seizure detection has been studied since the 70s (Babb et al., 1974) and over the past decades, a tremendous number of techniques on detecting and predicting seizure have been proposed with promising performance. Seizure prediction or forecasting has attracted growing attention as one of the most challenging predictive data analysis efforts to improve the life of patients with intractable epilepsy.

Electroencephalogram (EEG) signals have been widely used for diagnosing and monitoring of epileptic patients. Ambulatory EEG monitoring devices that can detect or forecast seizures could benefit the patients with drug-resistant epilepsy in terms of their safety and disease management. While many EEG-based seizure detection and prediction algorithms have been proposed in the literature with high performance, many of these studies relied on handcrafted feature extraction or tailored feature extraction, which is performed for each patient independently. This approach, however, is not generalizable and requires significant modifications for each new patient within a new dataset. These issues greatly limit their hardware implementations as part of implantable or wearable devices. In this thesis, we propose a deep learning-based

solution for generalized epileptic seizure detection and prediction that does not require handcrafted feature extraction.

Another problem that we would like to address is the lack of labeled EEG data for epilepsy. Today the process of accurate epileptic seizure identification and data labeling is done by neurologists. Most seizure forecasting algorithms use only labeled data for training purposes. As the seizure data is labeled manually by neurologists, preparing the labeled data is expensive and time-consuming. We propose an unsupervised learning approach to make use of unlabeled EEG data which is more accessible. Specifically, generative adversarial networks are trained with unlabeled EEG data to extract features from EEG signals that can be used for a seizure prediction task.

### 1.3 Research questions

1. Is epileptic seizure forecasting possible? What can be done to forecast the likelihood of incoming seizures effectively?
2. How can seizure detection/prediction algorithms be optimized towards reducing computation complexity and power consumption?
3. Can a hardware implementation of a high-performance seizure forecasting system operate in real-time with given low power constraints, e.g., wearable or portable devices?

### 1.4 Thesis organization

This thesis is divided into nine chapters. The first chapter provides an introduction to this thesis. From chapter 2 to 8, we try to address the research questions. Each chapter has its own introduction and conclusion of its specific problem to be solved. The last chapter summarizes the major contributions and concludes the thesis.

- In chapter 2, we first review the problems that patients with epilepsy encounter, especially those with intractable or drug-resistant epilepsy, that make detecting and forecasting epileptic seizure onset critical to improving their quality of life. Subsequently, we summarize existing algorithms in the literature performing seizure detection and forecasting, and their hardware implementation. We finally discuss the vision that goes beyond the scope of this Ph.D. project.

- Chapters 3 and 4 address the first research questions. In chapter 3, we propose a generalized convolutional neural network-based algorithm to forecast epileptic seizures across multiple epilepsy datasets effectively. In chapter 4, we propose an unsupervised feature learning to make use of unlabelled EEG signals which are more accessible.
  1. Is epileptic seizure forecasting possible? What can be done to forecast the likelihood of incoming seizures effectively?
- Chapters 5 to 7 address the second research question. The optimization for computational complexity and power consumption reduction is performed from two aspects: algorithm and input signal. In the first aspect, we propose two approaches: (1) automatic channel selection to reduce the number of necessary EEG electrodes (chapter 5), (2) Integer-Net, an integer convolutional neural network, to reduce computational complexity and required memory to store the algorithm (chapter 6). In the second aspect, we investigate how sensitive working seizure detection algorithms are with regard to EEG's resolution (chapter 7).
  2. How can seizure detection/prediction algorithms be optimized towards reducing computation complexity and power consumption?
- Chapter 8 addresses the last research question. In this chapter, we demonstrate a low-power hardware implementation of a seizure forecasting system that can operate in real-time.
  3. Can a hardware implementation of high-performance seizure forecasting system operate in real-time with given low power constraints, e.g., wearable or portable devices?

## 1.5 List of publications

The following publications form the core of this thesis. Sections from these publications are included in this thesis's chapters as indicated.

### 1.5.1 Journal publications

- Truong, N. D., L. Kuhlmann, M. R. Bonyadi, J. Yang, A. Faulks, and O. Kavehei (2017). “Supervised learning in automatic channel selection for epileptic seizure detection.” *Expert Systems with Applications* 86, 199-207. DOI:10.1016/j.eswa.2017.05.055.
- Truong, N. D., A. D. Nguyen, L. Kuhlmann, M. R. Bonyadi, J. Yang, S. Ippolito, and O. Kavehei (2018). “Integer Convolutional Neural Network for Seizure Detection.” *IEEE Journal on Emerging and Selected Topics in Circuits and Systems* 8.4, 849-857. DOI:10.1109/JETCAS.2018.2842761.
- Truong, N. D., A. D. Nguyen, L. Kuhlmann, M. R. Bonyadi, J. Yang, S. Ippolito, and O. Kavehei (2018). “Convolutional neural networks for seizure prediction using intracranial and scalp electroencephalogram.” *Neural Networks* 105, 104-111. DOI:10.1016/j.neunet.2018.04.018.
- Kavehei, O., T. J. Hamilton, N. D. Truong, and A. Nikpour (2019). “Opportunities for electroceuticals in Epilepsy.” *Trends in Pharmacological Sciences* 40.10, 735-746. DOI:10.1016/j.tips.2019.08.001.
- Truong, N. D., L. Kuhlmann, M. R. Bonyadi, D. Querlioz, L. Zhou, and O. Kavehei (2019). “Epileptic Seizure Forecasting with Generative Adversarial Networks.” *IEEE Access* 7, 143999-144009. DOI:10.1109/ACCESS.2019.2944691.

### 1.5.2 Conference publications

- Truong, N. D. and O. Kavehei (2019). “Low Precision Electroencephalogram for Seizure Detection with Convolutional Neural Network.” *Proc. IEEE International Conference on Artificial Intelligence Circuits and Systems*. DOI:10.1109/AICAS.2019.8771569.

### 1.5.3 Other publications

The following publications resulted from the main project and side projects during the duration of the degree but not being part of this thesis.

- Liu, T., N. D. Truong, A. Nikpour, L. Zhou, and O. Kavehei (2019). “Epileptic Seizure Classification with Hybrid Bilinear Models.” Under review with *IEEE Journal of Biomedical and Health Informatics*.
- Truong, N. D., L. Kuhlmann, M. R. Bonyadi, and O. Kavehei (2017). “A Generalised Seizure Prediction with Convolutional Neural Networks for Intracranial and Scalp Electroencephalogram Data Analysis.” *Poster presentation at the International Conference for Technology and AnaLysis of Seizures*.
- Truong, N. D., L. Zhou, and O. Kavehei (2019). “Semi-supervised Seizure Prediction with Generative Adversarial Networks.” *Proc. IEEE International Engineering in Medicine and Biology Conference*, 2369-2372.
- \*Truong, N. D., \*J. Y. Haw, S. M. Assad, P. K. Lam, and O. Kavehei (2019). “Machine Learning Cryptanalysis of a Quantum Random Number Generator.” *IEEE Transactions on Information Forensics and Security* 14.2, 403-414. DOI:10.1109/TIFS.2018.2850770.
- Kim, J., H. Nili, N. D. Truong, T. Ahmed, J. Yang, D. S. Jeong, S. Sriram, D. C. Ranasinghe, S. Ippolito, H. Chun, and O. Kavehei (2019). “Nano-Intrinsic True Random Number Generation: A Device to Data Study.” *IEEE Transactions on Circuits and Systems I: Regular Papers* 66.7, 2615-2626. DOI:10.1109/TCSI.2019.2895045.
- Kim, J., H. Nili, G. C. Adam, N. D. Truong, D. B. Strukov, and O. Kavehei (2018). “Predictive Analysis of 3D ReRAM-Based PUF for Securing the Internet of Things.” *IEEE Region Ten Symposium (Tensymp)* 91-94. DOI:10.1109/TENCONSpring.2018.8692038.

\* shared first authorship

## 1.6 List of source codes

- Truong, N. D., L. Kuhlmann, M. R. Bonyadi, J. Yang, A. Faulks, and O. Kavehei (2017). “Supervised learning in automatic channel selection for epileptic seizure detection.” *Expert Systems with Applications* 86, 199-207. DOI:10.1016/j.eswa.2017.05.055.  
<https://github.com/NeuroSyd/seizure-detection-ACS>
- Truong, N. D., A. D. Nguyen, L. Kuhlmann, M. R. Bonyadi, J. Yang, S. Ippolito, and O. Kavehei (2018). “Integer Convolutional Neural Network for Seizure Detection.” *IEEE Journal on Emerging and Selected Topics in Circuits and Systems* 8.4, 849-857. DOI:10.1109/JETCAS.2018.2842761.  
<https://github.com/NeuroSyd/Integer-Net>
- Truong, N. D., A. D. Nguyen, L. Kuhlmann, M. R. Bonyadi, J. Yang, S. Ippolito, and O. Kavehei (2018). “Convolutional neural networks for seizure prediction using intracranial and scalp electroencephalogram.” *Neural Networks* 105, 104-111. DOI:10.1016/j.neunet.2018.04.018.  
<https://github.com/NeuroSyd/seizure-prediction-CNN>
- Truong, N. D. and O. Kavehei (2019). “Low Precision Electroencephalogram for Seizure Detection with Convolutional Neural Network.” *Proc. IEEE International Conference on Artificial Intelligence Circuits and Systems*. DOI:10.1109/AICAS.2019.8771569.  
<https://github.com/NeuroSyd/seizure-detection-low-ADCbits>
- Truong, N. D., L. Kuhlmann, M. R. Bonyadi, D. Querlioz, L. Zhou, and O. Kavehei (2019). “Epileptic Seizure Forecasting with Generative Adversarial Networks.” *IEEE Access* (Early access). DOI:10.1109/ACCESS.2019.2944691.  
<https://github.com/NeuroSyd/seizure-prediction-GAN>

# Chapter 2

## Literature review

The content in this chapter has been adapted from the a journal paper published as:

- Kavehei, O., T. J. Hamilton, N. D. Truong, and A. Nikpour (2019). “Opportunities for electroceuticals in Epilepsy.” *Trends in Pharmacological Sciences* 40.10, 735-746. DOI:10.1016/j.tips.2019.08.001.

### **Statement of Contributions of Joint Authorship**

- Omid Kavehei (Principal Supervisor): first author, provided the main idea, writing, reviewing and editing the manuscript
- Tara Julia Hamilton: provided technical advice on the analysis and reviewing the manuscript
- Nhan Duy Truong (Candidate): writing, reviewing and editing of the manuscript. The candidate was in charge of reviewing treatment of drug-resistant epilepsy and methods for detecting and predicting epileptic seizures.
- Armin Nikpour: provided neurological and medical advice on the analysis and reviewing the manuscript

In addition to the statements above, in cases where I am not the corresponding author of a published item, permission to include the published material has been granted by the corresponding author.

Nhan Duy Truong

Date: 01 October 2019

As supervisor for the candidature upon which this thesis is based, I can confirm that the authorship attribution statements above are correct.

Dr. Omid Kavehei

Date: 01 October 2019

## 2.1 What is epilepsy?

Epilepsy is a neurological disease characterized by recurrent and unpredictable abnormal brain activities, called epileptic seizures (R. S. Fisher et al., 2017). Epilepsy can be caused by stroke, traumatic brain injury and encephalitis (Kullmann et al., 2014). There are many types of seizures (see Fig. 2.2) that affect different functions of the brain including sensory processing, movement, consciousness, emotion, memory, and behavior. Dependent on the mode of onset, seizures are classified as focal, generalized and unknown. Focal onset seizure is when electrical activities are only within a limited area of the brain while generalized onset seizure is when those activities originate at some point then rapidly spread in both hemispheres (Falco-Walter et al., 2018). Focal seizures are divided into aware and impaired awareness. A focal aware seizure means that the person is conscious of self and the surrounding environment, even if immobile. Otherwise, if the person loses awareness during any part of the seizure, it is classified as a focal impaired awareness seizure. Generalized seizures can be further classified as motor and non-motor (absence) seizures. Most common form of generalized motor seizure is tonic-clonic (R. S. Fisher et al., 2017).

In Australia, the national health insurance implements a co-payment scheme that represents 17% of the total cost of healthcare to reduce unnecessary services. As a consequence, low-income patients are most affected (C. L. Peterson and Walker, 2018). Particularly, the lowest-income group diagnosed with weekly income before tax of AUD250–500 spent 2.19% of their income on epilepsy. In New South Wales, Australia, during the five-year period from 2012 to 2016, total epilepsy related hospital direct costs were over AUD400 million (Mitchell et al., 2018).

Epilepsy affects nearly 1% of the global population, but only two thirds can be treated by medicine, and approximately 7-8% can be cured by surgery (Litt and Echauz, 2002). The point and lifetime prevalence of epilepsy is 6.4% and 7.6% per 1000 people, respectively (Fiest et al., 2017). In Australia, neurological conditions were accounted for 6.8% of all disability-adjusted life years in 2011. Epilepsy was responsible for 14.6% of the burden caused by the neurological conditions (see Fig. 2.1) (Australian Institute of Health Welfare, 2016). The most burden to epilepsy patients is that seizures can strike at any time, causing interruptions in their daily activities and potentially put them in danger. Therefore, seizure onset detection, prediction, and subsequent seizure suppression become important for the patients that cannot be cured by either drug or surgery. Early detection can allow early electrical stimulation to suppress the seizure (Echauz et al., 2007). Seizure prediction allows the patients to

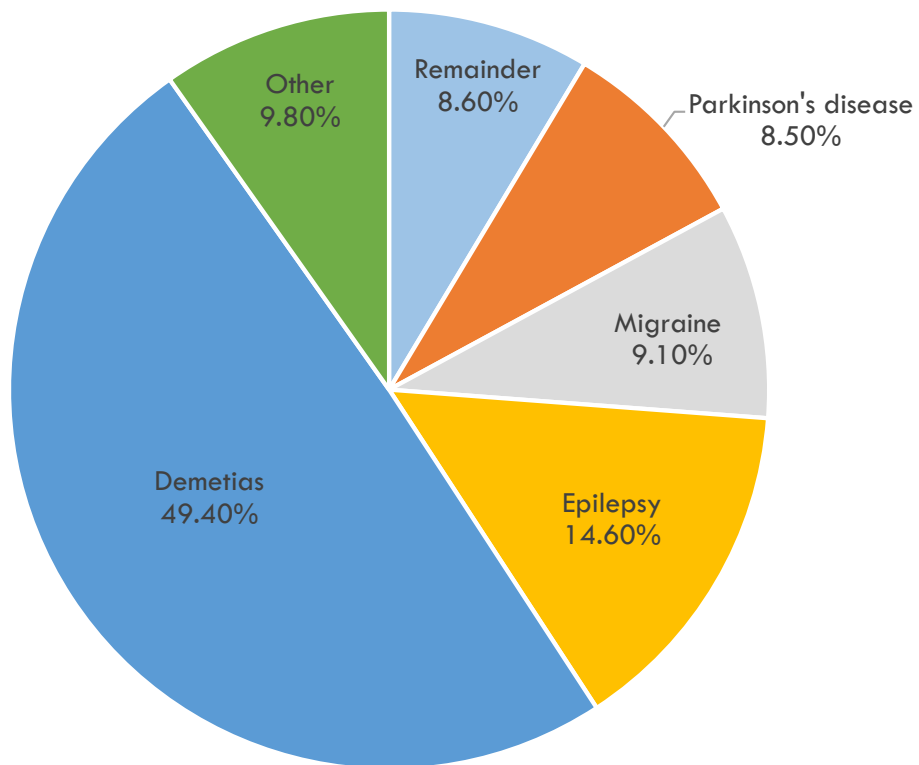


Figure 2.1: Proportions of disability-adjusted life years caused by neurological conditions in Australia. Adapted from (Australian Institute of Health Welfare, 2016).

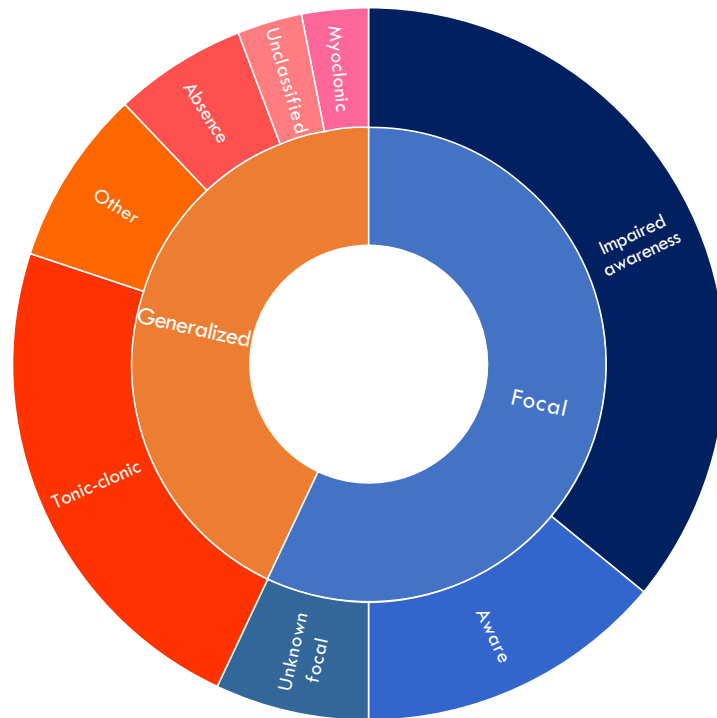


Figure 2.2: Different seizure types. Adapted from (CURE, 2019).

have time to take precautions if a seizure can be warned in minutes before its onset.

Patients diagnosed with epilepsy are firstly treated with appropriate epileptic drugs depending on the seizure types, properties of available drugs and other characteristics (Kwan and Brodie, 2000). Drug doses and combination of drugs are adjusted considering the efficacy and side effects. The International League Against Epilepsy (ILAE) defines drug-resistant epilepsy as “failure of adequate trials of two tolerated, appropriately chosen and used antiepileptic drug schedules (whether as monotherapies or in combination) to achieve sustained seizure freedom” (Kwan, Arzimanoglou, et al., 2010). Patients with drug-resistant epilepsy will be evaluated if they are appropriate candidate for surgical treatment (López González et al., 2015). Alternative treatments for those who do not respond satisfactorily to antiepileptic drugs or are not suitable for surgery are still in experimental stage (Kullmann et al., 2014).

In this chapter, we review the current drug-resistant epilepsy treatments, existing algorithms, and hardware implementation for seizure detection and prediction, and finally discuss the vision of this research.

## 2.2 Treatment of drug-resistant epilepsy

Non-invasive brain stimulation techniques that have been comprehensively studied and have therapeutic potential for epileptic patients are transcranial magnetic stimulation (TMS) and transcranial direct current stimulation (tDCS). TMS was originally designed to study human corticospinal motor conduction (Cattaneo, 2017). Single-pulse TMS uses a capacitor storing the electrical charge to produce a current in a coil. The coil is connected to a pulse generator, which is placed near the head, to deliver pulses at very low frequency (below 1 Hz). The magnetic field passes relatively painlessly through tissues of the head to generate a weak electrical current on the brain (Wassermann, 1998). Another form of TMS, repetitive TMS (rTMS) delivers repeated pulses with high frequency at up to 100 Hz by using multiple capacitors. rTMS shows the capability to modulate the excitability of cortical networks; hence, it has been considered as a promising therapy for treating epilepsy. However, TMS is yet to demonstrate clear evidence on the effectiveness in the treatment of seizures across a range of patients with different forms of epilepsy and different age group (Carrette et al., 2016).

tDCS is based on observations that low amplitude direct current can modulate the neuronal firing. Particularly, cathodal tDCS can reduce cortex excitability. Thus, it may be used for the treatment of seizures (Auvichayapat et al., 2013). tDCS devices are light-weight and can operate with a 9-V battery. tDCS devices are commercially available at an affordable price in the market with multiple providers, such as The Brain Stimulator<sup>1</sup>, Omni Stimulator<sup>2</sup>, tDCS Brain Care<sup>3</sup>. These products are claimed to have a positive effect on depression reduction and concentration improvement. Recent promising results on seizure reduction (Assenza et al., 2017) shows that it could also be used for the treatment of drug-resistant epilepsy.

Deep Brain Stimulation (DBS) is a neurostimulation therapy, whereas electrodes are implanted into subcortical regions and connected to an implanted pulse generator (IPG) typically placed in the front of the chest (Gooneratne et al., 2016). A variety of commercial DBS products are provided by Medtronic<sup>4</sup>, St. Jude Medical<sup>5</sup>, Boston Scientific<sup>6</sup>. DBS has been used as a therapy for Parkinson’s disease and essential tremor, where rhythmic shaking is a common feature. Typical stimulation for refractory

---

<sup>1</sup><https://thebrainstimulator.net/>

<sup>2</sup><http://www.omnistimulator.com/>

<sup>3</sup><http://tdcsbraincare.com.au/>

<sup>4</sup><http://professional.medtronic.com/pt/neuro/dbs-md/prod/index.htm>

<sup>5</sup><https://www.sjm.com/en/professionals/featured-products/neuromodulation/deep-brain-stimulation>

<sup>6</sup><https://www.bostonscientific.com/en-EU/products/deep-brain-stimulation-systems.html>

epilepsy is operated at a frequency around 145 Hz, 90  $\mu$ s pulse width, at voltages from 2 V increased to 5 V by 1 V each week, and cycle time of 1 min on and 5 min off (Ben-Menachem, 2012).

The efficacy of DBS was studied in a clinical trial of stimulation of the anterior nuclei of thalamus for epilepsy (SANTE) with 110 randomized participants with medically refractory partial seizures (R. Fisher et al., 2010). The DBS implantation was done with devices from Medtronic<sup>1</sup>. All participants underwent the same stimulation setting at a voltage of 5 V, 90  $\mu$ s pulse width, frequency of 145 Hz, 1 min on and 5 min off. The median percent seizure reduction was 41% at 1 year and 69% at 5 years. 16% of patients were reported seizure-free for at least 6 months in 5 years follow-up (Salanova et al., 2015). Another study on the efficacy of DBS in seizure treatment was conducted with 15 patients having refractory epilepsy (Lehtimäki et al., 2016). The locations of contacts were calculated from 3T MRI images obtained using scanner MAGNETOM Trio 3T, Siemens Healthcare Sector, Germany. Stimulation parameters were chosen at a frequency of 145 Hz, a pulse width of 90  $\mu$ s, 1 min on and 5 min off, and amplitude gradually increased to 5 V from 5–6 postoperative days to 2–3 weeks. As a result, 10 out of total 15 patients with refractory epilepsy were eventually responsive to ANT-DBS, whereas 4 of the 10 were initially not responsive but finally had seizure reduction after changes in active contacts. Overall, DBS is a highly invasive procedure that has some potentially dangerous side-effects.

Vagus nerve stimulation (VNS) is another approach of neurosurgical interventions for epilepsy. VNS uses an electrode placed around the vagal nerve in the left side of the neck and wired to a subcutaneous pulse generator. VNS is often set at 20–30 Hz, 250–500  $\mu$ s pulse width, a current between 1.5 and 2.25 mA, and cycle time of 30 s on and 3–5 min off (Ben-Menachem, 2012). VNS has been used as an FDA-approved therapy for refractory epilepsy (Clancy et al., 2014). Compared to DBS, VNS is less invasive and has fewer, less significant side effects such as changes in voice and coughing. Interestingly, patients with failed VNS seems to respond better to ANT-DBS (Gooneratne et al., 2016). In a study of 65 consecutive patients with implanted VNS over 10 years, the mean seizure reduction is 35.7% in six months and up to 75.5% after 10 years (Elliott et al., 2011). VNS Therapy, produced by LivaNova<sup>7</sup>, is a commercial FDA-approved device for drug-resistant epilepsy treatment. A non-invasive variant of VNS, namely transcutaneous vagus nerve stimulation (tVNS), has been investigated on the efficacy of seizure reduction. A randomized, double-blind trial with 67 patients was run with two stimulation frequencies, 1 Hz and 25 Hz (Bauer et al., 2016). The tVNS device that was

---

<sup>7</sup><http://www.livanova.cyberonics.com/>

used in the study is the NEMOS made by Cerbomed GmbH<sup>8</sup>. The results show a seizure reduction rate of 34.2% for patients in the 25 Hz group after 20 weeks of treatment.

In contrast to the aforementioned neurological therapies, where the stimuli are applied periodically without regard to the seizure onset, electroencephalogram (EEG) based neurostimulators monitor the brain's status and perform stimulation only when seizure-related patterns are detected (F. T. Sun and Morrell, 2014; Kassiri et al., 2016). Therefore, they may have a better chance of achieving the best possible, patient-specific outcome. EEG signals have been used extensively in the monitoring and diagnosis of patients with neurological disorders. The RNS system, for instance, is an FDA-approved implantable seizure treatment device produced by NeuroPace<sup>9</sup>. It hosts an implantable neurostimulator wired to leads that could be implanted into the brain or placed on the surface of the brain. The neurostimulator is capable of sensing the electrocorticographic (ECoG) signal, detect seizures, and perform electrical stimulation. The ECoG signals are recorded at a frequency of 250 Hz. The detection function is based on three detection tools: line length detection, area detection, and bandpass detection. The line length detection tool accumulates the differences between consecutive samples over a short-term window divided by the number of samples of that window, then compares with that of a long-term window. The area detection tool compares the average area under the curve over a short-time window with that of a long-time window. The bandpass detection tool first identifies half-waves by locating local minima and maxima points. The number of half-waves that exceed programmable thresholds of amplitude and duration is compared to a programmed threshold. Stimulation is typically initiated with a frequency of 200 Hz, 160 ms pulse width, 100 ms burst duration, and current from 1 mA up to 12 mA. The RNS system was studied with 191 subjects over two years (F. T. Sun and Morrell, 2014). The median seizure reduction is 44% at one year post-implant and 53% at two years post-implant.

Another implantable system that can record EEG signals and perform electrical stimulation, with regards to the detection and possible suppression of epileptic seizures, was proposed in (Kassiri et al., 2016). This battery-less system can operate at a maximum distance of 15 cm from an inductive powering link with a power transfer efficiency of up to 40%. The system was validated in a 100-hour study of 4 Wistar rats with temporal lobe epilepsy. Although the onset detection delay and the efficiency of the stimulation were not mentioned, the sensitivity was reported in the range of 88–96% and the selectivity of 89–97% (Kassiri et al., 2016).

---

<sup>8</sup><http://www.cerbomed.de>

<sup>9</sup><http://www.neuropace.com>

Besides electrical/magnetic simulations, ketogenic diet is another alternative treatments for drug-resistant epilepsy. A clinical trial with twenty-five children (median age of 6.1 years; range of 2.3-13.2) showed a response (with  $\leq 50\%$  reduction in seizure frequency) rate of 36%. The dietary ratio fat-to-carbohydrate varied from 3:1 to 4.2:1 (Mackay et al., 2005). Another trial on twenty-nine adults and adolescents (mean age of 32 years; range of 11-51) showed a similar response rate of 45%. However, due to small sample sizes and lack of long-term study on adverse effects, further research on ketogenic diet would be of benefit (Martin-McGill KJ and Cooper, 2018).

Gene therapy has been shown promising results on treating Parkinson's disease (Axelsen and Woldbye, 2018). For epilepsy, potential gene therapy approaches including manipulating endogenous genes, targeting cohorts of genes and introducing engineered proteins into the brain have been being investigated. Though there have been some successful results from experimental models, clinical trials are not ready yet due to concerns about safety, efficacy and human ethics (Kullmann et al., 2014).

There are other available solutions in the market sensing different important factors that are shown to be relevant to a seizure incident. For example, Seizure Sensor<sup>10</sup> uses heart rate and breathing patterns to detect epileptic seizures. Nikki G's temperature control clothing<sup>11</sup> monitors if the body temperature drops significantly below a threshold. Commonly used devices such as smartwatches are also demonstrated capabilities in detecting and logging seizure events. Smart mobile apps are also available with capabilities for seizure detection, seizure logging system, and automated carer alert<sup>12</sup>. While seizure detection is essential for 1) accurate seizure log keeping, 2) drug effectiveness studies and 3) automated EEG data labeling, seizure prediction is the only possible solution that delivers a meaningful quality-of-life improvement to patients living with the chronic disease.

## 2.3 Seizure detection and prediction

EEG has been commonly used in brain-computer interface thanks to the convenient real-time readings and high temporal resolution of EEG signals (H. Zhang et al., 2013). In recent years, EEG has provided a promising possibility to detect and even predict an epileptic seizure (Tieng et al., 2016; Fatichah et al., 2014; Parvez and Paul, 2015; Saab

---

<sup>10</sup><http://www.tunstallhealthcare.com.au>

<sup>11</sup><https://www.nikkigs.com.au>

<sup>12</sup><http://www.epdetect.com>

and Gotman, 2005; Osorio and Frei, 2009; Kuhlmann, Burkitt, et al., 2009). For seizure detection, a combination of principal component analysis (PCA) and neural network with fuzzy membership function can achieve an accuracy rate up to 97.64% (Faticah et al., 2014). The authors in (Tieng et al., 2016) combined wavelet de-noising with adapted Continuous Wavelet Transform in their algorithm and were able to achieve a sensitivity of 96.72% and a specificity of 94.69% with EEG data from mice. Another remarkable method is to transform EEG signals into images so as to leverage image processing techniques (Parvez and Paul, 2015). This approach was able to obtain 98.91% sensitivity and 94.35% specificity. (Zabihi et al., 2016) reconstructed EEG phase spaces using time-delay embedding method and PoinCare section. The phase spaces were then reduced by PCA before being fed to linear discriminant analysis (LDA) and Naive Bayesian classifiers. This approach achieved 88.27% sensitivity and 93.21% specificity in seizure detection.

The authors in (Shoeb, 2009) deployed eight filters spanning the frequency range of 0.5–24 Hz for each 2-second EEG epoch of all channels, then concatenated three epochs to form a feature set to be fed to a support vector machine (SVM) classifier. This approach was tested with the Boston Children’s Hospital (CHB)-MIT dataset and was able to detect 96% of 163 test seizures with a mean detection delay of 4.6 seconds. In another work, EEG signals were transformed into an image representation using 2-D projection of the patient electrodes and the magnitude of 3 different frequency bands spanning the range of 0–49 Hz of each 1-second block of EEG signal (Thodoroff et al., 2016). The recurrent convolutional neural network took 30 consecutive blocks as inputs to perform feature extraction and classification. The patient-specific detectors in this method have comparable performance compared to the proposed method by (Shoeb, 2009).

Prominent feature extraction techniques consider characteristics in both frequency and time domain. As an efficient tool for time-frequency-energy analysis, wavelet-based filters were used to extract a ratio of seizure content of the short foreground in comparison with the background (Saab and Gotman, 2005; Osorio and Frei, 2009). In another work, Bayes’ formula was applied on extracted features to estimate the probability of seizure in EEG signals (Saab and Gotman, 2005). This method achieved an impressively short onset detection delay of 9.8 s with 76% sensitivity and 0.34/h false positive rate. An extension of this method was done by combining extra features to find a superior detector (Kuhlmann, Burkitt, et al., 2009). The extended method was able to achieve a sensitivity of 81%, a false positive rate of 0.60/h, and a median detection delay of 16.9 s on a dataset of 525 h of scalp EEG data.

Detecting seizure using EEG signals has achieved high accuracy and low detection delay, however, computational efficiency gains are needed if state-of-the-art methods are to be implemented in implanted or wearable devices. One simple but non-trivial method to alleviate the computational burden is to reduce the amount of input signals. This can be done by leveraging bio-medical knowledge to manually select which channels genuinely contribute to the seizure. However, it is hard and time-consuming to disclose a set of channels that are significant for every patient. There have been several attempts to perform this channel selection in an automatic fashion (Duun-Henriksen et al., 2012; Shih et al., 2009). Alternative to reducing the amount of input signals is to reduce number of features extracted prior to classification (Minasyan et al., 2010; Subasi and Ismail Gursoy, 2010). However, this approach is less preferable because the feature selection has to be performed not only during training but also during run-time classification for the latter. In this thesis, we pursue the former approach where we propose a novel automatic channel selection engine to select the most relevant EEG channels for seizure detection. The work is presented in Chapter 5. The computational efficiency gains can be achieved by optimizing the detection algorithms themselves; i.e., making the algorithms more hardware friendly. The most common approach is to compress a pre-trained network by iteratively pruning connections and/or quantizing trained weights (Han, Pool, et al., 2015; Han, Mao, et al., 2015). Another approach is to design compact neural network by decomposing convolutional kernels into smaller ones (Iandola et al., 2016; Szegedy et al., 2017). A novel method, which is pursued in this work and is inspired by Rastegari et al. (2016), is to quantize weights during training phase.

Along with continuous improvements in recording electroencephalogram (EEG) signals, there has been an increasing number of EEG-based techniques for seizure prediction. There have been some articles on seizure prediction using the Freiburg Hospital dataset (University of Freiburg, 2003). For example, the dynamical similarity index, effective correlation dimension, and increments of accumulated energy were used as features (Maiwald et al., 2004). The dynamical similarity index yielded the highest performance, with a sensitivity of 42% and a false prediction rate (FPR) less than 0.15/h. The mean phase coherence and lag synchronization index of 32-s sliding EEG windows were used as features for seizure prediction (Winterhalder et al., 2006). This approach achieved a sensitivity of 60% and an FPR of 0.15/h. The approach was further improved by the combined use of bivariate empirical mode decomposition, and Hilbert-based mean phase coherence as additional features (Zheng et al., 2014). As a result, sensitivity was increased beyond 70%, while FPR dropped below 0.15/h. A lightweight approach based on the spike rate achieved 75.8% sensitivity and FPR of 0.09/h (S. Li et al., 2013). By

use of the synchronization information, a method based on phase-match error of two consecutive epochs and variation within each epoch resulted in 95.4% sensitivity and FPR of 0.36/h (Parvez and Paul, 2017). Another synchrony-based approach used the mean phase coherence between each pair of channels calculated over multiple window lengths as an indicator of incoming seizure onset (Kuhlmann, D. Freestone, et al., 2010).

Frequency bands of the power spectrum of each channel were used as a feature for seizure prediction (Park et al., 2011). These features were then fed to a support vector machine (SVM) classifier to learn the differences between preictal and interictal instances. This method was tested with the Freiburg Hospital dataset and achieved a sensitivity of 98.3% and an FPR of 0.29/h. A similar approach with additional features which are spectral power ratios between different frequency bands achieved sensitivity exceeding 98% and FPR less than 0.05/h (Z. Zhang and Parhi, 2016). However, this approach relied on tailoring features for each patient independently, hence offering reduced generalization as a result. Differently from the two approaches described, (Aarabi and He, 2014) applied a Bayesian inversion of power spectral density and then applied a rule-based decision to perform the seizure prediction task. This approach was tested with the Freiburg Hospital dataset, with a sensitivity of 87.07% and an FPR of 0.2/h. (Aarabi and He, 2017) recently extracted six univariate and bivariate features, including correlation dimension, correlation entropy, noise level, Lempel-Ziv complexity, largest Lyapunov exponent, and nonlinear interdependence, and achieved a comparable sensitivity of 86.7% and a lower FPR of 0.126/h. On the basis of the assumption that future events depend on a number of previous events, a multiresolution  $N$ -gram on amplitude patterns was used as features (Eftekhar et al., 2014). After optimization of the feature set per patient, this method yielded a high sensitivity of 90.95% and a low FPR of 0.06/h on the Freiburg Hospital dataset. Recently, the dynamics of EEG was captured by use of 64 fuzzy rules to estimate the trajectory of each sliding EEG window on a Poincaré plane (Sharif and Jafari, 2017). The principal component analysis was used to reduce interrelated features before classification by an SVM. This work achieved a sensitivity of more than 91% and an FPR below 0.08/h on the Freiburg Hospital dataset.

Many of these studies relied on handcraft feature extraction and/or tailored feature extraction to achieve a high sensitivity and a low false prediction rate. This approach, however, is not generalizable, and requires significant modifications for each new patient. Also, it is necessary to calibrate the seizure prediction because seizure characteristics may change over time. Minimum feature engineering allows faster and more frequent updates so that the patients can benefit the most from the seizure prediction algorithms. Recent

works on seizure prediction are moving towards using deep learning approaches which requires less feature engineering effort. These methods can take inputs as time-series EEG signals (Hosseini et al., 2017; Abdelhameed and Bayoumi, 2018) or spectrograms (Kiral-Kornek et al., 2018). Kiral-Kornek et al. (2018) generated spectrograms of each 30-second EEG segments and used a convolutional neural network to distinguish between preictal and interictal segments. The method achieved a mean sensitivity of 69% and a mean time in warning of 27% tested with a intracranial EEG dataset of ten patients. Hosseini et al. (2017) trained stacked autoencoders (SAE) with time-series EEG signals. The SAE’s features were then optimized with dimension reduction and combined with engineered features from a priori knowledge before being classified by an SVM. This approach was tested with two epilepsy patients and achieved a sensitivity of 95% and FPR of 0.06/h. In another work, Abdelhameed and Bayoumi (2018) used a deep convolutional autoencoder as an unsupervised feature extractor. The extracted features were classified by a bidirectional long-short term memory (Bi-LSTM). The method achieved a sensitivity of 94.6% and a FPR of 0.04/h tested with the CHB-MIT dataset.

## 2.4 Hardware implementation of seizure detection

Though there have been many promising algorithms for seizure prediction, a low-power or portable system that can perform seizure prediction has not been available yet. Regarding seizure detection, an 8-channel scalp EEG system for continuous detecting and recording seizure onset events was introduced in (Yoo et al., 2013). This system hosts an SoC that integrates 8 analog frontend channels, a machine-learning processor for seizure detection and a 64 KB SRAM. The machine-learning processor that implements support vector machine (SVM) as a classifier was able to perform an on-chip training and had comparable performance to MATLAB simulation when verifying with the CHB-MIT EEG database. However, the performance of this machine-learning processor was 82.7% in detection rate and 4.5% in false positive rate which is much lower than reported in (Goldberger et al., 2000), where the database was first introduced, with detection rate at 96% and 2 false detections per 24 hour period. The SoC was fabricated with 0.18  $\mu\text{m}$  1P6M CMOS process occupying 25  $\text{mm}^2$  area. The complete system was validated with an eye blink classification test and achieved an eye blink detection rate of 84.4% at 2.03  $\mu\text{J}$ /classification (Yoo et al., 2013).

An implantable system that can record EEG signals and perform electrical stimulation with regards to detection and suppression of epileptic seizures was proposed

in (Kassiri et al., 2016). This miniaturized system is composed of an inductive power receiver coil, a wireless interface board, and a neurostimulator board. This battery-less system can operate at a maximum distance of 15 cm from an inductive powering link with a power transfer efficiency of up to 40%. The wireless interface board performs power management and transmits signals recorded by the neurostimulator board to the outside of the body. The neurostimulator board hosts a 24-channel neurostimulator SoC that is responsible for neural signal recording, digital signal processing, and electrical stimulation for seizure suppression. The system was validated in a 100-hour study of 4 Wistar rats with temporal lobe epilepsy. The system was able to monitor and detect seizures in real-time and trigger electrical stimulation for seizure abortion. Although the onset detection delay and the efficiency of the stimulation were not mentioned, the sensitivity was reported in the range of 88–96% and the selectivity of 89–97% (Kassiri et al., 2016).

Using a much simpler seizure detection algorithm, an implantable hardware implementation for seizure detection in rats was proposed in (Raghunathan, Gupta, Markandeya, et al., 2010). The detection algorithm is based on events defined in relation to EEG signal amplitude during seizure period compared to baseline recordings. Specifically, if the amplitude is  $K_{\text{amp}}$  larger than the baseline, the signal is marked as an event. Inter-event intervals (IEIs) derived from marked events are less than or equal to a programmable threshold  $\text{IEI}_{\text{thresh}}$  are marked. The number of consecutive marked IEIs is used to determine whether there is a seizure onset by comparing with another threshold  $N_{\text{stage}}$ . This study was performed on 10 female long Evans rats and seizure data from 6 of 10 were used in the analysis. The data was recorded at 1526 Hz from a twisted-pair two-channel electrode through a data acquisition system connected to a computer. The set of  $(K_{\text{amp}}, \text{IEI}_{\text{thresh}}, N_{\text{stage}})$  is optimized per subject. The algorithm achieved a sensitivity of 95.3%, a selectivity of 88.9% and a mean detection delay of 8.5 seconds. The fully CMOS implementation of the algorithm has a power consumption per channel of 350 nW from a 250 mV power supply based on simulation results on the MIT 180 nm SOI process.

## 2.5 Discussions

Though seizure prediction is still challenging, seizure detection has achieved very high performance. Given a high-performance seizure detector, we can use it as part of a self-evaluation prediction system. The idea is that the seizure detector will keep evaluating the seizure prediction over a long period without the need for human

monitoring. The evaluation results can be used as feedback to improve (re-train) the prediction algorithm. As depicted in Fig. 2.3, the system performs seizure detection and seizure prediction in parallel. If a seizure is detected at time  $t_d$ , the system will check whether it was predicted within the period  $[t_d - SPH - SOP; t_d]$ , where  $SPH$  and  $SOP$  are the seizure prediction horizon and seizure occurrence period<sup>13</sup>. If yes, the prediction is correct; otherwise, it is a false negative prediction. In another scenario, if a seizure is predicted at time  $t_p$ , the system will check whether it will be detected within the period  $[t_p; t_p + SPH + SOP]$ . If yes, the prediction is correct; otherwise, it is a false positive prediction. Note that if there is a seizure and neither seizure detection nor prediction is triggered, the system will not be able to evaluate. Therefore, high-performance seizure detection is required for this system to work properly.

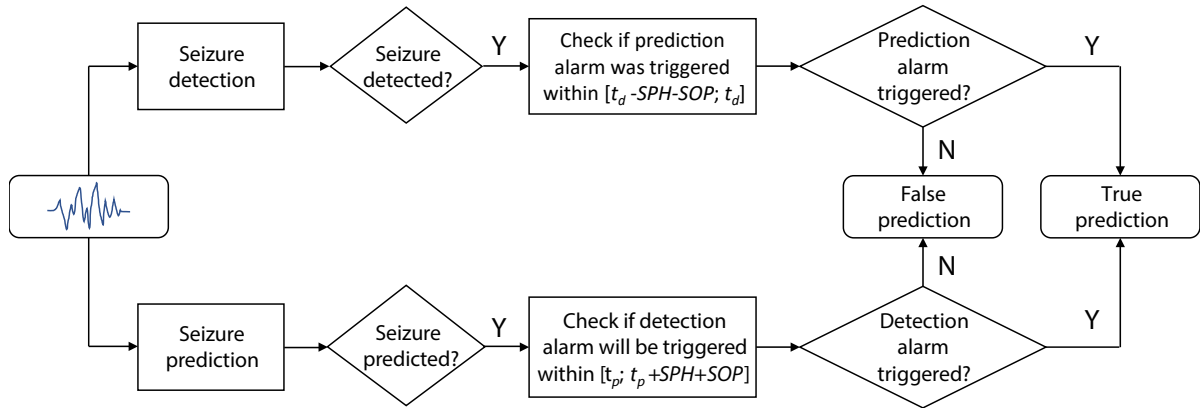


Figure 2.3: A self-evaluation prediction system. High-performance seizure detection is required for this system to work properly.  $t_d$  is the point of time when a seizure is detected.  $t_p$  is the point of time when an incoming seizure is predicted.

\* The seizure occurrence period (SOP) is the interval where the seizure is expected to occur. The period between the alarm and the beginning of the SOP is the seizure prediction horizon (SPH) (Truong, Nguyen, et al., 2018a)

<sup>13</sup>The seizure occurrence period (SOP) is the interval where the seizure is expected to occur. The period between the alarm and the beginning of the SOP is the seizure prediction horizon (SPH) (Truong, Nguyen, et al., 2018a).

## Chapter 3

# Seizure prediction with convolutional neural network

The content presented in this chapter is published as:

- Truong, N. D., A. D. Nguyen, L. Kuhlmann, M. R. Bonyadi, J. Yang, S. Ippolito, and O. Kavehei (2018). “Convolutional neural networks for seizure prediction using intracranial and scalp electroencephalogram.” *Neural Networks* 105, 104-111. DOI:10.1016/j.neunet.2018.04.018.

### **Statement of Contributions of Joint Authorship**

- Nhan Duy Truong (Candidate): First author, completed the analysis, writing, reviewing and editing of the manuscript
- Anh Duy Nguyen: aided in the analysis and reviewing of the manuscript
- Levin Kuhlmann: aided in the analysis, reviewing and editing the manuscript
- Mohammad Reza Bonyadi: aided in the analysis, reviewing and editing the manuscript
- Jiawei Yang: provided technical advice on the analysis, reviewing and editing the manuscript
- Omid Kavehei (Principal Supervisor): provided the main idea, reviewing and editing the manuscript

In addition to the statements above, in cases where I am not the corresponding author of a published item, permission to include the published material has been granted by the corresponding author.

Nhan Duy Truong

Date: 01 October 2019

As supervisor for the candidature upon which this thesis is based, I can confirm that the authorship attribution statements above are correct.

Dr. Omid Kavehei

Date: 01 October 2019

Seizure prediction has attracted growing attention as one of the most challenging predictive data analysis efforts to improve the life of patients with drug-resistant epilepsy and tonic seizures. Many outstanding studies have reported great results in providing sensible indirect (warning systems) or direct (interactive neural stimulation) control over refractory seizures, some of which achieved high performance. However, to achieve high sensitivity and a low false prediction rate, many of these studies relied on handcraft feature extraction and/or tailored feature extraction, which is performed for each patient independently. This approach, however, is not generalizable and requires significant modifications for each new patient within a new dataset. In this article, we apply convolutional neural networks to different intracranial and scalp electroencephalogram (EEG) datasets and propose a generalized retrospective and patient-specific seizure prediction method. We use the short-time Fourier transform on 30-s EEG windows to extract information in both the frequency domain and the time domain. The algorithm automatically generates optimized features for each patient to best classify preictal and interictal segments. The method can be applied to any other patient from any dataset without the need for manual feature extraction. The proposed approach achieves a sensitivity of 81.4%, 81.2%, and 75% and a false prediction rate of 0.06/h, 0.16/h, and 0.21/h on the Freiburg Hospital intracranial EEG dataset, the Boston Children’s Hospital-MIT scalp EEG dataset, and the American Epilepsy Society Seizure Prediction Challenge dataset, respectively. Our prediction method is also statistically better than an unspecific random predictor for most of the patients in all three datasets.

### 3.1 Introduction

Advances in data mining and machine learning in the past few decades have attracted significantly more attention to the application of these techniques in detective and predictive data analytics, especially in health care, medical practices, and biomedical engineering (Kuhlmann, Grayden, Wendling, et al., 2015; D. R. Freestone, P. J. Karoly, A. D. H. Peterson, et al., 2015; Xiao et al., 2017; Bou Assi et al., 2017; Kuhlmann, Grayden, and Cook, 2017; D. R. Freestone, P. J. Karoly, and Cook, 2017; Sinha et al., 2017). While the body of available proven knowledge lacks a convincing and comprehensive understanding of the sources of epileptic seizures, some early studies showed the possibility of predicting seemingly unpredictable seizures (Rogowski et al., 1981; Salant et al., 1998). Along with continuous improvements in recording electroencephalogram (EEG) signals, there has been an increasing number of EEG-based techniques for seizure prediction (Szostak et al., 2017). There have been some articles on

seizure prediction using the Freiburg Hospital dataset (University of Freiburg, 2003). For example, the dynamical similarity index, effective correlation dimension, and increments of accumulated energy were used as features (Maiwald et al., 2004). The dynamical similarity index yielded the highest performance with a sensitivity of 42% and a false prediction rate (FPR) less than 0.15/h. A lightweight approach based on spike rate achieved a sensitivity of 75.8% and an FPR of 0.09/h (S. Li et al., 2013). By the use of the synchronization information, a method based on phase-match error of two consecutive epochs and variation within each epoch resulted in a sensitivity of 95.4% and an FPR of 0.36/h (Parvez and Paul, 2017). The mean phase coherence and lag synchronization index of 32-s sliding EEG windows could be used as features for seizure prediction (Winterhalder et al., 2006). This approach achieved sensitivity of 60% and FPR of 0.15/h. The approach was further improved by the combination of bivariate empirical mode decomposition and Hilbert-based mean phase coherence as additional features (Zheng et al., 2014). As a result, sensitivity was increased beyond 70%, while FPR dropped below 0.15/h. Another synchrony-based approach used the mean phase coherence between each pair of channels calculated over multiple window lengths as an indicator of incoming seizure onset (Kuhlmann, D. Freestone, et al., 2010).

Feature engineering and support vector machine have been used effectively in the seizure prediction task. Park et al. (2011) calculated frequency bands of the power spectrum of each channel and used a support vector machine (SVM) classifier to distinguish between preictal and interictal EEG segments. This method was tested with the Freiburg Hospital dataset, and achieved a sensitivity of 98.3% and an FPR of 0.29/h. In a similar approach, Z. Zhang and Parhi (2016) added additional features that were spectral power ratios between different frequency bands. The method achieved a sensitivity and an FPR of (100%, 0.032/h) and (98.68%, 0.046/h) tested with the CHB-MIT and the Freiburg Hospital datasets, respectively. However, this approach relied on tailoring features for each patient independently, hence offering limited generalization as a result. Differently from the two approaches described, Aarabi and He (2014) applied a Bayesian inversion of power spectral density and then applied a rule-based decision to perform the seizure prediction task. This approach was tested with the Freiburg Hospital dataset, achieving a sensitivity of 87.07% and an FPR of 0.2/h. Aarabi and He (2017) extracted six univariate and bivariate features, including correlation dimension, correlation entropy, noise level, Lempel-Ziv complexity, largest Lyapunov exponent, and nonlinear interdependence, and achieved a comparable sensitivity of 86.7% and a lower FPR of 0.126/h. On the basis of the assumption that future events depend on a number of previous events, a multiresolution  $N$ -gram on amplitude patterns was used as features (Eftekhar et al., 2014). After optimization

of the feature set per patient, this method yielded a high sensitivity of 90.95% and a low FPR of 0.06/h on the Freiburg Hospital dataset. Recently, the dynamics of EEG was captured by use of 64 fuzzy rules to estimate the trajectory of each sliding EEG window on a Poincaré plane (Sharif and Jafari, 2017). Principal component analysis was used to reduce interrelated features before classification by an SVM. This work achieved sensitivity of more than 91% and FPR below 0.08/h on the Freiburg Hospital dataset.

Patient-specific feature engineering techniques have been successful in seizure prediction tasks by achieving perfect sensitivity (100%) and a very low false alarm rate: 0.05/h (Z. Zhang and Parhi, 2016) or 0/h (Mirowski et al., 2008). Such techniques, however, use numerous pre-engineered features, selected manually, for each patient, and require lots of resources (e.g., subject domain experts) and time. For example, Mirowski et al. (2008) used six different feature extraction methods and three machine learning algorithms. Z. Zhang and Parhi (2016) used 44 features and a set of 91 cost-sensitive linear SVM classifiers to search for the optimal single features or feature combinations that perform best for each patient. For both of these approaches, not only is the best combination of features and classifiers not known for each patient, but an optimal feature set and classifier may be suboptimal in the future because of the dynamic changes in the brain.

Because of the drawbacks of feature engineering techniques, a generalized approach for seizure prediction is highly beneficial. In this work, we use a convolutional neural network (CNN) for seizure prediction. The main contributions of this work are as follows: (1) we propose an efficient method to preprocess raw EEG data into a form suitable for a CNN; (2) we propose a guideline to help the CNN perform well with the seizure prediction task with minimum feature engineering; and (3) we provide an algorithm that works well across multiple datasets; namely, the Freiburg Hospital dataset (University of Freiburg, 2003), the Boston Children’s Hospital (CHB)-MIT dataset (Shoeb, 2009), and the American Epilepsy Society Seizure Prediction Challenge (Kaggle) dataset (Kaggle, 2014a). The third main contribution will also reveal factors that describe (unrealistically) high performance of other seizure prediction methods. This confounder is mitigated here by the consideration of numerous datasets.

## 3.2 Dataset

Three datasets were used in this work: the Freiburg Hospital dataset (University of Freiburg, 2003), the CHB-MIT dataset (Shoeb, 2009), and the American Epilepsy

Society Seizure Prediction Challenge (Kaggle) dataset (Kaggle, 2014a). The three datasets are summarized in Table 3.1. The Freiburg Hospital dataset consists of intracranial EEG (iEEG) recordings of 21 patients with intractable epilepsy. Because of lack of availability of the dataset, we are able to use data from only 13 patients with 59 seizures and 311.4 interictal hours in total. A sampling rate of 256 Hz was used to record iEEG signals. In this dataset, there are six recording channels from six selected contacts, where three of them are from epileptogenic regions and the other three are from the remote regions. For each patient, there is at least 50 min of preictal data and 24 h of interictal data.

Table 3.1: Summary of the three datasets used in this work.

Dataset	EEG type	No. of patients	No. of channels	No. of seizures	Interictal hours
Freiburg Hospital	Intracranial	13 patients	6	59	311.4
Boston Children’s Hospital–MIT	Scalp	13 patients	22	64	209
American Epilepsy Society Seizure Prediction Challenge (Kaggle)	Intracranial	5 dogs, 2 patients	16	48	627.7

The CHB-MIT dataset contains scalp EEG (sEEG) data from 23 pediatric patients with 844 h of continuous sEEG recording and 163 seizures. The sEEG signals were captured with the use of 22 electrodes at a sampling rate of 256 Hz (Shoeb, 2009). We define interictal periods as being between at least 4 h before seizure onset and 4 h after seizure ends. In this dataset, there are cases where multiple seizures occur close to each other. For the seizure prediction task, we are interested in predicting the leading seizures. Therefore for seizures that are less than 30 min from the previous seizure, we consider them as only one seizure and use the onset of the leading seizure as the onset of the combined seizure. Besides, we consider only patients with fewer than 10 seizures per day for the prediction task because it is not very critical to perform the task for patients having a seizure every 2 h on average. With these definitions and considerations, there are 13 patients with sufficient data (at least three leading seizures and 3 h of interictal recording) that consists of 64 leading seizures and 209 interictal hours in total.

The American Epilepsy Society Seizure Prediction Challenge dataset has iEEG data from five dogs and two patients with 48 seizures and 627.7 h of interictal recording (Kaggle, 2014a). Intracranial EEG (iEEG) canine data were recorded from 16 implanted electrodes with a sampling rate of 400 Hz. Recorded iEEG data from the two patients were from 15 depth electrodes (patient 1) and 24 subdural electrodes (patient 2) at a sampling rate of 5 kHz. Preictal and interictal 10-min segments were extracted by the

organizers. Specifically, for each lead seizure, six preictal segments were extracted from 66 min to 5 min before seizure onset with 10 s apart. Interictal segments were randomly selected at least one week from any seizure.

## 3.3 Proposed method

### 3.3.1 Preprocessing

Since a two-dimensional CNN is used in this work, it is necessary to convert raw EEG data into a matrix (i.e., image-like format). The conversion must be able to keep the most important information from the EEG signals. Wavelet and Fourier transforms are commonly used to convert time-series EEG signals into image shape (Kaggle, 2014a; Khan et al., 2018). They are also used as an effective feature extraction method for seizure detection and prediction. In this work, we use the short-time Fourier transform (STFT) and apply  $\log_{10}$  on the amplitudes to translate raw EEG signals into a two-dimensional matrix composed of frequency and time axes. We use an EEG window length of 30 s. Most of the EEG recordings were contaminated by power line noise at 50 Hz (see Fig. 3.1a) for the Freiburg Hospital dataset and 60 Hz for the CHB-MIT dataset. In the frequency domain, it is convenient to effectively remove the power line noise by excluding components in the frequency ranges of 47–53 Hz and 97–103 Hz for a power line frequency of 50 Hz and components in the frequency ranges of 57–63 Hz and 117–123 Hz for a power line frequency of 60 Hz. The DC component (at 0 Hz) was also removed. Fig. 3.1b shows the STFT of a 30-s window after removal of power line noise.

One challenge in many classification tasks is the imbalance of the dataset; that is, more instances in one class than in others (Branco et al., 2016). Seizure prediction also encounters this issue; for example, in the Freiburg Hospital dataset, the interictal-to-preictal ratio per patient ranges from 9.5:1 to 15.9:1. To overcome this, we generate more preictal segments by using an overlapped sampling technique during the training phase. We adopt the idea of data augmentation in computer vision where images are shifted and rotated by small amounts to generate more samples. This data augmentation helps the deep learning models to be more robust with input variation. In particular, we create extra preictal samples for training by sliding a 30-s window along the time axis at every step  $S$  over preictal time-series EEG signals (see Fig. 3.2).  $S$  is chosen per subject so that we have a similar number of samples per class (preictal or interictal) in the training set. The chosen  $S$  value for each patient is provided in Table 3.2.

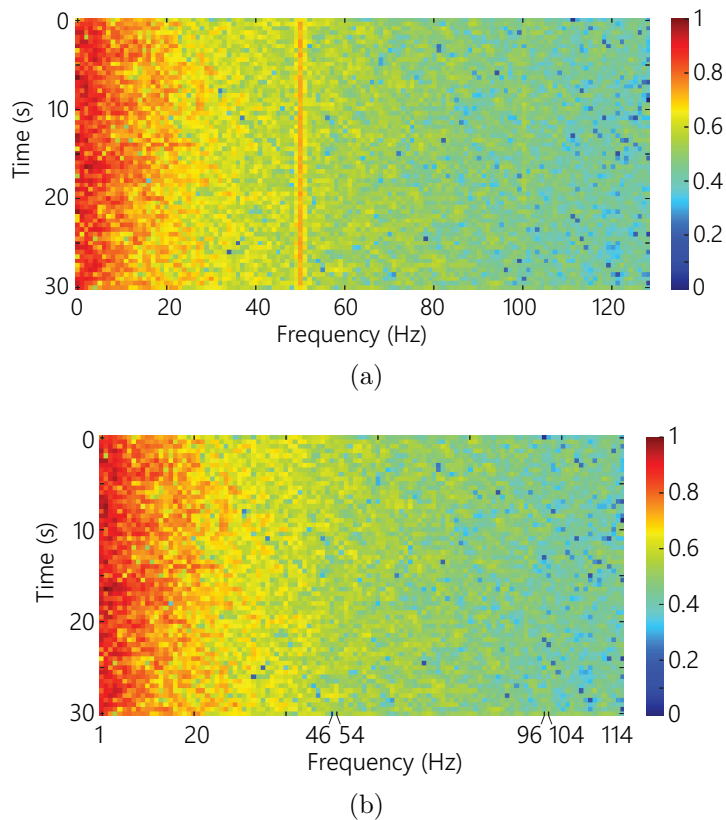


Figure 3.1: (a) Example spectrogram of a 30-s window. (b) Same window after removal of power line noise.

### 3.3.2 Convolutional neural network

CNNs have been used extensively for computer vision and natural language processing (Krizhevsky et al., 2012; Sainath et al., 2013). In this work, we use a CNN with three convolution blocks as described in Fig. 3.3. Each convolution block consists of a batch normalization, a convolution layer with a rectified linear unit activation function, and a max-pooling layer. The batch normalization ensures the inputs to the convolution layer have zero mean and unit variance. As we desire to capture the correlation across channels, we design a three-dimension kernel so that one dimension covers all the channels and the other two extract time and frequency information. Specifically, the first convolution layer has sixteen  $n \times 5 \times 5$  kernels, where  $n$  is the number of EEG channels, with stride of  $1 \times 2 \times 2$ . For the rest of the network, we keep it simple by using typical configuration for convolutional layers. Particularly, the next two convolution blocks have 32 and 64 convolution kernels, respectively, and both have a kernel size of

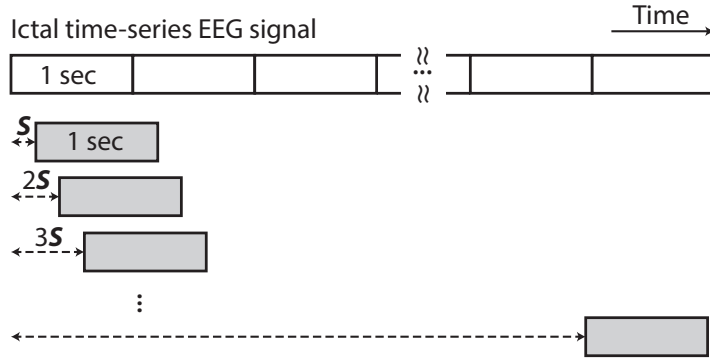


Figure 3.2: Generate extra preictal segments to balance the training dataset by sliding a 30-s window along the time axis at every step  $S$  over preictal signals.  $S$  is chosen per subject so that there are a similar number of samples per class (preictal or interictal) in the training set.

$3 \times 3$ , stride of  $1 \times 1$ , and max-pooling over a  $2 \times 2$  region. Following the three convolution blocks are two fully connected layers with sigmoid activation and output sizes of 256 and 2, respectively. The former fully connected layer uses a sigmoid activation function, while the latter uses a soft-max activation function. Both of the fully connected layers have a dropout rate of 0.5. Our model is implemented in Python 2.7 with the use of Keras 2.0 with a Tensorflow 1.4.0 backend. The model was configured to run in parallel on four NVIDIA K80 graphics cards.

Because of the limited available datasets, it is important to prevent the CNN from overfitting the data. First, we keep the CNN architecture simple and shallow as described above (Ba and Caruana, 2014). Second, we propose an approach to prevent overfitting during the training of the neural network. A common practice is to randomly split 20% of the training set for use as a validation set. After each training epoch, a loss and/or accuracy is calculated with respect to the validation set to check if the network starts to overfit the training set. This approach works well with datasets where time information is not involved (e.g., images for the classification task). For seizure prediction, we need to use samples from a period different from that of those during training to monitor if the model starts to overfit the data. In this work, we select 25% of later samples from preictal and interictal recordings in the training set for monitoring and the rest for training (see Fig. 3.4).

Table 3.2: The chosen  $S$  value for each patient.

(a) Freiburg Hospital		(b) CHB-MIT	
Subject	$S$ (seconds)	Subject	$S$ (seconds)
Pat1	2.7	Pat1	7.5
Pat3	3.6	Pat2	2.4
Pat5	3.6	Pat3	4.5
Pat6	2.1	Pat5	7.2
Pat13	1.5	Pat9	1.3
Pat14	2.9	Pat10	4.5
Pat15	2.7	Pat13	7.2
Pat16	3.6	Pat14	30
Pat17	3.6	Pat18	3.6
Pat18	3.6	Pat19	2
Pat19	2.7	Pat20	5.1
Pat20	3.6	Pat21	3
Pat21	3.6	Pat23	7.5

### 3.3.3 Postprocessing

It is common to have isolated false positives during interictal periods. These isolated false predictions can be effectively reduced by use of a discrete-time Kalman filter (Park et al., 2011). In this work, we propose a simple method, called  $k$ -of- $n$ , in which an alarm is set only if at least  $k$  predictions among the last  $n$  predictions were positive. Our experiments showed that  $k = 8$  and  $n = 10$  are good choices for the purpose of efficient prediction. This means that if during the last 300 s at least 240 s led to a positive prediction, then the alarm is set. Because of the postprocessing, the prediction latency of the proposed method is 5 minutes which is reasonable given that the SOP is 30 minutes.

### 3.3.4 System evaluation

The seizure prediction horizon (SPH) and seizure occurrence period (SOP) need to be defined before performance metrics such as sensitivity and FPR are estimated. In this work, we follow the definitions of the SOP and SPH proposed by Maiwald et al. (2004) (see Fig. 3.5). The SOP is the interval where the seizure is expected to occur. The period between the alarm and the beginning of the SOP is the SPH. For a correct prediction, a seizure onset must be after the SPH and within the SOP. Likewise, a false alarm occurs when the prediction system returns a positive result but no seizure occurs during the

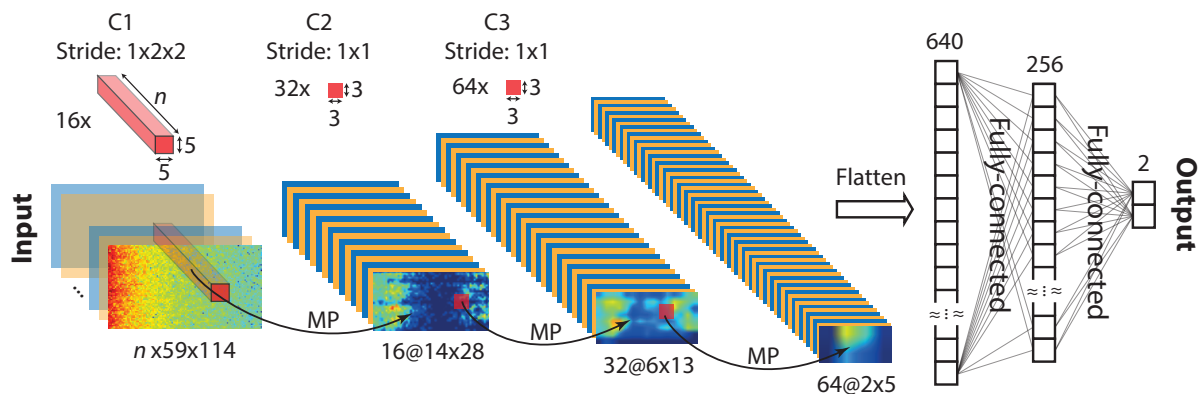


Figure 3.3: Convolutional neural network architecture. This illustration is applied to the Freiburg Hospital and Boston Children’s Hospital–MIT datasets. For the American Epilepsy Society Seizure Prediction Challenge dataset, the feature sizes are different because of the different recording sampling rate. Short-time Fourier transforms of 30-s windows of raw EEG signals are input. There are three convolution blocks, named  $C1$ ,  $C2$ , and  $C3$ . Each block consists of a batch normalization, a convolution layer with a rectified linear unit (ReLU) activation function, and a max-pooling layer. For simplicity, max-pooling layers are not shown and are noted as  $MP$ . For  $C1$ , there are 16  $n \times 5 \times 5$  kernels, where  $n$  is the number of EEG channels, with stride of  $1 \times 2 \times 2$ . ReLU activation is applied on convolution results before they are subsampled by a max-pooling over a  $1 \times 2 \times 2$  region. The same steps are applied in  $C2$  and  $C3$  except the convolution kernel size is  $3 \times 3$ , stride is  $1 \times 1$ , and max-pooling size is  $2 \times 2$ . Blocks  $C2$  and  $C3$  have 32 and 64 convolution kernels, respectively. Features extracted by the three convolution blocks are flattened and connected to two fully connected layers with output sizes of 256 and 2, respectively. The former fully connected layer uses a sigmoid activation function, while the latter uses a soft-max activation function. Both of the fully connected layers have a dropout rate of 0.5.

SOP. When an alarm occurs, it will last until the end of the SOP. Sensitivity is defined as the percentage of seizures correctly predicted divided by the total number of seizures. The FPR is defined as the number of false alarms per hour.

Regarding clinical use, the SPH must be long enough to allow sufficient intervention or precautions (SPH is also called *intervention time*; (Bou Assi et al., 2017)). In contrast, the SOP should be not too long to reduce the patient’s anxiety. Inconsistency in defining the SPH and SOP makes the benchmarking among methods difficult and confusing. Park et al. (2011) reported using an SPH of 30 min, but from their explanation what they were implicitly using was an SPH of 0 min and an SOP of 30 min (i.e., if an alarm occurs at any point within 30 min before seizure onset, it is considered a successful prediction).



Figure 3.4: Practice to prevent the convolutional neural network from overfitting the data during training. Twenty-five percent of later samples (diagonal lines) from preictal and interictal recordings in the training dataset are used for monitoring and the rest are used for training.

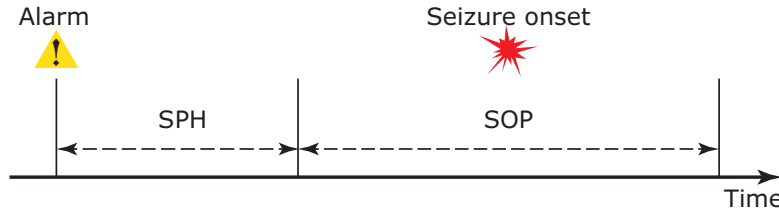


Figure 3.5: Definition of the seizure occurrence period (SOP) and the seizure prediction horizon (SPH). For a correct prediction, a seizure onset must be after the SPH and within the SOP.

Similarly, Z. Zhang and Parhi (2016) provided a different definition of the SPH: the interval between the alarm and seizure onset.

The metrics used to test the proposed approach are sensitivity and FPR with an SPH of 5 min and an SOP of 30 min. To have a robust evaluation, we follow a leave-one-out cross-validation approach for each subject. If a subject has  $N$  seizures,  $(N - 1)$  seizures will be used for training, and the remaining seizure will be used for validation. This round is done  $N$  times, so all seizures will be used for validation exactly once. Interictal segments are randomly split into  $N$  parts.  $(N - 1)$  parts are used for training and the remaining part is used for validation. The  $(N - 1)$  parts are further split into monitoring and training sets to prevent overfitting as depicted in Fig. 3.4.

We also compare the prediction performance of our approach with that of an unspecific random predictor. Given an FPR, the probability to raise an alarm in an SOP can be approximated by Schelter et al. (2006)

$$P \approx 1 - e^{-\text{FPR} \cdot \text{SOP}} . \quad (3.1)$$

Therefore the probability of predicting at least  $m$  of  $M$  independent seizures by chance is given by

$$p = \sum_{i \geq m} \binom{M}{i} P^i (1 - P)^{M-i} . \quad (3.2)$$

We calculated  $p$  for each patient by using the FPR of that patient and the number of seizures ( $m$ ) predicted by our method. If  $p$  is less than 0.05, we can conclude that our prediction method is significantly better than a random predictor at a significance level of 0.05.

### 3.4 Results

In this section, we test our approach with three datasets: (1) the Freiburg Hospital iEEG dataset, (2) the CHB-MIT sEEG dataset, and (3) the American Epilepsy Society Seizure Prediction Challenge iEEG dataset. An SOP of 30 min and an SPH of 5 min were used in our calculating all metrics in this work. Each fold of the leave-one-out cross-validation was executed twice, and average results with standard deviations were reported. Table 6.1 summarizes the seizure prediction results for the Freiburg Hospital iEEG dataset. Prediction sensitivity is 81.4% (i.e., 48 of 59 seizures are successfully predicted). The FPR is very low at 0.06/h. Our method achieves a similar sensitivity of 81.2% on the CHB-MIT sEEG dataset but with a higher FPR of 0.16/h (see Table 6.2). This is reasonable since sEEG recordings tend to be noisier than sEEG onset. For the American Epilepsy Society Seizure Prediction Challenge dataset, the overall sensitivity is 75% and FPR is 0.21/h (see Table 3.5). It is important to note that our approach works comparably with both iEEG and sEEG recordings without any denoising techniques except power line noise removal.

Table 3.6 demonstrates a benchmark of recent seizure prediction approaches and this work. It is complicated to tell which approach is the best because each approach was tested with one dataset that is limited in the amount of data. In other words, one approach may perform well on one dataset and poorly on another. Therefore we added an extra indicator on whether the same feature engineering or feature set is applied across all patients to evaluate generalization of each method. From a clinical perspective, it is desirable to have a long enough SPH to allow effective therapeutic intervention and/or precautions. The SOP, however, should be short to minimize the patient’s anxiety (Maiwald et al., 2004). Some studies that implicitly used zero SPH disregarded clinical considerations, and hence could have overestimated the prediction

Table 3.3: Seizure prediction results obtained with the Freiburg Hospital interictal EEG dataset. The model was executed twice, and average results with standard deviations were reported. The seizure occurrence period (SOP) was 30 min and the seizure prediction horizon (SPH) was 5 min. The  $p$  value was calculated for the worst case for each patient; that is, with minimum sensitivity and maximum false prediction rate (FPR). Our seizure prediction approach achieves significantly better performance than an unspecific random predictor for all patients except Pat14, where the convolutional neural network results are only marginally better than the random predictor’s.

Patient	No. of seizures	Interictal hours	Sensitivity (%)	FPR (/h)	$p$
Pat1	4	23.9	100 ± 0.0	0.00 ± 0.00	< 0.001
Pat3	5	23.9	100 ± 0.0	0.00 ± 0.00	< 0.001
Pat4	5	23.9	100 ± 0.0	0.00 ± 0.00	< 0.001
Pat5	5	23.9	40 ± 0.0	0.13 ± 0.00	0.032
Pat6	3	23.8	100 ± 0.0	0.00 ± 0.00	< 0.001
Pat14	4	22.6	50 ± 0.0	0.27 ± 0.00	0.078
Pat15	4	23.7	100 ± 0.0	0.02 ± 0.02	< 0.001
Pat16	5	23.9	80 ± 0.0	0.17 ± 0.13	0.001
Pat17	5	24	80 ± 0.0	0.00 ± 0.00	< 0.001
Pat18	5	24.8	100 ± 0.0	0.00 ± 0.00	< 0.001
Pat19	4	24.3	50 ± 0.0	0.16 ± 0.00	0.033
Pat20	5	24.8	60 ± 0.0	0.04 ± 0.00	< 0.001
Pat21	5	23.9	100 ± 0.0	0.00 ± 0.00	< 0.001
Total	59	311.4	81.4 ± 0.0	0.06 ± 0.00	

Table 3.4: Seizure prediction results obtained with the Boston Children’s Hospital–MIT scalp EEG dataset. The model was executed twice, and average results with standard deviations were reported. The seizure occurrence period (SOP) was 30 min and the seizure prediction horizon (SPH) was 5 min. The  $p$  value was calculated for the worst case for each patient; that is, with minimum sensitivity and maximum false prediction rate (FPR). Our seizure prediction approach achieves significantly better performance than an unspecific random predictor for all patients except Pat9, where the convolutional neural network results are only marginally better than the random predictor’s.

Patient	No. of seizures	Interictal hours	Sensitivity (%)	FPR (/h)	$p$
Pat1	7	17	$85.7 \pm 0.0$	$0.24 \pm 0.00$	$< 0.001$
Pat2	3	22.9	$33.3 \pm 0.0$	$0.00 \pm 0.00$	$< 0.001$
Pat3	6	21.9	$100 \pm 0.0$	$0.18 \pm 0.00$	$< 0.001$
Pat5	5	13	$80 \pm 20$	$0.19 \pm 0.03$	0.010
Pat9	4	12.3	$50 \pm 0.0$	$0.12 \pm 0.12$	0.067
Pat10	6	11.1	$33.3 \pm 0.0$	$0.00 \pm 0.00$	0.025
Pat13	5	14	$80 \pm 0.0$	$0.14 \pm 0.00$	$< 0.001$
Pat14	5	5	$80 \pm 0.0$	$0.40 \pm 0.00$	0.004
Pat18	6	23	$100 \pm 0.0$	$0.28 \pm 0.02$	$< 0.001$
Pat19	3	24.9	$100 \pm 0.0$	$0.00 \pm 0.00$	$< 0.001$
Pat20	5	20	$100 \pm 0.0$	$0.25 \pm 0.05$	$< 0.001$
Pat21	4	20.9	$100 \pm 0.0$	$0.23 \pm 0.09$	$< 0.001$
Pat23	5	3	$100 \pm 0.0$	$0.33 \pm 0.00$	$< 0.001$
Total	64	209	$81.2 \pm 1.5$	$0.16 \pm 0.00$	

Table 3.5: Seizure prediction results obtained with the American Epilepsy Society Seizure Prediction Challenge dataset. The model was executed twice, and average results with standard deviations were reported. The seizure occurrence period (SOP) was 30 min and the seizure prediction horizon (SPH) was 5 min. The  $p$  value was calculated for the worst case for each participant; that is, with minimum sensitivity and maximum false prediction rate (FPR). Our seizure prediction approach achieves significantly better performance than an unspecific random predictor for four of five dogs and for Pat1.

Participant	No. of seizures	Interictal hours	Sensitivity (%)	FPR (/h)	$p$
Dog1	4	80	$50 \pm 0.0$	$0.19 \pm 0.02$	0.053
Dog2	7	83.3	$100 \pm 0.0$	$0.04 \pm 0.03$	< 0.001
Dog3	12	240	$58.3 \pm 0.0$	$0.14 \pm 0.09$	< 0.001
Dog4	14	134	$78.6 \pm 0.0$	$0.48 \pm 0.07$	< 0.001
Dog5	5	75	$80 \pm 0.0$	$0.08 \pm 0.01$	< 0.001
Pat1	3	8.3	$100 \pm 0.0$	$0.42 \pm 0.06$	0.009
Pat2	3	7	$66.7 \pm 0.0$	$0.86 \pm 0.00$	0.693
Total	48	627.7	$75 \pm 0.0$	$0.21 \pm 0.04$	

accuracy. The approach proposed by Park et al. (2011) achieved a very high sensitivity of 98.3% and FPR of 0.29/h in testing with 18 patients from the Freiburg Hospital dataset. Our method yields a lower sensitivity of 81.4% but a much better FPR of 0.06/h. It is nontrivial to note that the SPH was implicitly set to zero, which means prediction at a time close to or at seizure onset can be counted as a successful prediction. Likewise, research conducted by Z. Zhang and Parhi (2016) and Parvez and Paul (2017) also implied the use of zero SPH, which will not be compared directly with our results. Among the rest of the studies listed in Table 3.6, Eftekhari et al. (2014) reported a very good prediction sensitivity of 90.95% and a low FPR of 0.06/h for an SOP of 20 min and an SPH of 10 min. They fine-tuned the feature set for each patient to achieve the maximum performance. This, however, leads to the need for adequate expertise and time to perform the feature engineering for a new dataset. Sharif and Jafari (2017) applied the same set of features to all patients and performed classification using an SVM. This approach achieved a high sensitivity of 91.8–96.6% and a low FPR of 0.05–0.08 in testing with the Freiburg Hospital iEEG dataset. However, no studies have reported the successful use of a similar approach on sEEG signals.

Table 3.6: Benchmarking of recent seizure prediction approaches and this work

Year	Authors	Dataset	Feature	Classifier	Same FE <sup>a</sup>	No. of seizures	Sensitivity (%)	FPR (/h)	SOP	SPH
2004	(Maiwald et al., 2004)	FB, 21 patients	Dynamical similarity index	Threshold crossing	Yes	88	42	< 0.15	30 min	2 min
2006	(Winterhalder et al., 2006)	FB, 21 patients	Phase coherence, lag synchronization	Threshold crossing	No	88	60	0.15	30 min	10 min
2011	(Park et al., 2011)	FB, 18 patients	Univariate spectral power	SVM	Yes	80	98.3	0.29	30 min	0 <sup>b</sup>
2013	(S. Li et al., 2013)	FB, 21 patients	Spike rate	Threshold crossing	Yes	87	72.7	0.11	50 min	10 s
2014	(Zheng et al., 2014)	FB, 10 patients	Mean phase coherence	Threshold crossing	No	50	> 70	< 0.15	30 min	10 min
2014	(Eftekhar et al., 2014)	FB, 21 patients	Multiresolution $N$ -gram	Threshold crossing	No	87	90.95	0.06	20 min	10 min
2014	(Aarabi and He, 2014)	FB, 21 patients	Bayesian inversion of power spectral density	Rule-based decision	Yes	87	87.07	0.20	30 min	10 s
2016	(Z. Zhang and Parhi, 2016)	FB, 18 patients	Power spectral density ratio	SVM	No	80	100	0.03	50 min	0 <sup>b</sup>
2016	(Z. Zhang and Parhi, 2016)	MIT, 17 patients	Power spectral density ratio	SVM	No	76	98.68	0.05	50 min	0 <sup>b</sup>
2017	(Parvez and Paul, 2017)	FB, 21 patients	Phase-match error, deviation, fluctuation	LS-SVM	Yes	87	95.4	0.36	30 min	0 <sup>b</sup>
2017	(Sharif and Jafari, 2017)	FB, 19 patients	Fuzzy rules on Poincaré plane	SVM	Yes	83	91.8–96.6	0.05–0.08	15min	2–42 min
2017	(Aarabi and He, 2017)	FB, 10 patients	Univariate and bivariate features	Rule-based decision	Yes	28	86.7	0.126	30 min	10 s
2017	(Khan et al., 2018)	MIT, MSSM	Wavelet transform	CNN	Yes	131	87.8	0.14	10 min	0 <sup>b</sup>
2017	This work	FB, 13 patients	Short-time Fourier transform	CNN	Yes	59	81.4	0.06	30 min	5 min
2017	This work	MIT, 13 patients	Short-time Fourier transform	CNN	Yes	64	81.2	0.16	30 min	5 min
2017	This work	Kaggle <sup>c</sup> , 5 dogs, 2 patients	Short-time Fourier transform	CNN	Yes	48	75	0.21	30 min	5 min

CNN, convolutional neural network, FB, Freiburg Hospital intracranial EEG dataset; FE, feature engineering; FPR, false prediction rate; LS, least squares; MIT, Massachusetts Institute of Technology scalp EEG dataset; MSSM, Mount Sinai Hospital dataset (intracranial EEG); SPH, seizure prediction horizon; SOP, seizure occurrence period; SVM, support vector machine.

<sup>a</sup>Same FE across all patients. “No” means feature engineering is tailored for each patient.

<sup>b</sup>The authors implicitly used zero SPH and disregarded clinical considerations, and hence the results could be overestimated.

<sup>c</sup>American Epilepsy Society Seizure Prediction Challenge dataset (intracranial EEG).

## 3.5 Discussion

Information extracted from EEG signals in frequency and time (synchronization) domains has been used widely to predict seizures. We proposed a novel way to exploit both frequency and time aspects of EEG signals without handcrafted feature engineering. The STFT of an EEG window has two dimensions; namely, the frequency and the time. A two-dimensional convolution filter was slid throughout the STFT to collect the changes in both the frequency and the time of EEG signals. The filter weights are automatically adjusted during the training phase and the CNN acts like a feature extraction method in an automatic fashion.

In the work proposed by Khan et al. (2018), continuous wavelet transform (CWT) was used as a preprocessing step and the wavelet transform of raw EEG signals was used as input to a CNN. In this section, we implement the same CWT and compare it with the STFT in terms of seizure prediction performance. Following Khan et al. (2018), we apply a set of ten scales from  $2^0$  to  $2^9$  and the Mexican-hat mother wavelet, then downsample the time axis of the wavelet transform so that the final dimension is  $n \times 10 \times 128$ . Here we use the area under the receiver operating characteristic curve (AUC) as a comparison criterion instead of sensitivity and FPR. The AUC is a threshold-free metric, so it can be used to directly compare the performance of different methods. The results are illustrated in Fig. 3.6. With the use of the Wilcoxon signed-rank test on the three datasets with a significance level of 0.05, the STFT is significantly better than the CWT, with  $p = 0.0135$ .

We used the oversampling technique to overcome the imbalance of the datasets. Cost-sensitive learning has been used widely in the literature for the same purpose (Branco et al., 2016). We applied cost-sensitive learning by changing the cost function in a way that the misclassification cost of preictal samples is multiplied by the ratio of interictal samples to preictal samples for each patient. We used STFT as the preprocessing step for cost-sensitive learning. The results are illustrated in Fig. 3.6. Although our oversampling technique does not result in a significant improvement as compared with cost-sensitive learning when applied on the three datasets, we argue that our oversampling technique is a more intuitive way to address the overfitting problem caused by the imbalance of time-series datasets.

Tables 6.1 and 6.2 show that our prediction method is significantly superior to an unspecific random predictor for all patients except Pat14 in the Freiburg Hospital dataset and Pat9 in the CHB-MIT dataset. It is worth remembering that the Freiburg Hospital dataset consists of iEEG recordings and the CHB-MIT dataset consists of

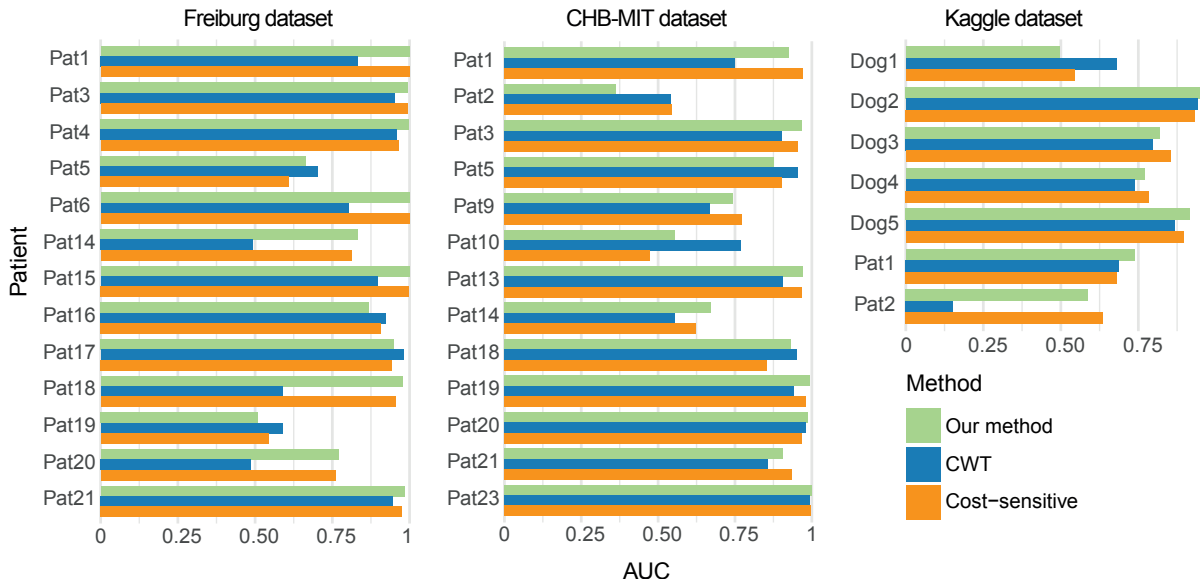


Figure 3.6: Comparison among our method, the preprocessing step using the continuous wavelet transform (CWT) (Khan et al., 2018), and cost-sensitive learning. AUC, area under the receiver operating characteristic curve; CHB, Boston Children’s Hospital.

sEEG recordings. In other words, our method works well with both types of EEG signals. Regarding the American Epilepsy Society Seizure Prediction Challenge dataset, our method results in significantly better performance than a random predictor for four of five dogs (see Table 3.5) and for Pat1. Note that the results above are collected by a retrospective analysis where the data is clean and all disruptions during recording are effectively removed. One may expect a degradation in performance when testing a prospective seizure prediction because of potential issues during EEG recording.

As seizure characteristics may change over time, calibration of the seizure prediction algorithm is necessary. Minimum feature engineering has a great advantage in that it does not require an expert to carefully extract and select the optimum features for the prediction task. Hence it allows faster and more frequent updates so that patients are able to benefit the most from the seizure prediction algorithm. Also, minimum feature engineering allows seizure prediction to be available to more patients. Since the feature extraction task is undertaken by the CNN, neurophysiologists and clinical staff can spend more time in monitoring and recording EEG signals for diagnostic purposes and/or training data collection.

Our method can be further improved by non-EEG data such as information on the time when seizures occur. Epileptic seizures have been shown to have biases in

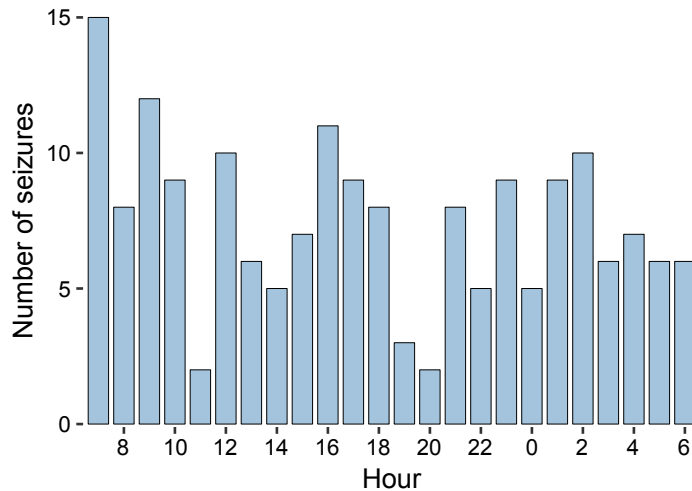


Figure 3.7: Number of seizures versus time of day across patients for the Boston Children’s Hospital—MIT dataset. Most seizures occur in the early morning. Two lower peaks occur around 4 p.m. and 2 a.m.

distribution over time at various intervals that can be as long as 1 year or as short as 1 h (Griffiths and Fox, 1938). Importantly, Griffiths and Fox (1938) showed that there were more incidences of seizure around sunrise, noon, and midnight in their dataset of 101 patients with 39,929 seizures. However, this pattern is patient specific. Adopting the same observation, P. J. Karoly et al. (2017) leveraged this pattern to significantly improve their seizure forecasting system. Unfortunately, the three datasets investigated in this article are not large enough to assess if the time of day information is useful because the maximum recording period per patient was 3 days. Nevertheless, it is still worth seeing how incidences of seizure are distributed over the day across patients in the CHB-MIT dataset, the only dataset from which we can access the time of seizure occurrence. On the basis of the CHB-MIT data, the greatest incidence occurs in the early morning, and there two lower peaks around 4 p.m. and 2 a.m. (see Fig. 3.7).

### 3.6 Conclusion

Seizure prediction capability has been studied and improved over the last four decades. A perfect prediction is not yet available, but with current prediction performance, it appears possible to provide patients with a warning so they can take some precautions for their safety. We proposed a novel approach of using CNNs with minimum feature engineering. The proposed approach showed its good generalization in working well

with both iEEG and sEEG data. This gives more patients the opportunity to possess a seizure prediction device that can help them have a more manageable life.

## **Acknowledgments**

This research was supported by Sydney Informatics Hub, funded by the University of Sydney. The authors appreciate the support of Benjamin H. Brinkmann from Mayo Systems Electrophysiology Laboratory for providing information on some unlabeled datasets. O. Kavehei acknowledges support provided by a 2018 Early Career Research grant from the Faculty of Engineering and Information Technology, University of Sydney. L. Kuhlmann acknowledges support from National Health and Medical Research Council project grants APP1065638 and APP1130468. N. Truong acknowledges partial financial support from the Commonwealth Scientific and Industrial Research Organisation via a PhD scholarship (PN 50041400). J. Yang acknowledges the National Natural Science Foundation of China for financial support under grant 61501332.

# Chapter 4

## Semi-supervised learning for seizure prediction

The content presented in this chapter is published as:

- Truong, N. D., L. Kuhlmann, M. R. Bonyadi, D. Querlioz, L. Zhou, and O. Kavehei (2019). “Epileptic Seizure Forecasting with Generative Adversarial Networks.” *IEEE Access* 7, 143999-144009. DOI:10.1109/ACCESS.2019.2944691.

### **Statement of Contributions of Joint Authorship**

- Nhan Duy Truong (Candidate): First author, completed the analysis, writing, reviewing and editing of the manuscript
- Levin Kuhlmann: aided in the analysis, reviewing and editing the manuscript
- Mohammad Reza Bonyadi: aided in the analysis, reviewing and editing the manuscript
- Damien Querlioz: aided in the analysis and reviewing the manuscript
- Luping Zhou (Auxiliary Supervisor): aided in the analysis, reviewing and editing the manuscript
- Omid Kavehei (Principal Supervisor): provided the main idea, reviewing and editing the manuscript

In addition to the statements above, in cases where I am not the corresponding author of a published item, permission to include the published material has been granted by the corresponding author.

Nhan Duy Truong

Date: 01 October 2019

As supervisor for the candidature upon which this thesis is based, I can confirm that the authorship attribution statements above are correct.

Dr. Omid Kavehei

Date: 01 October 2019

Many outstanding studies have reported promising results in seizure forecasting, one of the most challenging predictive data analysis problems. This is mainly because electroencephalogram (EEG) bio-signal intensity is very small, in  $\mu V$  range, and there are significant sensing difficulties given physiological and non-physiological artifacts. Today the process of accurate epileptic seizure identification and data labeling is done by neurologists. The current unpredictability of epileptic seizure activities together with the lack of reliable treatment for patients living with drug-resistant forms of epilepsy creates an urgency for research into accurate, sensitive and patient-specific seizure forecasting. Most seizure forecasting algorithms use only labeled data for training purposes. As the seizure data is labeled manually by neurologists, preparing the labeled data is expensive and time-consuming, making the best use of the data critical. In this article, we propose an approach that can make use of not only labeled EEG signals but also the unlabeled ones which are more accessible. We use the short-time Fourier transform on 28-s EEG windows as a pre-processing step. A generative adversarial network (GAN) is trained in an unsupervised manner where information of seizure onset is disregarded. The trained Discriminator of the GAN is then used as a feature extractor. Features generated by the feature extractor are classified by two fully-connected layers (can be replaced by any classifier) for the labeled EEG signals. This semi-supervised patient-specific seizure forecasting method achieves an out-of-sample testing area under the operating characteristic curve (AUC) of 77.68%, 75.47% and 65.05% for the CHB-MIT scalp EEG dataset, the Freiburg Hospital intracranial EEG dataset and the EPILEPSIAE dataset, respectively. Unsupervised training without the need for labeling is important because not only it can be performed in real-time during EEG signal recording, but also it does not require feature engineering effort for each patient. To the best of our knowledge, this is the first application of GAN to seizure forecasting.

## 4.1 Introduction

Epilepsy affects almost 1% of the global population and considerably impacts the quality of life of those patients diagnosed with the disease (Kuhlmann, Lehnertz, et al., 2018; R. S. Fisher et al., 2017; Kuhlmann, P. Karoly, et al., 2018). Over the past two decades, a tremendous number of techniques on predicting seizure has been proposed with promising performance. An early approach based on similarity, correlation, and energy of EEG signals achieved a modest sensitivity of 42% and a false prediction rate (FPR) less than 0.15/h tested with the Freiburg Hospital dataset (Maiwald et al., 2004). The performance improved with the use phase coherence and synchronization information

in EEG signals, resulting in sensitivity 60% and FPR of 0.15/h in (Winterhalder et al., 2006) and 95.4% and FPR of 0.36/h in (Parvez and Paul, 2017). A similar approach with additional features by combining bivariate empirical mode decomposition and Hilbert-based mean phase coherence improved sensitivity to over 70% and FPR to below 0.15/h (Zheng et al., 2014). Different from the methods above, Aarabi and He (2014) used Bayesian inversion of power spectral density and then applied a rule-based decision. Their method achieved a sensitivity of 87.07% and FPR of 0.2/h on the Freiburg Hospital dataset.

Advances in machine learning have enabled major improvements in computer vision, language processing and medical applications (Kuhlmann, P. Karoly, et al., 2018). Support vector machine (SVM) with frequency bands of the spectral energy as inputs further boosted the performance to 98.3% and FPR of 0.29/h (Park et al., 2011) and 98% and FPR less than 0.05/h (Z. Zhang and Parhi, 2016) tested with the Freiburg Hospital dataset. In another work, features of EEG signals were estimated on a Poincaré plane using 64 fuzzy rules (Sharif and Jafari, 2017). The features were processed with principal component analysis (PCA) to reduce dimension before being classified by an SVM. This approach achieved a high sensitivity of more than 91% and an FPR below 0.08/h on the Freiburg Hospital dataset. In our recent work (Truong, Nguyen, et al., 2018a), we showed that convolutional neural networks (CNNs) can be used as an effective seizure prediction method.

Note that all high-performance seizure forecasting algorithms were fully supervised; i.e., only labeled data were used for training. However, labeling seizure data is performed manually by neurologists and is an expensive and time-consuming task. There has been an increasing need to make use of unlabelled data with unsupervised feature learning such as clustering, Gaussian mixture models, Hidden Markov Models and autoencoders (Smart and Chen, 2015; Wen and Z. Zhang, 2018). Most of these unsupervised learning techniques have been applied to seizure detection and achieved high sensitivity and specificity (Bizopoulos et al., 2013; Supratak et al., 2014; Smart and Chen, 2015). However, there are few works successfully applying unsupervised learning in the seizure forecasting context. Hosseini et al. (2017) trained unsupervised stacked autoencoders (SAE) then optimized the SAE’s features with principal component analysis, independent component analysis, and differential search algorithm. These features were combined with engineered features from a priori knowledge before being classified by an SVM. This approach achieved a sensitivity of 95% and FPR of 0.06/h tested with a dataset of two epilepsy patients developed and released by the University of Pennsylvania and the Mayo Clinic. In another work, a deep convolutional autoencoder

was used as an unsupervised feature extractor (Abdelhameed and Bayoumi, 2018). The extracted features were fed to a bidirectional long-short term memory (Bi-LSTM) to perform the seizure prediction task. This method was tested with the CHB-MIT dataset with a sensitivity of 94.6% and an FPR of 0.04/h.

In this work, we exploit a deep convolutional generative adversarial network (GAN) (Radford et al., 2015) as an unsupervised technique to extract features from unlabeled EEG signals that can be used for seizure forecasting task. The extracted features can be classified by any classifier (a neural network with two fully-connected layers in this work). The structure of this article is as follows. We first introduce the datasets being used in this work. Next, we describe how EEG signals are pre-processed. Then we provide details on GAN and how it can be used as a feature extractor for seizure forecasting. Lastly, we evaluate our approach and discuss the results on three datasets. A preliminary version of this work has been reported by Truong, Zhou, et al. (2019). The contribution of this work includes:

- Confirming unsupervised feature learning using GAN for seizure forecasting is generalizable across multiple epilepsy EEG datasets,
- Bridging the gap between supervised and semi-supervised approaches,
- Linking patient-specific characteristics to seizure forecasting performance.

## 4.2 Dataset

Table 4.1 summarizes the three datasets being used in this work: the CHB-MIT dataset (Shoeb, 2009), the Freiburg Hospital dataset (University of Freiburg, 2003), and the EPILEPSIAE dataset (Klatt et al., 2012). The CHB-MIT dataset contains scalp EEG (sEEG) data of 23 pediatric patients with 844 hours of continuous sEEG recording and 163 seizures. Scalp EEG signals were captured using 22 electrodes at a sampling rate of 256 Hz (Shoeb, 2009). We define interictal periods that are at least 4 h away before seizure onset and after the seizure ends. In this dataset, there are cases that multiple seizures occur close to each other. For the seizure forecasting task, we are interested in predicting the leading seizures. Therefore, for seizures that are less than 30 min away from the previous one, we consider them as only one seizure and use the onset of leading seizure as the onset of the combined seizure. Besides, we only consider patients with less than 10 seizures a day for the prediction task because it is not very critical to perform

the task for patients having a seizure every 2 hours on average. With the above definition and consideration, there are 13 patients with sufficient data (at least 3 leading seizures and 3 interictal hours) that is consisted of 64 leading seizures and 209 interictal hours in total.

The Freiburg Hospital dataset consists of intracranial EEG (iEEG) recordings of 21 patients with intractable epilepsy. Due to the lack of availability of the dataset, we are only able to use data from 13 patients with 59 seizures and 311.4 interictal hours. A sampling rate of 256 Hz was used to record iEEG signals. In this dataset, there are 6 recording channels from 6 selected contacts where three of them are from epileptogenic regions, and the other three are from the remote regions. For each patient, there are at least 50 min preictal data and 24 h of interictal. More details about Freiburg dataset can be found in (Maiwald et al., 2004).

EPILEPSIAE is the largest epilepsy database that contains EEG data from 275 patients (Klatt et al., 2012). In this work, we analyze scalp EEG of 30 patients with 261 leading seizures and 2881.4 interictal hours in total. The time-series EEG signals were recorded at a sampling rate of 256 Hz and from 19 electrodes. Seizure onset information obtained by two methods, namely EEG based and video analysis, is provided. In our study, we use seizure onset information using EEG based technique where the onsets were determined by visual inspection of EEG signals performed by an experienced clinician (Klatt et al., 2012).

Table 4.1: Summary of the three datasets used in this work.

Dataset	EEG type	No. of patients	No. of channels	No. of seizures*	Interictal hours
Freiburg	intracranial	13	6	59	311.4
CHB-MIT	scalp	13	22	64	209
EPILEPSIAE	scalp	30	19	261	2881.4

\* We are considering leading seizures only. Seizures that are less than 30 min away from the previous one are considered as one seizure only, and the onset of leading seizure is used as the onset of the combined seizure.

## 4.3 Proposed Method

### 4.3.1 Pre-processing

Since we will use a Generative Neural Network (GAN) architecture with three de-convolution layers, dimensions of GAN’s input must be divisible by  $2^3$ , except the

number of channels. Specific to the CHB-MIT dataset, some patients have less than 22 channels of recording EEG due to changes in electrodes. Particularly, Pat13 and Pat17 have only 17 available channels; Pat4, Pat9 have 20, 21 channels, respectively. Since we are interested in whether GAN can be effectively trained with non-patient specific data, all patients must have the same number of channels so that data from all patients can be combined. We follow the approach proposed by Truong, Kuhlmann, et al. (2017) to select 16 channels for each patient in CHB-MIT dataset. With regards to CHB-MIT and Freiburg datasets, we use Short-Time Fourier Transform (STFT) to translate 28 seconds of time-series EEG signal into a two-dimensional matrix comprised of frequency and time axes. For the STFT, we use cosine window of 1-second length and 50% overlap. Most of EEG recordings were contaminated by power line noise at 60 Hz (see Fig. 4.1a) for CHB-MIT dataset and 50 Hz for Freiburg dataset. The power line noise can be removed by excluding components at the frequency range of 47–53 Hz and 97–103 Hz if the power frequency is 50 Hz and components at the frequency range of 57–63 Hz and 117–123 Hz for the power line frequency of 60 Hz. The DC component (at 0 Hz) was also removed. Fig. 4.1b shows the STFT of a 28-s window after removing power line noise. We also trim components at the last two frequencies 127–128 Hz to have the final dimension of each pre-processed 28 s be  $(\text{number-of-channels} \times X \times Y) = (n \times 56 \times 112)$ , where  $X$  and  $Y$  are time and frequency dimensions, respectively.  $n$  is 16, 6, 19 for the CHB-MIT dataset, the Freiburg Hosiptal dataset and the EPIELEPSIA dataset, respectively.

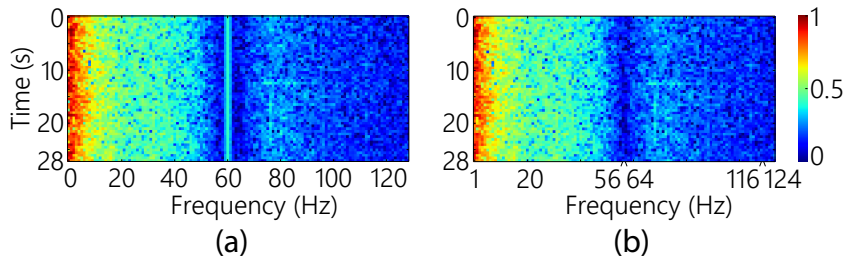


Figure 4.1: (a) Example spectrogram of a 28-second window. (b) Spectrogram of the same window after removing power line noise.

### 4.3.2 Adversarial Neural Network

In this work, we use a Deep Convolutional Generative Adversarial Network (DCGAN) (Radford et al., 2015) as depicted in Fig. 4.2 as an unsupervised feature extraction technique. Note that here we explain for the CHB-MIT dataset. The same explanation is applied to the other two datasets with the change in input dimension as mentioned in

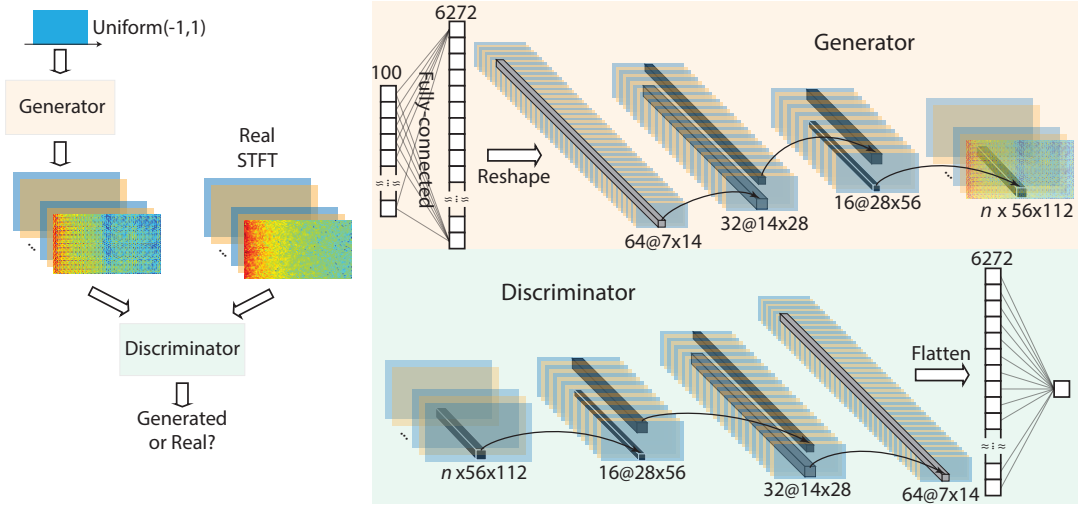


Figure 4.2: The Generator takes a random sample of 100 data points from a uniform distribution  $\mathcal{U}(-1, 1)$  as input. The input is fully-connected with a hidden layer with the output size of 6272 which is then reshaped to  $64 \times 7 \times 14$ . The hidden layer is followed by three de-convolution layers with filter size  $5 \times 5$ , stride  $2 \times 2$ . The numbers of filters of the three de-convolution layers are 32, 16 and  $n$ , respectively. The Discriminator consists of three convolution layers with filter size  $5 \times 5$ , stride  $2 \times 2$ . The numbers of filters of the three convolution layers are 16, 32 and 64, respectively.

Section 4.3.1. The Generator takes a 100 dimensional sample from a uniform distribution  $\mathcal{U}(-1, 1)$  as input. The input is fully-connected with a hidden layer with the output size of 6272 which is then reshaped to  $64 \times 7 \times 14$ . The hidden layer is followed by three de-convolution layers with filter size  $5 \times 5$ , stride  $2 \times 2$ . The number of filters of the three de-convolution layers are 32, 16 and  $n$ , respectively. Outputs of the Generator have the same dimension with STFT of 28 seconds EEG signals. The Discriminator, on the other hand, is configured to discriminate the generated EEG signals from the original ones. The Discriminator consists of three convolution layers with filter size  $5 \times 5$ , stride  $2 \times 2$ . Note that the choice of convolution filter size in both convolution and de-convolution layers is based on the CNN architecture reported by Truong, Nguyen, et al. (2018a) that was shown to be effective in predicting seizures. The number of filters of the three convolution layers are 16, 32 and 64, respectively. During training, the Generator tries to generate signals that are apparently similar to the original ones while the Discriminator is optimized to detect those generated signals. As a result, the Discriminator learns how to extract unique features in the original EEG signals by adjusting its parameters in the three convolution layers. This training process is unsupervised because we do not provide labels (preictal or interictal) to the network.



Figure 4.3: Seizure forecasting with features extracted by DCGAN’s Discriminator. Inputs are short-time Fourier transform (STFT) of 28-s windows of raw electroencephalogram (EEG) signals. Features extracted by the three convolution blocks of the Discriminator are flattened and connected to a neural network consisting of 2 fully-connected layers with the output sizes 256 and 2, respectively. The former fully-connected layer uses a sigmoid activation function while the latter uses a soft-max activation function. Both of the two layers have drop-out rate of 0.5. Note that the two-layer neural network can be replaced with any other binary classifier.

The Discriminator’s loss,  $D_{\text{loss}}$ , and the Generator’s loss,  $G_{\text{loss}}$ , are defined as (Goodfellow et al., 2014):

$$D_{\text{loss}} = \frac{1}{m} \sum_{i=1}^m \left[ \log D(x^{(i)}) + \log \left( 1 - D(G(z^{(i)})) \right) \right], \quad (4.1)$$

$$G_{\text{loss}} = \frac{1}{m} \sum_{i=1}^m \log \left( 1 - D(G(z^{(i)})) \right), \quad (4.2)$$

where  $m$  is the batch size (64),  $x$  is the original STFT of EEG signals,  $z$  is sampled from the distribution  $\mathcal{U}(-1, 1)$ .

The idea of training a generative adversarial network is that the Discriminator ( $D$ ) and Generator ( $G$ ) compete with each other until they finally reach an equilibrium (Goodfellow et al., 2014). However, when we first started training the DCGAN, we observed that the Discriminator converged too fast. When the Discriminator converges too fast, the term  $D(G(z^{(i)}))$  gets very close to 0 causing  $G_{\text{loss}}$  very close to 0. Hence, the gradient of  $G_{\text{loss}}$  is almost 0. This prevents the Generator from learning how to generate high quality STFT samples that are not distinguishable from real STFT samples. As a result, the classification between generated STFT samples and original ones becomes a trivial task. To overcome this, we update the Generator twice instead of once every mini-batch as suggested by S.-H. Sun (2017) and configure an early-stopping

monitor to keep track of loss values of the Discriminator and Generator (defined in Eqs. 4.1 and 4.2 (Goodfellow et al., 2014)). The monitor stops the DCGAN training if  $D_{\text{loss}}$  keeps being larger than  $G_{\text{loss}}$  over  $k$  consecutive training batches. In this work, we used  $k = 20$ , batch size of 64, and Adam optimizer for gradient-based learning with a learning rate of  $1e^{-4}$ ,  $\beta_1 = 0.5$ ,  $\beta_2 = 0.999$ , and  $\epsilon = 1e^{-8}$ . The effect of updating the Generator twice can be verified by visualizing the loss values. In Fig. 4.4, we plot the Discriminator and the Generator’s loss values in two scenarios: update the Generator (1) once, and (2) twice every mini-batch using data of Patient 1 from the CHB-MIT dataset. One can observe that the Generator’s loss ( $G_{\text{loss}}$ ) is lower and has less variation in scenario (2) which means the generated STFT samples better resemble the original ones. A better Generator, in turn, helps to improve the discriminant performance of the Discriminator. The Generator and the Discriminator reach their equilibrium after around 2000 steps where the early-stopping monitor stops the training. Note that the early-stopping was turned off when collecting loss values to produce Fig. 4.4.

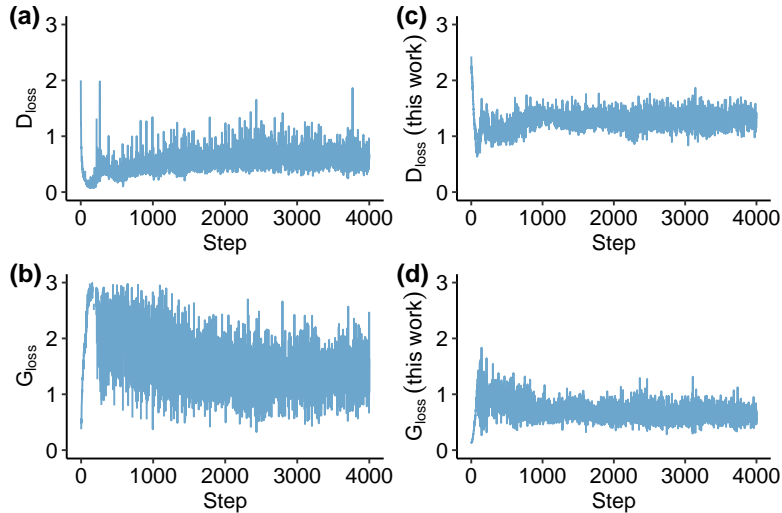


Figure 4.4: The Discriminator’s and the Generator’s loss values in two scenarios: update the Generator (1) once (a-b) and (2) twice (c-d) every mini-batch using data of Patient 1 from the CHB-MIT dataset.

We investigate the system performance in three scenarios: (1) GAN is trained with data of all patients combined (from the same dataset), (2) GAN is trained in a patient-specific fashion, and (3) GAN is trained in a patient-specific fashion with improvement. In scenario (3), similar to the dataset balancing technique proposed by Truong, Nguyen, et al. (2018a), we generate extra samples from existing ones. As a result, the training set in scenario (3) is ten times larger compared to the one in scenario

(2). Our model training is performed on an NVIDIA P100 graphic card using Tensorflow 1.4.0 framework.

### 4.3.3 Seizure forecasting with features extracted by DCGAN

We use the trained convolution layers in the DCGAN’s Discriminator as a feature extractor (see Fig. 4.3). Specifically, we feed STFT of 28-second EEG signals into the Discriminator and collect the flatten features at its last convolution layer’s output ( $64 \times 7 \times 14$ ). Those features can now be used with any classifier to perform the seizure forecasting task. In this work, we use a simple neural network consisting of two fully-connected layers with output sizes of 256 and 2, respectively. The former layer uses a sigmoid activation function while the latter uses soft-max activation function. Both of the two layers have a drop-out rate of 0.5. The training of this two-layer neural network is patient-specific. We also apply a practice proposed by Truong, Nguyen, et al. (2018a) to prevent over-fitting during the training of the neural network. In particular, we perform dataset balancing and then choose 25% later preictal and interictal samples from the training set to monitor if over-fitting occurs and use the rest to train the network.

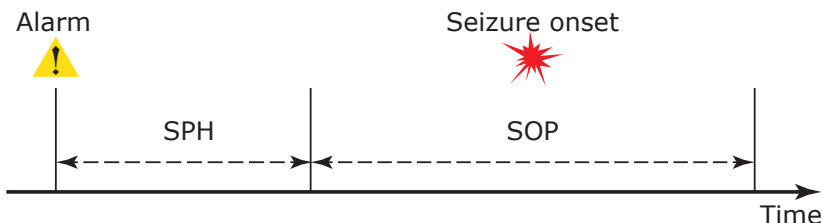


Figure 4.5: Definition of seizure occurrence period (SOP) and seizure prediction horizon (SPH). For a correct prediction, a seizure onset must be after the SPH and within the SOP.

### 4.3.4 System evaluation

Seizure prediction horizon (SPH) and seizure occurrence period (SOP) need to be defined before estimating the system’s performance. In this work, we follow the definition of SOP and SPH that was proposed by Maiwald et al. (2004) (see Fig. 4.5). SOP is the interval where the seizure is expected to occur. The period between the alarm and the beginning of SOP is called SPH. For a correct prediction, a seizure onset must be after

the SPH and within the SOP. Likewise, a false alarm rises when the prediction system returns a positive but there is no seizure occurring during SOP. When an alarm rises, it will last until the end of the SOP. Regarding clinical use, SPH must be long enough to allow sufficient intervention or precautions. In contrast, SOP should be not too long to reduce the patient’s anxiety.

We use the area under the receiver operating characteristics curve (AUC) with SPH of 5 min and SOP of 30 min. To have a robust evaluation, we follow a leave-one-out cross-validation approach for each subject. If a subject has  $N$  seizures,  $(N - 1)$  seizures will be used for the supervised training and the withheld seizure for validation. This round is repeated  $N$  times so all seizures will be used for validation exactly one time. Interictal segments are randomly split into  $N$  parts.  $(N - 1)$  parts are used for training and the rest for validation. The  $(N - 1)$  parts are further split into monitoring and training sets to prevent over-fitting (Truong, Nguyen, et al., 2018a).

We compare our semi-supervised learning models with a fully-supervised approach using CNN reported in our previous work (Truong, Nguyen, et al., 2018a). We also compare the forecasting performance with a random predictor. Specifically, we use the single-tailed Hanley-McNeil AUC test (Hanley and McNeil, 1983) to compare our AUC scores with the chance level (AUC= 0.5). The AUC values used for the Hanley-McNeil AUC test are calculated from all seizure forecasting scores during the leave-one-out cross-validation for each patient.

## 4.4 Results

In this section, we test our approach with three datasets: the CHB-MIT sEEG dataset, the Freiburg Hospital iEEG dataset, and the EPILEPSIAE sEEG dataset. SOP = 30 min and SPH = 5 min were used in calculating all metrics in this work. Each fold of leave-one-out cross-validation was executed twice, and average results with standard deviations were reported. Fig. 4.6 summarizes seizure forecasting results with SOP of 30 min and SPH of 5 min. Results in detail are provided in Tables A1-A3.

Compared to the fully supervised CNN, GAN-NN introduces  $\sim 6\%$ ,  $\sim 12\%$  and  $\sim 6.6\%$  loss in AUC for the CHB-MIT sEEG dataset, the Freiburg Hospital iEEG dataset, and the EPILEPSIAE sEEG dataset, respectively. When GAN is trained per patient (GAN-PS-NN), the average AUC drops further to 72.63%, 60.91% and 63.6% for the three datasets. This can be explained by the limited amount of data from each patient. By applying  $10\times$  up-sampling (GAN-PS-USPL-NN), the average

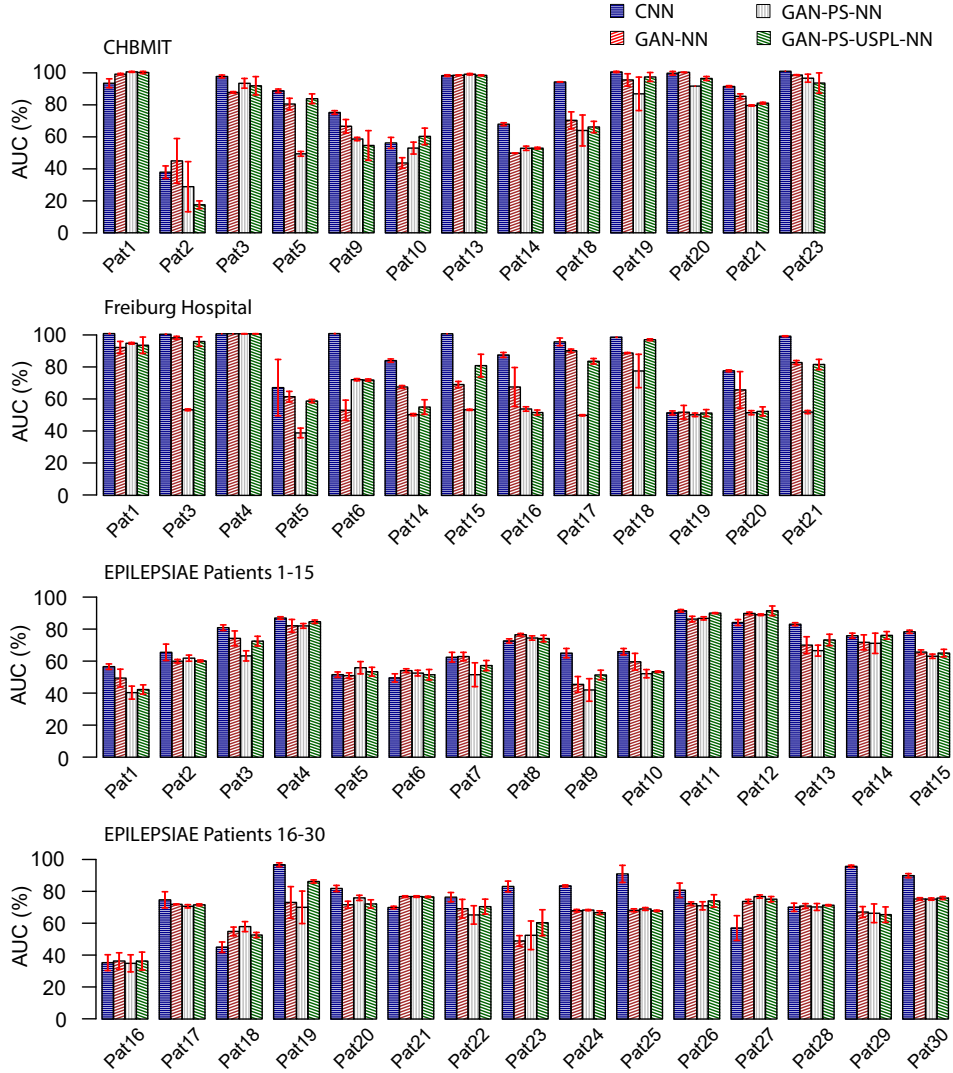


Figure 4.6: Seizure forecasting performance for the CHB-MIT dataset, the Freiburg Hospital dataset, and the EPILEPSIAE dataset. Four methods are evaluated: (1) CNN: convolutional neural network (Truong, Nguyen, et al., 2018a) (global means:  $83.89 \pm 1.28\%$ ,  $88.86 \pm 1.87\%$ ,  $71.65 \pm 2.44\%$ ), (2) GAN-NN: unsupervised feature extraction using generative adversarial network (GAN) and classification performed by a two-layer neural network (global means:  $77.68 \pm 2.85\%$ ,  $75.35 \pm 3.62\%$ ,  $65.05 \pm 2.78\%$ ), (3) GAN-PS-NN: similar to (2) but GAN is done patient-specific (global means:  $72.63 \pm 3.80\%$ ,  $60.91 \pm 1.62\%$ ,  $63.60 \pm 3.16\%$ ), (4) GAN-PS-USPL-NN: similar to (3) but  $10\times$  over-sampling of samples is performed when training GAN (global means:  $75.66 \pm 3.15\%$ ,  $74.33 \pm 2.54\%$ ,  $65.76 \pm 2.33\%$ )

AUC is boosted to 75.66% and 74.33% for the CHB-MIT dataset and the Freiburg Hospital dataset, respectively, which are 1–2% lower than those of GAN-NN. Regarding the EPILEPSIAE dataset, up-sampling technique improves overall AUC by 2% higher compared to patient-specific GAN without up-sampling (GAN-PS-NN) and 0.7% higher compared to non-patient-specific GAN (GAN-CNN). Fig. A1 demonstrates the overall seizure performance across different models and datasets. Tables A1-A3 show that our seizure forecasting method is significantly better than the chance level for most of the patients at a significance level of 0.05. The supervised and semi-supervised learning methods (namely CNN, and GAN-PS-USPL-NN) outperform the random predictor for most of the patients. The percentages of patients with forecasting performance above the chance level for the two methods are (92.30%, 84.61%), (100%, 84.61%), and (86.67%, 86.67%) for the CHB-MIT dataset, the Freiburg Hospital dataset, and the EPILEPSIAE dataset, respectively.

## 4.5 Discussion

We have shown that feature extraction for seizure forecasting can be performed in an unsupervised way. Though the overall AUC degraded by  $\sim 6\text{--}12\%$  across the three datasets, our unsupervised feature extraction can help to minimize the EEG labeling task that is costly and time-consuming. Specifically, unlabeled EEG signals are used to train the GAN. The trained GAN plays like a feature extractor. Extracted features from labeled EEG data (that can be much smaller than unlabeled one) can be fed to any classifier (two fully-connected layers in our work) for the seizure forecasting task.

There is still a gap in seizure forecasting performance between fully-supervised (CNN) and semi-supervised approaches. We argue that this is because the size of training data for GAN is not big enough. This argument is supported by the results of over-sampling data for training GAN. We have shown that over-sampling the inputs during training GAN helps to fill the gap for some patients and boost the seizure forecasting performance in overall. It is reasonable to argue that with more EEG data, the prediction accuracy can be improved. The advantage of using unsupervised feature extraction is that we can train the feature extractor (GAN) while recording EEG data, i.e., online training, without inducing extra efforts from clinicians.

Previous works using autoencoder-based unsupervised feature extraction (Hosseini et al., 2017; Abdelhameed and Bayoumi, 2018) achieved sensitivity higher than 94% and FPR lower than 0.06/h, which, however, cannot be directly compared with the

performance of our method. The work proposed by Hosseini et al. (2017) not only utilized the unsupervised feature extraction by stacked autoencoders but also engineered features from a priori knowledge. Therefore, it is not clear how much the extracted features from the stacked autoencoders contribute to the final performance. Also, the method was tested with only two patients with intracranial EEG signals. The other work proposed by Abdelhameed and Bayoumi (2018) defined preictal period right next to ictal period which means seizure prediction period (SPH) is zero. However, from a clinical perspective, SPH needs to be long enough to allow sufficient intervention (Truong, Nguyen, et al., 2018a).

In the field of computer vision, GAN can help to reduce the amount of labeled data without compromising the classification performance (Kingma et al., 2014). Unfortunately, with the current sizes of the datasets available to us, we could not replicate a similar claim for seizure forecasting using GAN as an unsupervised feature extractor.

Another aspect that we believe it is important is that how patient-specific characteristics, such as seizure types (R. S. Fisher et al., 2017; Espay et al., 2018), age, and gender, affects seizure forecasting performance testing with the EPILEPSIAE dataset. In this dataset, seizures are categorized into focal aware (simple partial), focal impaired awareness (complex partial), focal to bilateral tonic-clonic (secondarily generalized tonic-clonic) and unclassified. The age of the patients is ranging from 13 to 67. In terms of seizure type, focal aware seizures have the least variation in seizure forecasting. This observation could be helpful for clinical trial consideration; e.g., focus on patients with focal aware seizures first. Regarding the gender, seizure forecasting is better for female patients overall, with an exception that there is one female who has a very low AUC score (below 35%). It is most interesting to observe that patients with age in the range of 10 to 30 have considerably higher AUC scores and less variation compared to other groups. In fact, if we exclude the patient with a very low AUC score which is an outlier from group 10 to 30, it can be seen that seizures of young patients (30 and below) can be predicted with the highest accuracy. The reason behind this observation is not clear and is not in the scope of this article.

## 4.6 Conclusion

Seizure forecasting capability has been studied and improved over the last four decades. A perfect prediction is yet available but with current prediction performance, it is useful

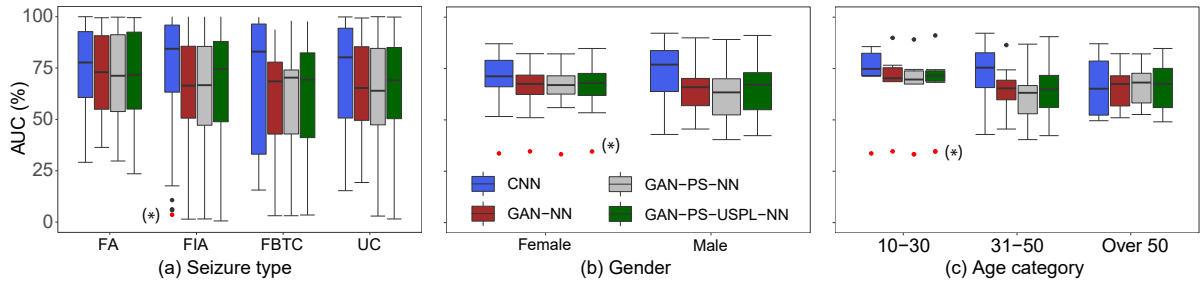


Figure 4.7: Seizure forecasting performance (AUC) across different patient-specific characteristics for the EPILEPSIAE dataset: (a) - Seizure type, (b) - Gender, (c) - Age. Refer to Table A4 for the patients’ details. Dots indicate outliers. Data points in red (\*) are from the same patient. FA: focal aware, FIA: focal impaired awareness, FBTC: focal to bilateral tonic-clonic, UC: unclassified.

to provide the patients with warning messages so they can take some precautions for their safety. We have shown that feature extraction for seizure forecasting can be done using unsupervised deep learning or GAN particularly. Using semi-supervised seizure forecasting approach, 61.53% of the patients in the CHB-MIT dataset, 53.84% in the Freiburg Hospital dataset and 13.33% in the EPILEPSIAE dataset have very good seizure forecasting performance (with AUC above 80%).

## Acknowledgment

This research is funded by a Sydney Research Accelerator (SOAR) Fellowship and an Early Career Research grant through the University of Sydney. N.D.T. acknowledges partial support provided via John Makepeace Bennett Gift Scholarship funded by the Australian Institute for Nanoscale Science and Technology (AINST) and administered by the University of Sydney Nano Institute. The authors also acknowledge the support by Sydney Informatics Hub via the University of Sydney’s Core Research Facilities.

## Appendix

Table A1: Seizure forecasting performance for the CHB-MIT dataset.  $p$ -values are from the single-tailed Hanley-McNeil AUC test to compare our seizure forecasting performance with the chance level (AUC= 0.5). Patients with  $p$ -values not being highlighted in gray color have seizure forecasting performance significantly better than the chance level with the significance level of 0.05.

Patient	CNN	$p$ -value	GAN-NN	$p$ -value	GAN-PS-NN	$p$ -value	GAN-PS-USPL-NN	$p$ -value
Pat1	92.48 ± 2.73	< 0.001	98.09 ± 0.48	< 0.001	99.52 ± 0.29	< 0.001	99.13 ± 0.68	< 0.001
Pat2	37.50 ± 3.85	<b>1</b>	44.47 ± 13.8	< 0.001	28.52 ± 15.4	<b>1</b>	17.34 ± 2.39	<b>1</b>
Pat3	96.66 ± 0.88	< 0.001	86.79 ± 0.51	< 0.001	92.43 ± 3.01	< 0.001	90.91 ± 5.66	< 0.001
Pat5	87.80 ± 1.09	< 0.001	79.62 ± 3.56	< 0.001	48.83 ± 1.47	<b>0.400</b>	82.90 ± 2.99	< 0.001
Pat9	74.41 ± 1.12	< 0.001	65.87 ± 4.18	< 0.001	57.99 ± 1.01	< 0.001	54.00 ± 9.17	< 0.001
Pat10	55.59 ± 3.39	< 0.001	43.17 ± 3.26	<b>0.088</b>	52.38 ± 3.67	0.028	59.63 ± 5.09	< 0.001
Pat13	97.21 ± 0.50	< 0.001	97.42 ± 0.23	< 0.001	98.04 ± 0.44	< 0.001	97.35 ± 0.25	< 0.001
Pat14	67.16 ± 0.88	< 0.001	49.22 ± 0.08	<b>0.566</b>	52.28 ± 1.31	<b>0.302</b>	52.34 ± 0.55	<b>0.395</b>
Pat18	93.29 ± 0.13	< 0.001	69.54 ± 5.24	< 0.001	63.27 ± 9.56	< 0.001	65.44 ± 3.47	< 0.001
Pat19	99.48 ± 0.37	< 0.001	94.53 ± 3.82	< 0.001	85.93 ± 10.3	< 0.001	96.36 ± 2.75	< 0.001
Pat20	98.67 ± 1.12	< 0.001	99.21 ± 0.08	< 0.001	90.70 ± 0.01	< 0.001	95.43 ± 1.22	< 0.001
Pat21	90.47 ± 0.50	< 0.001	84.38 ± 1.53	< 0.001	78.71 ± 0.36	< 0.001	80.17 ± 0.53	< 0.001
Pat23	99.90 ± 0.02	< 0.001	97.55 ± 0.23	< 0.001	95.59 ± 2.46	< 0.001	92.60 ± 6.26	< 0.001
Average	83.89 ± 1.28		77.68 ± 2.85		72.63 ± 3.80		75.66 ± 3.15	

Table A2: Seizure forecasting performance for the Freiburg Hospital dataset.  $p$ -values are from the single-tailed Hanley-McNeil AUC test to compare our seizure forecasting performance with the chance level (AUC= 0.5). Patients with  $p$ -values not being highlighted in gray color have seizure forecasting performance significantly better than the chance level with the significance level of 0.05.

Patient	CNN	$p$ -value	GAN-NN	$p$ -value	GAN-PS-NN	$p$ -value	GAN-PS-USPL-NN	$p$ -value
Pat1	100 ± 0.00	< 0.001	91.43 ± 3.75	< 0.001	94.02 ± 0.51	< 0.001	92.78 ± 5.05	< 0.001
Pat3	99.59 ± 0.00	< 0.001	97.44 ± 0.90	< 0.001	52.89 ± 0.53	<b>0.306</b>	95.13 ± 2.91	< 0.001
Pat4	99.93 ± 0.01	< 0.001	99.92 ± 0.01	< 0.001	99.88 ± 0.05	< 0.001	99.88 ± 0.04	< 0.001
Pat5	66.58 ± 17.4	< 0.001	61.04 ± 3.28	<b>1</b>	38.60 ± 2.97	<b>1</b>	58.28 ± 0.95	< 0.001
Pat6	100 ± 0.00	< 0.001	52.58 ± 6.26	< 0.001	71.51 ± 0.66	< 0.001	71.27 ± 0.64	< 0.001
Pat14	83.28 ± 1.02	< 0.001	67.01 ± 0.87	0.015	49.86 ± 0.65	0.044	54.60 ± 4.51	< 0.001
Pat15	99.95 ± 0.02	< 0.001	68.50 ± 1.93	< 0.001	52.88 ± 0.35	<b>0.052</b>	80.18 ± 7.01	< 0.001
Pat16	86.81 ± 1.53	< 0.001	67.01 ± 12.0	< 0.001	53.44 ± 1.36	<b>1</b>	51.17 ± 1.55	< 0.001
Pat17	94.92 ± 2.36	< 0.001	89.44 ± 1.01	< 0.001	49.49 ± 0.37	< 0.001	82.91 ± 1.70	< 0.001
Pat18	97.69 ± 0.00	< 0.001	87.99 ± 0.30	< 0.001	76.90 ± 10.3	< 0.001	96.25 ± 0.55	< 0.001
Pat19	50.97 ± 1.19	< 0.001	51.35 ± 4.19	<b>0.991</b>	49.77 ± 1.08	<b>0.088</b>	50.93 ± 2.12	<b>0.345</b>
Pat20	77.02 ± 0.55	< 0.001	65.24 ± 11.2	< 0.001	51.11 ± 1.27	<b>0.677</b>	51.91 ± 2.80	<b>0.157</b>
Pat21	98.40 ± 0.25	< 0.001	80.56 ± 1.26	< 0.001	51.51 ± 0.95	<b>0.379</b>	80.94 ± 3.16	< 0.001
Average	88.86 ± 1.87		75.35 ± 3.62		60.91 ± 1.62		74.33 ± 2.54	

Table A3: Seizure forecasting performance for the EPILEPSIAE dataset.  $p$ -values are from the single-tailed Hanley-McNeil AUC test to compare our seizure forecasting performance with the chance level (AUC= 0.5). Patients with  $p$ -values not being highlighted in gray color have seizure forecasting performance significantly better than the chance level with the significance level of 0.05.

Patient	CNN	$p$ -value	GAN-NN	$p$ -value	GAN-PS-NN	$p$ -value	GAN-PS-USPL-NN	$p$ -value
Pat1	56.66 ± 1.70	< 0.001	49.49 ± 5.57	0.228	40.40 ± 4.06	1	42.34 ± 2.91	1
Pat2	65.63 ± 5.12	< 0.001	60.05 ± 1.11	< 0.001	61.96 ± 1.91	< 0.001	60.24 ± 0.57	< 0.001
Pat3	81.03 ± 1.75	< 0.001	74.35 ± 4.65	< 0.001	63.39 ± 3.17	< 0.001	72.62 ± 3.04	< 0.001
Pat4	87.07 ± 0.80	< 0.001	82.23 ± 3.95	< 0.001	82.14 ± 1.48	< 0.001	84.76 ± 1.05	< 0.001
Pat5	51.64 ± 1.70	0.259	51.04 ± 1.75	0.279	55.98 ± 3.83	< 0.001	53.48 ± 2.76	< 0.001
Pat6	49.60 ± 2.57	0.975	54.16 ± 1.16	0.577	52.62 ± 1.77	1	51.59 ± 3.28	1
Pat7	62.56 ± 3.04	< 0.001	62.96 ± 2.64	< 0.001	51.62 ± 7.44	< 0.001	57.33 ± 3.16	< 0.001
Pat8	72.76 ± 1.29	< 0.001	76.61 ± 0.79	< 0.001	74.57 ± 1.33	< 0.001	74.24 ± 2.07	< 0.001
Pat9	65.12 ± 2.91	< 0.001	45.55 ± 4.91	1	42.07 ± 7.06	1	51.46 ± 2.96	0.014
Pat10	66.02 ± 1.99	< 0.001	59.70 ± 5.26	0.002	52.25 ± 2.57	0.687	53.50 ± 0.44	0.001
Pat11	91.58 ± 0.80	< 0.001	86.41 ± 1.73	< 0.001	86.87 ± 1.00	< 0.001	90.15 ± 0.30	< 0.001
Pat12	84.27 ± 1.87	< 0.001	89.94 ± 0.82	< 0.001	89.13 ± 0.48	< 0.001	91.61 ± 2.99	< 0.001
Pat13	83.21 ± 0.94	< 0.001	70.12 ± 5.24	< 0.001	66.67 ± 3.41	< 0.001	73.35 ± 3.58	< 0.001
Pat14	76.00 ± 1.60	< 0.001	71.86 ± 4.68	< 0.001	71.26 ± 6.33	< 0.001	76.23 ± 2.36	< 0.001
Pat15	78.47 ± 1.00	< 0.001	65.76 ± 1.38	< 0.001	63.16 ± 1.33	< 0.001	65.14 ± 2.34	< 0.001
Pat16	33.69 ± 4.73	1	34.67 ± 4.91	1	33.28 ± 5.09	1	34.64 ± 5.34	1
Pat17	71.22 ± 4.83	< 0.001	68.53 ± 0.22	< 0.001	67.37 ± 0.96	< 0.001	68.23 ± 0.55	< 0.001
Pat18	42.91 ± 3.12	1	52.35 ± 2.58	0.999	55.22 ± 2.98	0.030	50.20 ± 1.53	1
Pat19	92.19 ± 1.13	< 0.001	69.66 ± 9.44	< 0.001	66.74 ± 9.68	< 0.001	82.17 ± 0.94	< 0.001
Pat20	78.01 ± 1.83	< 0.001	68.28 ± 2.08	< 0.001	72.39 ± 1.55	< 0.001	68.76 ± 2.48	< 0.001
Pat21	66.62 ± 0.76	< 0.001	73.15 ± 0.49	< 0.001	73.17 ± 0.46	< 0.001	72.98 ± 0.39	< 0.001
Pat22	72.81 ± 2.77	< 0.001	65.93 ± 5.55	< 0.001	62.20 ± 5.49	< 0.001	67.14 ± 4.47	< 0.001
Pat23	79.20 ± 3.20	< 0.001	46.65 ± 3.18	1	50.04 ± 8.54	< 0.001	57.56 ± 7.74	< 0.001
Pat24	79.52 ± 0.59	< 0.001	64.73 ± 0.74	< 0.001	65.09 ± 0.33	< 0.001	63.55 ± 1.08	< 0.001
Pat25	86.71 ± 5.11	< 0.001	64.97 ± 0.88	< 0.001	65.76 ± 0.83	< 0.001	64.68 ± 0.39	< 0.001
Pat26	76.91 ± 4.31	< 0.001	68.87 ± 1.08	< 0.001	67.66 ± 2.42	< 0.001	70.58 ± 3.69	< 0.001
Pat27	54.36 ± 7.39	< 0.001	70.26 ± 1.19	< 0.001	73.16 ± 0.97	< 0.001	71.60 ± 1.58	< 0.001
Pat28	66.76 ± 2.45	< 0.001	67.51 ± 1.43	< 0.001	66.95 ± 2.04	< 0.001	67.99 ± 0.35	< 0.001
Pat29	91.22 ± 0.70	< 0.001	63.93 ± 3.24	< 0.001	63.19 ± 5.57	< 0.001	62.38 ± 4.61	< 0.001
Pat30	85.67 ± 1.21	< 0.001	71.72 ± 0.75	< 0.001	71.66 ± 0.66	< 0.001	72.28 ± 0.86	< 0.001
Average	71.65 ± 2.44		65.05 ± 2.78		63.60 ± 3.16		65.76 ± 2.33	

Table A4: The EPILEPSIAE scalp EEG dataset.

Patient	Gender	Age	No. of seizures	No. of leading seizures*	Interictal hours
Pat1	male	36	11	11	68.9
Pat2	female	46	8	8	114.9
Pat3	male	41	8	8	96.3
Pat4	female	67	5	5	126
Pat5	female	52	8	8	204.1
Pat6	male	65	8	7	92.2
Pat7	male	36	5	5	75.7
Pat8	male	26	22	11	65.6
Pat9	male	47	6	6	51.1
Pat10	male	44	11	11	60.7
Pat11	male	48	14	14	57.8
Pat12	male	28	9	9	94.1
Pat13	male	46	8	8	101.3
Pat14	female	62	6	6	115.7
Pat15	female	41	5	5	82.8
Pat16	female	15	6	6	51.1
Pat17	female	17	9	9	82.4
Pat18	male	47	7	6	133
Pat19	male	32	22	21	75.4
Pat20	male	47	7	7	115.3
Pat21	female	31	8	8	106.6
Pat22	male	38	7	7	88.2
Pat23	male	50	9	9	179.6
Pat24	female	54	10	10	36.2
Pat25	male	42	8	8	109.8
Pat26	male	13	9	9	97.1
Pat27	male	58	9	8	99.9
Pat28	female	35	9	9	95.2
Pat29	male	50	10	10	111.9
Pat30	female	16	12	12	92.5

\* We are considering leading seizures only. Seizures that are less than 30 min away from the previous one are considered as one seizure only and the onset of leading seizure is used as the onset of the combined seizure.

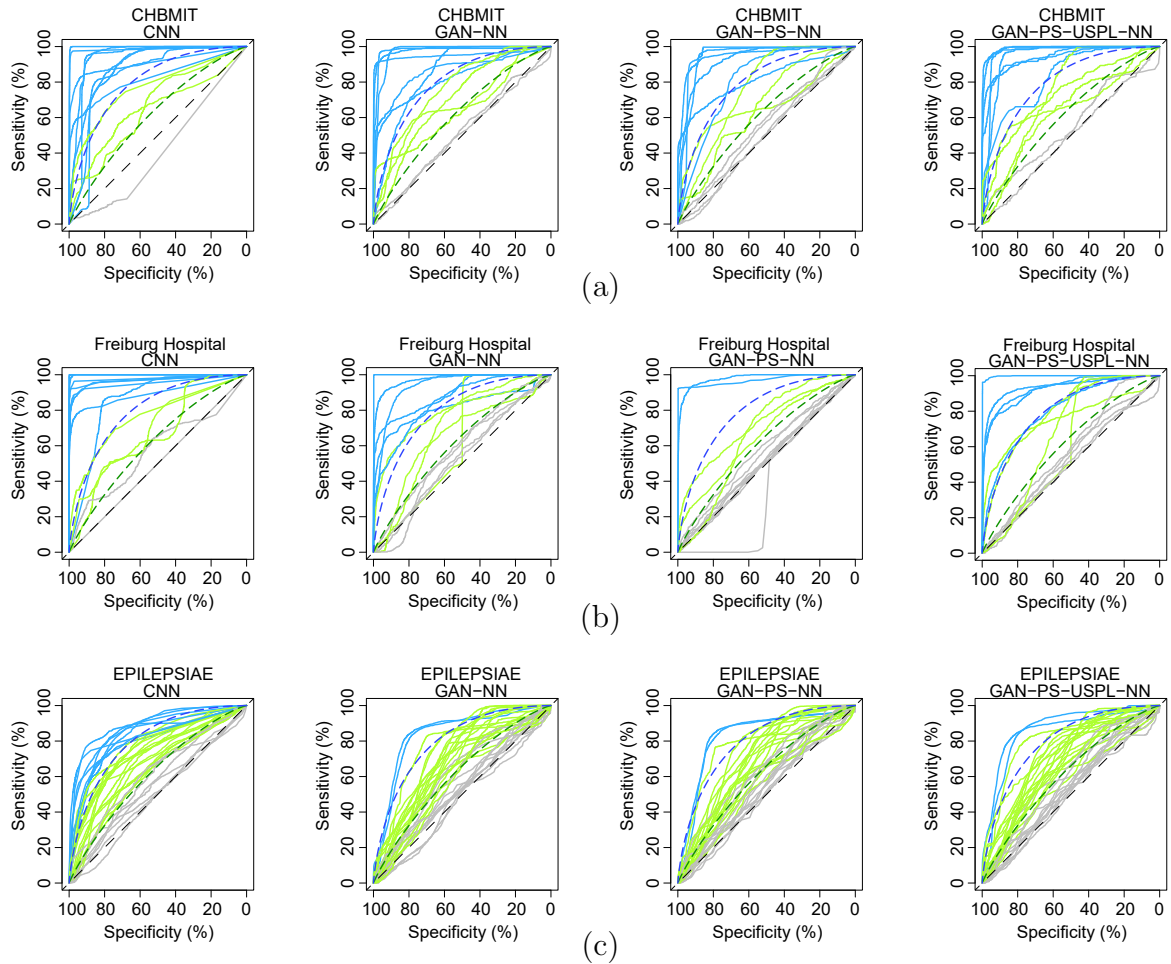


Figure A1: Receiver operating characteristics (ROC) curves of seizure forecasting performance testing for different patients of the three datasets: (a) - the CHB-MIT sEEG dataset, (b) - the Freiburg Hospital iEEG dataset, and (c) - the EPILEPSIAE sEEG dataset. Each line corresponds to one patient. Above the green dash line: good performance; above the blue dash line: very good performance (adapted from (Kuhlmann, Lehnertz, et al., 2018)).

# Chapter 5

## Automatic channel selection for seizure detection

The content presented in this chapter is published as:

- Truong, N. D., L. Kuhlmann, M. R. Bonyadi, J. Yang, A. Faulks, and O. Kavehei (2017). “Supervised learning in automatic channel selection for epileptic seizure detection.” *Expert Systems with Applications* 86, 199-207. DOI:10.1016/j.eswa.2017.05.055.

### **Statement of Contributions of Joint Authorship**

- Nhan Duy Truong (Candidate): First author, completed the analysis, writing, reviewing and editing of the manuscript
- Levin Kuhlmann: aided in the analysis, reviewing and editing the manuscript
- Mohammad Reza Bonyadi: aided in the analysis, reviewing and editing the manuscript
- Jiawei Yang: provided technical advice on the analysis, reviewing and editing the manuscript
- Andrew Faulks: reviewing and editing the manuscript
- Omid Kavehei (Principal Supervisor): provided the main idea, reviewing and editing the manuscript

In addition to the statements above, in cases where I am not the corresponding author of a published item, permission to include the published material has been granted by the corresponding author.

Nhan Duy Truong

Date: 01 October 2019

As supervisor for the candidature upon which this thesis is based, I can confirm that the authorship attribution statements above are correct.

Dr. Omid Kavehei

Date: 01 October 2019

Detecting seizure using brain neuroactivations recorded by intracranial electroencephalogram (iEEG) has been widely used for monitoring, diagnosing, and closed-loop therapy of epileptic patients, however, computational efficiency gains are needed if state-of-the-art methods are to be implemented in implanted devices. We present a novel method for automatic seizure detection based on iEEG data that outperforms current state-of-the-art seizure detection methods in terms of computational efficiency while maintaining the accuracy. The proposed algorithm incorporates an automatic channel selection (ACS) engine as a pre-processing stage to the seizure detection procedure. The ACS engine consists of supervised classifiers which aim to find iEEG channels which contribute the most to a seizure. Seizure detection stage involves feature extraction and classification. Feature extraction is performed in both frequency and time domains where spectral power and correlation between channel pairs are calculated. Random Forest is used in classification of interictal, ictal and early ictal periods of iEEG signals. Seizure detection in this work is retrospective and patient-specific. iEEG data is accessed via Kaggle, provided by International Epilepsy Electro-physiology Portal. The dataset includes a training set of 6.5 hours of interictal data and 41 min in ictal data and a test set of 9.14 hours. Compared to the state-of-the-art on the same dataset, we achieve 2 times faster in run-time seizure detection. The proposed model is able to detect a seizure onset at 89.40% sensitivity and 89.24% specificity with a mean detection delay of 2.63 s for the test set. The area under the ROC curve (AUC) is 96.94%, that is comparable to the current state-of-the-art with AUC of 96.29%.

## 5.1 Introduction

Epileptic seizure affects nearly 1% of global population but only two thirds can be treated by medicine and approximately 7–8% can be cured by surgery (Litt and Echauz, 2002). Therefore, seizure onset detection and subsequent seizure suppression becomes important for the patients that cannot be cured by neither drug nor surgery. Early detection can allow early electrical stimulation to suppress the seizure (Echauz et al., 2007). In this work, we focus on how to effectively and reliably detect seizure onset based on iEEG patterns. Note that cause and treatment of epilepsy is beyond the scope of this work.

EEG has been commonly used in brain-computer interface thanks to the convenient real-time readings and high temporal resolution of EEG signals (Zeng and Song, 2015; H. Zhang et al., 2013). In recent years, EEG has provided a promising possibility to detect and even predict an epileptic seizure (Tieng et al., 2016; Fatichah et al., 2014;

Parvez and Paul, 2015; Saab and Gotman, 2005; Osorio and Frei, 2009; Kuhlmann, Burkitt, et al., 2009). For seizure detection, Faticchah et al. (2014) used a combination of principle component analysis (PCA) and neural network with fuzzy membership function that can achieve accuracy rate up to 97.64%. In another work, wavelet de-noising was combined with adapted Continuous Wavelet Transform as feature extraction achieving a sensitivity of 96.72% and a specificity of 94.69% with EEG data from mice (Tieng et al., 2016). Another remarkable method is to transform EEG signals into images so as to leverage image processing techniques (Parvez and Paul, 2015). This approach was able to obtain 98.91% sensitivity and 94.35% specificity. In another approach, EEG phase spaces were constructed using time-delay embedding method and PoinCare section (Zabihi et al., 2016). The phase spaces were then reduced by PCA before being fed to linear discriminant analysis (LDA) and Naive Bayesian classifiers. This approach achieved 88.27% sensitivity and 93.21% specificity in seizure detection.

Shoeb (2009) deployed 8 filters spanning the frequency range of 0.5–24 Hz for each 2-s EEG epoch of all channels, then concatenated 3 epochs to form a feature set to be fed to a SVM classifier. This approach was tested with the CHB-MIT EEG dataset and was able to detect 96% of 163 test seizures with a mean detection delay of 4.6 seconds. Using the same CHB-MIT dataset, EEG signal was transformed into an image representation using 2-D projection of the patient electrodes and the magnitude of 3 different frequency bands spanning the range of 0–49 Hz of each 1 s block of EEG signal (Thodoroff et al., 2016). The recurrent convolutional neural network took 30 consecutive blocks as inputs to perform feature extraction and classification. The patient-specific detectors in this method have comparable performance compared to the proposed method by Shoeb (2009). The downside of the work proposed by Thodoroff et al. (2016) is that the detection delay is at least 30 seconds which is not preferable.

Table 5.1: Summary of existing EEG-based seizure detection methods

Ref.	EEG type	No. of patients	No. of seizures	Data duration ictal	Data duration interictal	Patient -specific	Split data for training	Testing sensitivity	FDR*	Mean detection delay
(Saab and Gotman, 2005)	scalp	44	195	1012 h <sup>†</sup>		No	64%	76%	0.34/h	9.8s
(Kuhlmann, Burkitt, et al., 2009)	scalp	21	88	525 h <sup>†</sup>		No	70%	81%	0.60/h	16.9s
(G. Wang et al., 2016)	scalp	10	44	72 min	121 h	Yes	80%	91.44%	99.34%	n/a
(Zabihi et al., 2016)	scalp	24	161	2.55 h	169 h	Yes	25%	88.27%	93.21%	n/a
(Faticchah et al., 2014)	intracranial <sup>‡</sup>	n/a	n/a	39.3 min	2.62 h	n/a	90%	94.55%	98.41%	n/a
(Hills, 2014)	intracranial	12	48	41 min	6.5 h	Yes	50%	91.33%	94.02%	3.17s
(Parvez and Paul, 2015)	intracranial	21	87	58 h	490 h	n/a	80%	100%	97%	n/a

\* False detection rate (FDR) or specificity.

<sup>†</sup> Duration of ictal and interictal were not provided separately.

<sup>‡</sup> Intracranial EEG for seizure class and both intracranial and extracranial for non-seizure class.

Prominent feature extraction techniques consider characteristics in both frequency and time domain. As an efficient tool for time-frequency-energy analysis, wavelet-based

filters were used to extract a ratio of seizure content of the short foreground in comparison with the background (Saab and Gotman, 2005; Osorio and Frei, 2009). Saab and Gotman (2005) applied Bayes' formula on extracted features to estimate the probability of seizure in EEG signals. This method achieved an onset detection delay of 9.8 s with 76% sensitivity and 0.34/h false positive rate. The method was then extended by combining extra features to find a superior detector (Kuhlmann, Burkitt, et al., 2009). Their method was able to achieve a sensitivity of 81%, a false positive rate of 0.60/h, and a median detection delay of 16.9 s on a dataset of 525 h of scalp EEG data.

EEG signals can be recorded using many channels. Large number of channels yields higher computational complexity as it requires more data to be analyzed. This can also deteriorate the diversity of iEEG data, hence degrade the performance of seizure detection, because some channels may capture irrelevant information (Guyon and Elisseeff, 2003). One can leverage bio-medical knowledge to manually select which channels genuinely contribute to the seizure. However, it is hard, if not impossible, to disclose a set of channels that are significant for all subjects. It is required to use the expertise to analyze every subject (or group of subjects) to proclaim a list of significant channels with regards to each subject (or group of subjects) which is manifestly a time-consuming task. There have been attempts to reduce the number of channels to be analyzed (Duun-Henriksen et al., 2012; Shih et al., 2009) or reduce number of features extracted prior to classification (Minasyan et al., 2010; Subasi and Ismail Gursoy, 2010). Duun-Henriksen et al. (2012) proposed an automated channel selection based on variance of EEG signal amplitude where channels with largest variance would be chosen. The detection performance using 3 channels selected by their algorithm was similar to using 3 channels selected by a clinical neurophysiologist. In another work, a greedy backward elimination algorithm was used to find the subset of features that results in lowest false positive rate (Shih et al., 2009). Seven features are extracted per each channel. The algorithm starts with all features and gradually removes the least influential ones by doing cross-validation on all subset of features. The authors were able to reduce the number of channels from 18 to 4.6 with an improvement in FPR (0.35 to 0.19/h) but degradation in sensitivity (from 99% to 97%) and detection delay (from 7.8 to 11.2 s). This approach, however, is less favorable when the number of channels per subject is too high because the number of subsets increases exponentially. In another work, feature selection was performed using mutual information between individual features and output where features with less mutual information are discarded (Minasyan et al., 2010). It is worth noting that this feature selection has to be performed not only during training but also during run-time classification. In

other words, this approach induces extra processing time and makes it less suitable for portable device implementation. Subasi and Ismail Gursoy (2010) applied PCA, ICA, LDA for feature dimension reduction and used SVM classifier to distinguish between seizure and non-seizure segments. They tested with an 80 min subset of University Hospital of Bonn’s dataset. They showed LDA achieved the best performance while PCA obtained the worst. However, their approaches also induce extra processing time during both training and run-time classification, similar to the work proposed by Minasyan et al. (2010).

The current state-of-the-art seizure detection method proposed by Hills (2014) for the dataset considered here is implemented and extended in this work. The dataset is derived from a Kaggle seizure detection competition in which Hills (2014) scored AUC of 96.29% and announced as the winner. Description of the dataset is provided in Section 5.2. In this work, we significantly enhanced computational efficiency of Hill’s method by employing an automatic channel selection algorithm. This enabled us to process data as accurately with reduced number of channels. Table 5.1 summarizes the existing EEG-based seizure detection methods in recent years. We have made the research’s source code publicly available on GitHub via <https://goo.gl/Bc89mJ>.

The remainder of this work is organized as follows. In Section 5.3, after describing the dataset, we propose automatic channel selection engine that helps to reduce the number of channels to be processed. This section also presents spatio-temporal feature extraction and Random Forest classifier used for seizure detection. Section 5.4 evaluates the performance of the proposed model with comparison against the state-of-the-art method on the same dataset. Section 5.5 concludes the achievement of the work.

## 5.2 Dataset

Dataset being analyzed in this work is obtained from Kaggle (2014b). Intracranial EEG signals were recorded from 4 dogs and 8 patients with epileptic seizures. Recordings were sampled at 400 Hz from 16 electrodes for dogs, and sampled at 500 Hz or 5 kHz from varying number of electrodes (ranging from 16 to 72) for humans. The data was pre-organized into 1 s iEEG epochs annotated as ictal for seizure states or interictal for seizure-free states. Interictal data was captured not less than one hour before or after a seizure onset and randomly chosen from the recorded data. Each ictal segment also came with the time in seconds between the seizure onset and first data point of the segment. The training dataset is consisted of 41 min of ictal data and 6.5 hours of interictal data.

Summary of the training dataset is presented in Table 5.2. Note that early ictal state in this work is the ictal state occurring within the first 15 s from the seizure onset. The proposed method was tested with a hidden dataset provided by Kaggle. This dataset consists of 9.14 hours of unlabeled iEEG data (Kaggle, 2014b).

Table 5.2: Summary of the dataset

Subject	No. of electrodes	Ictal data length (s)	Interictal data length (s)	Unlabeled data length (s)	Train/Test ratio
Dog-1	16	178	418	3181	0.19
Dog-2	16	172	1148	2997	0.44
Dog-3	16	480	4760	4450	1.18
Dog-4	16	257	2790	3013	1.01
Patient-1	68	70	104	2050	0.08
Patient-2	16	151	2990	3894	0.81
Patient-3	55	327	714	1281	0.81
Patient-4	72	20	190	543	0.39
Patient-5	64	135	2610	2986	0.92
Patient-6	30	225	2772	2997	1
Patient-7	36	282	3239	3601	0.98
Patient-8	16	180	1710	1922	0.98
<b>Total</b>		<b>2477</b>	<b>23445</b>	<b>32915</b>	<b>0.79</b>

### 5.3 Proposed method

The intracranial EEG data was recorded on multiple subjects with varying number of channels and sampling rates. We propose an automatic channel selection engine to filter out channels which are less relevant to seizure. The engine accepts raw iEEG data, their corresponding labels, and the number of channels to be selected,  $M$ , and determines indexes of channels that are most relevant for seizure detection. Indexes of these  $M$  channels are stored on hard-disk so the engine only needs to be executed one time at the beginning for each subject. Feature extraction was performed in both frequency and time domain on the selected channels. Information extracted in frequency and time domains was concatenated and fed to a Random Forest classifier. Fig. 5.1 presents flowchart of the proposed method.

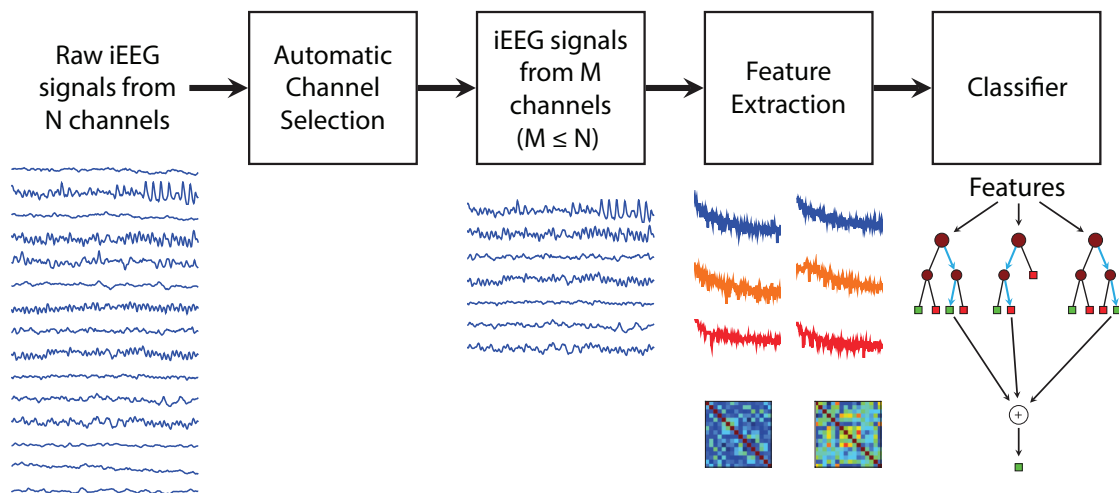


Figure 5.1: Flowchart of the proposed method. Raw iEEG data from all  $N$  channels is fed to ACS to find  $M$  channels which contribute the most to a seizure. The ACS engine is executed one time only for each subject at the beginning and indexes of the  $M$  channels are stored on hard-disk. Feature extraction in both frequency and time domains is done on the  $M$  channels. Extracted features are fed to a classifier using Random Forest algorithm to discriminate interictal, ictal and early ictal epochs.

### 5.3.1 Automatic channels selection

We propose a novel approach for automatic channels selection (ACS) as follows. The approach is designed to be run offline in order to select channels for future online analysis. The labeled data is first transformed to obtain frequency information. Specifically, FFT is applied onto the raw iEEG data on all  $N$  channels. FFT values are then sliced to extract data in 1-Hz bins in the range of 1–47 Hz.  $\log_{10}$  is then applied to the magnitudes. The transformed data is a  $N \times 47$  matrix where 47 is the number of 1-Hz bins in the range of 1–47 Hz. If the channels correlation is involved in ACS stage, it will be confusing to identify which channels are the most important based on the importance level of the correlation between each pair of channels. Therefore, the correlation among channels is disregarded in this stage. Each individual channel becomes a feature to be fed to classifiers. One or a set of classifiers determine the importance level of each feature or channel. There are several options of classifiers using different ensemble algorithms such as Gradient Boosting, AdaBoost and Random Forest. If multiple classifiers are used, the final importance level of each channel is the sum of importance values obtained from all classifiers. The measure of feature importance in this work is implemented using scikit-learn ensemble library (Scikit-learn, 2014). The importance of a feature is

estimated by how often that feature is used in split points of each individual decision tree of the ensemble classifier (Scikit-learn, 2014). It is important to note that only train dataset was involved in the ACS stage.

The output of the channel selection algorithm is a set of  $M$  channels sorted based on the level of their contribution to the detection of a seizure. In this work, we selected the value of  $M$  through some experiments aiming at maximising the final AUC score. Particularly, we gradually drop channels with lowest rank and check the cross-validation performance using the rest of channels. It is important to differentiate our approach to the one proposed by Shih et al. (2009) that we are able to rank the channels prior to channel reduction. This helps us to know which channel should be dropped at each round, instead of extensively dropping one by one channel and comparing performance for all cases to decide which channel should be dropped. We also use coarse to fine approach to accelerate this selection. Typically, we start the selection by dropping 20% of channels with lowest rank until the performance decreases. Then we start next round with the number of channels present just before the aforementioned performance drops.

### 5.3.2 Feature extraction

#### Feature extraction in frequency domain

The iEEG signals from  $M$  selected channels are transformed by FFT. The transformed data then is filtered to discard high frequency noise and low frequency artifacts. Frequency range of 1–47 Hz was shown to achieve the best performance for the dataset (Hills, 2014). Eigenvalues have been used as an effective technique to discriminate ictal epochs in (Z. Zhang and Parhi, 2016; Hills, 2014; Sardouie et al., 2015). In order to compute eigenvalues, spectral power is primarily normalized over each 1-s window (zero mean and standard deviation of one) along each channel before estimating cross spectral matrix (Hills, 2014). Contrary to the Hills feature extraction, we did not use cross spectral coefficients as a feature because our empirical observation shows that such feature could worsen detection accuracy. Sample recordings and corresponding power spectrum for ictal and interictal segments of Patient–1 are illustrated in Figs. 5.2 and 5.3.

The feature set in frequency domain consists of:

- Spectral power in 1 Hz bins in range of 1–47 Hz by applying  $\log_{10}$  to the magnitude of FFT transformation, and

- Eigenvalues, sorted in descending order, of cross spectral matrix on all selected channels of the above spectral power.

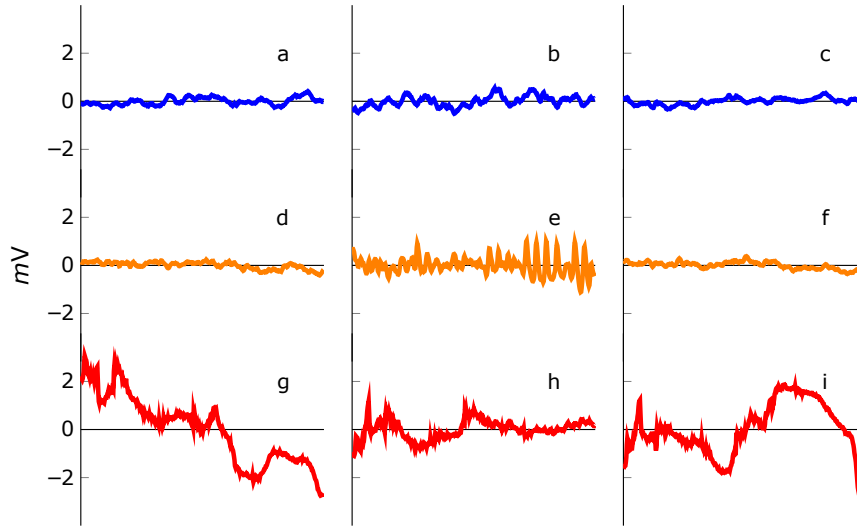


Figure 5.2: Sample 1 s iEEG recordings. (a, b and c) interictal; (d, e and f) ictal at early state (within 15 s from seizure onset); (g, h and i): ictal after early state. iEEG signals presented in one column, (e.g. a, d and g) are recorded from the same channel.

### Feature extraction in time domain

Raw iEEG signals are firstly re-sampled to 400 Hz. Similarly to frequency domain, filtered iEEG data is normalized over each 1-s window to zero mean and unity standard deviation along each channel prior to computing covariance matrix and its eigenvalues. As illustrated in Fig. 5.4, iEEG data from 16 selected channels of Patient-1 have a very low correlation to each others in interictal states. The correlation slightly increases when seizure is at early state and becomes remarkable beyond the early state.

The feature set in time domain consists of:

- Coefficients in upper triangle of correlation matrix of iEEG signals from selected channels, and
- Eigenvalues of the correlation matrix above, sorted in descending order.

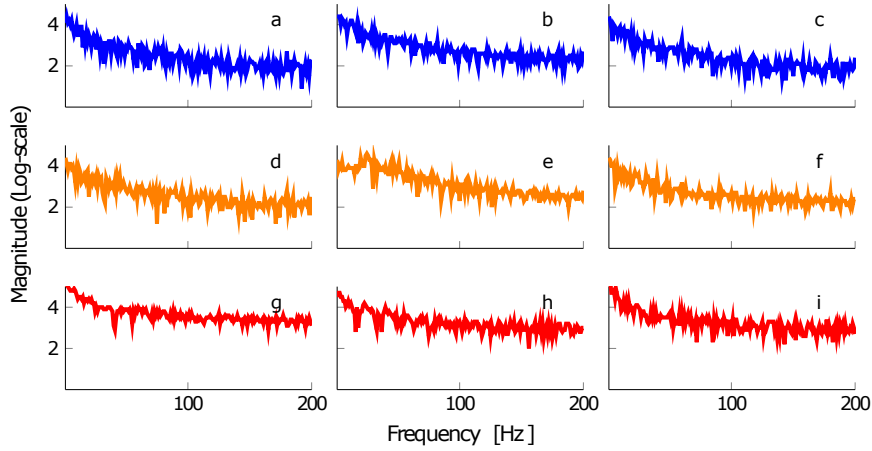


Figure 5.3: Sample 1 s iEEG recordings power spectrum. (a, b and c) interictal; (d, e and f) ictal at early state; (g, h and i): ictal after early state. iEEG signals presented in one column, (e.g. a, d and g) are recorded from the same channel. Subplots in this figure are one-by-one associated with subplots in Fig. 5.2.

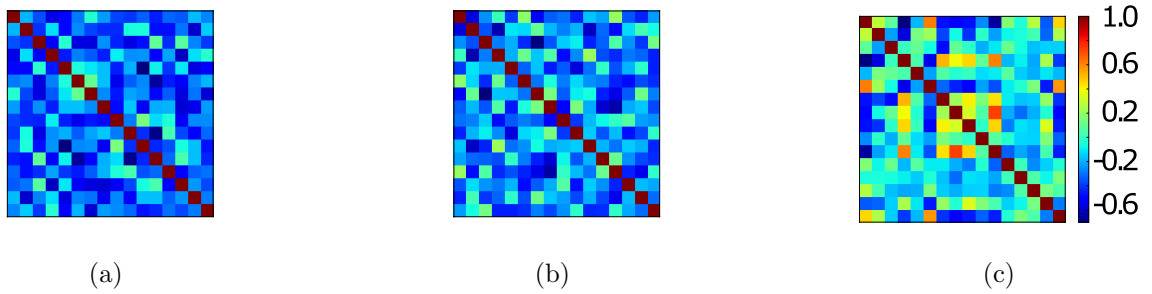


Figure 5.4: Covariance matrix: a) interictal; b) ictal at early state; c) ictal. Correlation between channels is very low in interictal period. The channels are more correlated after the seizure onset and highly correlated in ictal state.

### 5.3.3 Classifier

Random Forest algorithm was first proposed by Breiman (2001). The algorithm uses a large set of decision trees to acquire an average results. Random Forest has been shown with good performance on dataset with high dimensional datasets in biology and medical fields (Scornet, 2016; Huynh et al., 2016; Cabezas et al., 2016). This work will not go in deep about its mathematical properties as they can be found in (Breiman, 2001; Scornet, 2016) but rather on fine-tuning the parameters to achieve the highest performance with the given feature sets.

Random Forest classifier in this work is implemented using scikit-learn library

(Scikit-learn, 2014). Parameters of the classifier are reused from the approach proposed by Hills (2014) with 3000 decision trees. The classifier analyses each 1 s iEEG epoch and categorizes them into 3 classes as outputs: early ictal (ictal within 15 s from the onset), ictal, and interictal. Regarding sensitivity, specificity, F1-score and detection delay evaluation, the Random Forest classifier is adjusted from three-class classifier to binary classifier which detects whether a 1 s iEEG signal is ictal or interictal.

### 5.3.4 System evaluation

Here our method is compared with a visual inspection based focal channel selection (channels where seizures first appear) method and the variance-based method (Duun-Henriksen et al., 2012). We skip the method introduced by Shih et al. (2009) because we have high number of channels, the greedy backward elimination method becomes impractical. For patient-4 with 72 channels, for example, we need to evaluate a factorial of 72 subsets in the worst case. Though we can stop the search when the performance of subsets starts to drop, the number of cases to be analyzed is still huge.

Metrics used to test the proposed approach are area under the receiver operating characteristic curve (AUC), sensitivity, specificity, F1-score and onset detection delay. To have a robust evaluation, we follow a leave-one-out cross-validation approach for each subject. If a subject has  $\mathcal{N}$  seizures,  $(\mathcal{N} - 1)$  seizures will be used for training and the withheld seizure for validation. This round is repeated  $\mathcal{N}$  times so all seizures will be used for validation exactly one time. Interictal segments are randomly split into  $\mathcal{N}$  parts.  $(\mathcal{N} - 1)$  parts are used for training and the rest for validation. The metrics to be reported are the average of all rounds. The cross-validation will be based on the labeled iEEG dataset of 7.2 hours. We will also test the system after being trained by 7.2 hours of labeled iEEG data with the hidden dataset consisting of 9.14 hours of unlabeled iEEG data provided by Kaggle.

The dataset used in this work is from a competition to detect whether a given 1 s iEEG segment represents a seizure and whether that segment is within the first 15 s (early) of its respective seizure. The overall AUC is the average of the two AUC scores of the two detections (Kaggle, 2014b), and is given by

$$\text{AUC} = \frac{1}{2}(\text{AUC}_S + \text{AUC}_E), \quad (5.1)$$

where,

- $\text{AUC}_S$  is AUC for two classes: ictal (including early seizure) and interictal, and

- $AUC_E$  is AUC for two classes: early seizure and non-early-seizure (including ictal states after 15 s from onset and interictal states).

Sensitivity, specificity and F1-score are commonly used in evaluating a seizure detection system and are given by

$$\text{Sensitivity (or Recall)} = \frac{TP}{TP + FN} \quad (5.2)$$

$$\text{Specificity} = \frac{TN}{TN + FP} \quad (5.3)$$

$$\text{Precision} = \frac{TP}{TP + FP} \quad (5.4)$$

$$\text{F1-score} = 2 \times \frac{\text{Precision} \times \text{Recall}}{\text{Precision} + \text{Recall}}, \quad (5.5)$$

where,

- $TP$  is the total number of 1 s ictal segments are correctly classified as ictal, and
- $TN$  is the total number of 1 s interictal segments are correctly classified as interictal, and
- $FP$  is the total number of 1 s interictal segments are wrongly classified as ictal, and
- $FN$  is the total number of 1 s ictal segments are wrongly classified as interictal.

## 5.4 Results

Using same setup proposed by Duun-Henriksen et al. (2012), 3 channels are selected for each method. Fig. 5.5 illustrates the iEEG signal from seizure onset for a seizure of Dog-1. For this subject, selected channels using focal, variance-based, and our methods are (9, 10, 13), (3, 8, 9), and (4, 10, 12) respectively. A completed set of channels selected using the three methods is presented in Table A1. To benchmark the efficiency of the three methods, we calculated AUC through leave-one-out cross-validation as shown in Fig. 5.6 and more details in Table 5.3. As seen from Fig. 5.6, our method is better than the other two. Here we use a two-tailed signed rank test at a significance level

of 0.05 to compare the three methods. Since there are multiple comparisons, the significance level should be adjusted to be  $0.05/3 = 0.01667$  using Bonferroni correction. A two-tailed signed rank test on AUC scores of focal channel method and our method has p-value of 0.373 which indicates that the two methods has no statistical difference at the adjusted significance level of 0.01667. However, the same test between variance-based method and our method shows a significant result at p-value of 0.0076. This result confirms our channel selection method superior to the variance-based method proposed by Duun-Henriksen et al. (2012).

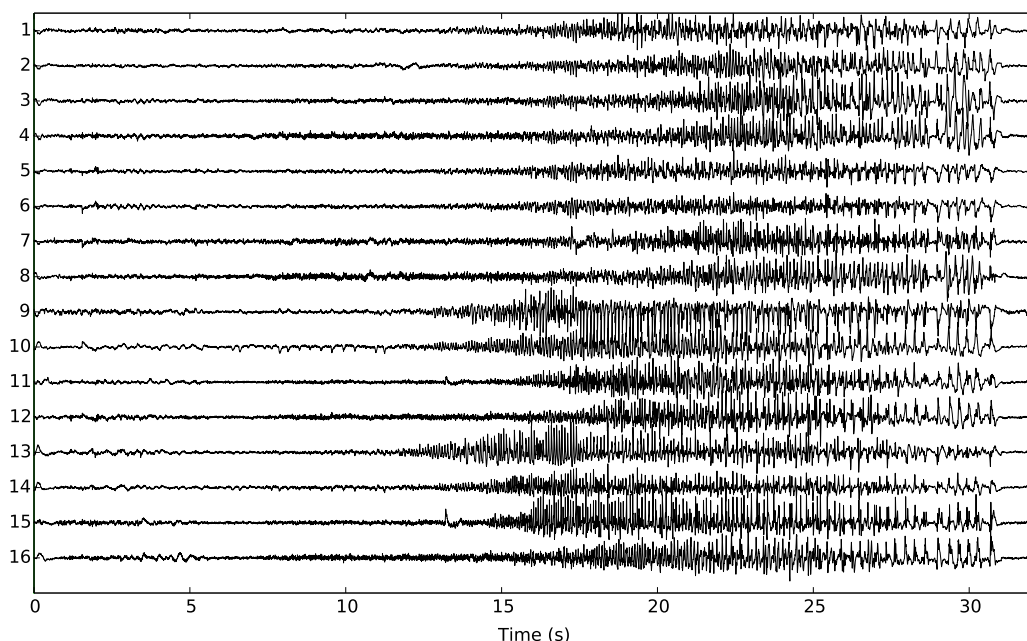


Figure 5.5: iEEG recording of a seizure since its onset from Dog-1. Selected channels using focal, variance-based, and our methods are (9, 10, 13), (3, 8, 9). and (4, 10, 12) respectively.

We now compare the efficacy of the proposed method with the current state-of-the-art method proposed by Hills (2014) on the same dataset. The algorithm was implemented in Python 2.7 in Ubuntu 14.04 LTS. Random Forest classifier was implemented using *scikit-learn* library (Scikit-learn, 2014). FFT was performed with *numpy* library. All simulations were performed on a workstation with CPU Xeon (4 cores enabled) and 16 GB of RAM. Using our approach, average number of channels can be reduced from 35.1 to 10.3. Consequently, training time and test time are improved by 39.2% and 49.7% respectively (see Table 5.4). With 49.7% reduction in test time, our seizure detection system is 2 times faster at run-time than Hills approach. Therefore, the automatic

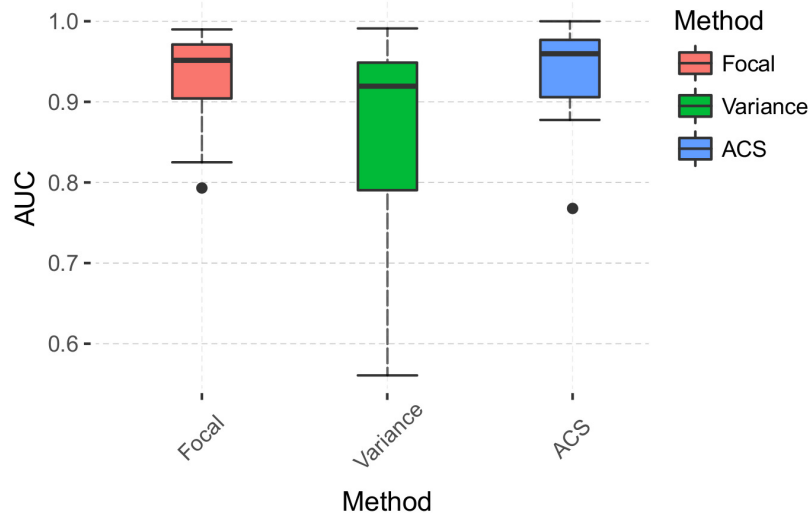


Figure 5.6: Channel selection method comparison on overall AUC scores. The dots are for outliers. Focal: focal channel method; Variance: variance-based method; ACS: automatic channel selection (our method).

channel selection is promising for real-time seizure detection application.

Table A2 describes the comparison between the state-of-the-art and proposed method on AUC, sensitivity, specificity, F1-score and onset detection delay for the modified leave-one-out cross-validation applied to the training set. Regarding sensitivity and specificity evaluation, the Random Forest classifier is adjusted from three-class classifier to binary classifier which detects whether a 1 s iEEG signal is ictal or interictal. The classifier’s outputs range from 0 to 1 indicating how likely the input signal is ictal. The threshold of the classifier’s output used to separate whether a 1 s iEEG segment is ictal or interictal was determined per subject. The value of threshold was selected to achieve the balance between sensitivity and specificity (ie., the higher threshold value yields the higher specificity but the lower sensitivity and vice versa). Moreover, the threshold selection must result in similar specificity scores across the methods to have a meaningful sensitivity and mean detection delay comparisons. As seen from Table A2, our proposed method achieved better score on all metrics though not significant. However, the proposed method yields a considerable improvement in mean onset detection delay. Onset detection delay indicates the time in seconds after that the classifier can detect a seizure onset. Delay is 1 s if the first 1 s ictal iEEG segment at seizure onset can be correctly detected. Since iEEG signals are divided into 1 s epochs, the minimum onset detection delay could be achieved is 1 s. Our work has a mean detection delay of 3.31 s

Table 5.3: Comparison among three channel selection methods.

Subject	Focal channel			Variance-based			Proposed method		
	$AUC_E$ (%)	$AUC_S$ (%)	AUC (%)	$AUC_E$ (%)	$AUC_S$ (%)	AUC (%)	$AUC_E$ (%)	$AUC_S$ (%)	AUC (%)
Dog-1	95.02	98.46	96.74	95.03	98.47	96.75	94.79	98.44	96.62
Dog-2	92.32	95.20	93.76	91.31	96.74	94.03	94.35	96.30	95.32
Dog-3	95.72	98.92	97.32	92.05	98.02	95.03	95.90	98.88	97.39
Dog-4	98.76	91.11	94.94	98.49	89.15	93.82	98.79	94.62	96.71
Patient-1	94.29	96.46	95.38	71.72	89.77	80.75	82.03	93.49	87.76
Patient-2	99.22	98.75	98.98	99.20	99.04	99.12	99.17	98.72	98.95
Patient-3	88.62	92.75	90.68	87.89	92.25	90.07	87.61	94.68	91.15
Patient-4	97.05	97.05	97.05	94.82	94.82	94.82	100	100	100
Patient-5	76.69	88.31	82.50	65.86	77.16	71.51	69.73	83.83	76.78
Patient-6	97.33	99.51	98.42	74.48	87.75	81.11	97.56	99.61	98.58
Patient-7	79.22	79.41	79.32	71.13	76.75	73.94	89.21	94.24	91.72
Patient-8	81.29	97.99	89.64	27.37	84.76	56.07	80.06	97.71	88.88
Average	91.29	94.49	92.89	80.78	90.39	85.59	90.77	95.88	93.32

which is comparable with that of Hills method. Fig. 5.7 demonstrates the advantages of the proposed method in terms of processing time, number of channels to be analyzed and detection delay.

We also test our method with the unlabeled dataset from the Kaggle competition. Labels for this dataset is not publicly available. The Kaggle competition organizers provided us the labels so we are able to evaluate the performance metrics per subject. Table A3 describes the seizure detection performance on the unlabeled dataset. It is non-trivial to note that all the thresholds were kept the same as they were during the cross-validation. A two-tailed signed rank test on the AUC between Hills and our methods result in a  $p$ -value of 0.6599 which means the difference is not significant at  $p$ -value  $< 0.05$ . F1-scores of the two methods are comparable. Our method has sensitivity of 89.40%, specificity of 89.24% and mean detection delay of 2.63 s. Since our proposed method has better specificity but worse sensitivity, comparison on detection delay may not be meaningful here. However, both methods achieve a good mean detection delay at less than 3 seconds. Finally, the overall AUC score across all subject of our method is 96.94%, slightly higher than that of Hills method at 96.29%.

## 5.5 Discussions

We presented a seizure detection method based on a novel approach for automatic iEEG channel selection that provides comparable performance to the state-of-the-art method for the dataset considered. Although this leads to an extra overhead computing time

Table 5.4: Comparison between state-of-the-art and proposed method on computational efficiency.

Subject	No. of electrodes	$M$	Training data (min)	Test data (min)	(Hills, 2014)		Proposed method			Training time improvement	Test time improvement
					Training <sup>†</sup> (s)	Test <sup>◊</sup> (s)	ACS* (s)	Training <sup>†</sup> (s)	Test <sup>◊</sup> (s)		
Dog-1	16	9	9.9	53	24.9	18	6.3	22.8	13.5	8.43%	25.00%
Dog-2	16	10	22	50	66	15.3	15.4	56.1	11.8	15.00%	22.88%
Dog-3	16	8	87.3	74.2	365.5	22.6	78.1	245	14.7	32.97%	34.96%
Dog-4	16	13	50.8	50.2	159.8	16.7	37.7	135.7	14.9	15.08%	10.78%
Patient-1	68	16	2.9	34.2	19	54.9	4.9	14.5	16.3	23.68%	70.31%
Patient-2	16	11	52.4	64.9	138.4	41.8	39.7	97	25.5	29.91%	39.00%
Patient-3	55	8	17.4	21.4	120.2	49.5	32.4	53	13.7	55.91%	72.32%
Patient-4	72	4	3.5	9.1	23.5	32.1	7.9	12.1	8.7	48.51%	72.9%
Patient-5	64	16	45.8	49.8	652.1	136.3	119.7	197	35.5	69.79%	73.95%
Patient-6	30	8	50	50	202.7	57.9	57.5	73.4	20.8	63.79%	64.08%
Patient-7	36	13	58.7	60	523.8	87.2	119.8	223.6	30	57.31%	65.6%
Patient-8	16	8	31.5	32	82.5	21.9	23.1	51.2	12.2	37.94%	44.29%
<b>Average</b>	<b>35.1</b>	<b>10.3</b>								<b>38.19%</b>	<b>49.67%</b>

\* Automatic channel selection (ACS) time.

† Training time includes time for feature extraction and classifier training.

◊ Test time includes time for feature extraction and classification.

in the beginning, the impact overall processing time is negligible because the channel selection need only be computed offline for each subject, before any future online seizure detection would be performed. One may argue that different channels may provide better performance over time; hence, channel selection is necessary over time. For the current dataset which was linked to a Kaggle seizure detection competition and downloaded from Kaggle (2014b), the precise information about the times of the inter-seizure and seizure windows is not available. Therefore, investigating channel selection over time is not possible with this dataset. In our approach, data collected in real-time implementation would be transferred from a seizure control implant for off-line processing to update approximately every 1–6 months the optimal seizure detection channel for use during real-time implementation. The advantages of the automatic channel selection, on the other hand, are remarkable. Firstly, redundant and unrelated iEEG signals are eliminated which helps to improve efficacy of seizure detection system. Secondly, since the amount of data to processed is reduced, the processing time is also reduced. Gain in computational complexity becomes visible and significant for subjects with large number of channels. For instance, by reducing number of channels to be analyzed from 64 to 16 for Patient-5 (see Table 5.4, classification time can be improved by 74%. Depending on the practical use, more speed can be achieved at the cost of performance.

Our channel selection method showed significantly better performance compared to the variance-based method proposed by Duun-Henriksen et al. (2012). Although the focal channel method has comparable performance with our method, it is more

demanding to select focal channels for subjects with large number of channels. We can use our channel selection method to automatically select channels whereas selecting focal channels requires visual inspection by a neurophysiologist. In the scenario where we continuously collect data and re-select the best channels every 1–6 months, an offline automated approach may be more cost/time effective with regards to person hours and neurophysiologist time. In other words, there are more offline computation hours but more importantly less time spent by clinical staff labeling data so they can pay more attention to the other needs of their patients. Moreover, our method has an important advantage over approaches proposed by Minasyan et al. (2010) and Subasi and Ismail Gursoy (2010) since our automatic channel selection only runs during training phase, not in run-time classification.

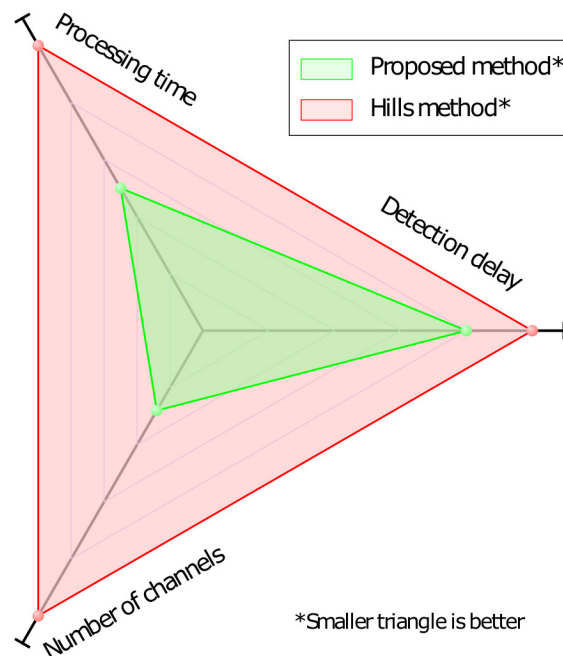


Figure 5.7: Comparison between the method reported by Hills (2014) and the proposed method in terms of detection delay, number of processed channels and processing time.

Spectral power, correlation matrix and its eigenvalues on iEEG channels in both frequency and time domains have been shown as important features in seizure detection using iEEG recordings. The proposed subject-specific approach has a mean seizure onset detection delay of 2.63 s that is critical, for example, for an electrical stimulator to suppress the seizure on time.

## 5.6 Conclusion

Detection of seizure, especially at its early state, is crucial for patients who cannot be treated by drugs or surgery. Precise seizure detection allows electrical stimulation to timely interrupt the alteration of consciousness and subsequent convulsions. Although high performing seizure detectors are available, translating state-of-the-art seizure detection methods into battery-saving hardware implementations in implantable seizure control devices requires greater gains in computational efficiency. This work proposed automatic channels selection engine as a mechanism to adequately determine most informative iEEG recordings prior to feature extraction. The engine gave rise to significant computational efficiency improvements on subjects having large number of recording channels. The overall results of the proposed method were comparable with that of the state-of-the-art while it save 49.4% of the processing time and reduced the average number of channels requiring analysis by 71%, both critical factors for real-world applications.

## Acknowledgement

The authors appreciate Dr Benjamin H. Brinkmann support from Mayo Systems Electrophysiology Lab for providing information on some unlabeled datasets. N. Truong acknowledges The Commonwealth Scientific and Industrial Research Organisation (CSIRO) partial financial support via a PhD Scholarship, PN 50041400. J. Yang acknowledges National Natural Science Foundation of China for their financial support under Grant 61501332.

## Appendix

Table A1: Channels selected using the three channel selection methods.

	Focal channel	Variance-based	Our method
Dog-1	(9, 10, 13)	(3, 8, 9)	(4, 10, 12)
Dog-2	(1, 5, 13)	(1, 2, 5)	(1, 9, 12)
Dog-3	(8, 13, 14)	(1, 4, 9)	(7, 13, 14)
Dog-4	(1, 5, 13)	(2, 7, 9)	(7, 8, 15)
Patient-1	(11, 13, 14)	(1, 27, 44)	(19, 27, 30)
Patient-2	(1, 2, 3)	(1, 2, 3)	(1, 2, 3)
Patient-3	(5, 9, 14)	(5, 9, 11)	(5, 6, 26)
Patient-4	(7, 10, 15)	(26, 31, 47)	(37, 45, 66)
Patient-5	(5, 9, 12)	(10, 12, 49)	(9, 18, 25)
Patient-6	(2, 8, 15)	(2, 9, 18)	(15, 23, 24)
Patient-7	(8, 11, 15)	(7, 8, 28)	(26, 28, 36)
Patient-8	(3, 10, 11)	(2, 3, 4)	(3, 10, 11)

Table A2: Comparison between state-of-the-art and proposed method on AUC, sensitivity (SEN), specificity (SPE) and F1-score for binary classification of seizure and non-seizure states for the modified leave-one-out cross-validation of the training set. Threshold values were chosen to achieve best SEN-SPE balance and similar specificity scores between the two methods. This helps the sensitivity and mean detection delay comparisons meaningful.

Subject	(Hills, 2014)								Proposed method							
	$AUC_E$ (%)	$AUC_S$ (%)	AUC (%)	SEN (%)	SPE (%)	F1 (%)	Delay (s)	Thres.	$AUC_E$ (%)	$AUC_S$ (%)	AUC (%)	SEN (%)	SPE (%)	F1 (%)	Delay (s)	Thres.
Dog-1	98.53	99.69	99.11	96.79	99.29	97.49	1.60	0.30	97.79	99.43	98.77	96.79	98.81	96.96	1.60	0.29
Dog-2	97.47	99.66	98.57	87.68	99.30	91.00	2.00	0.28	99.58	99.58	98.58	90.86	98.87	91.41	1.00	0.26
Dog-3	97.76	99.58	98.67	95.21	98.17	89.20	2.08	0.28	96.71	99.25	98.08	92.08	98.34	88.16	3.08	0.35
Dog-4	99.86	97.15	98.51	57.06	99.28	69.49	1.00	0.26	99.70	97.34	98.56	69.54	98.03	73.11	1.00	0.20
Patient-1	90.94	98.13	94.54	91.03	96.15	92.27	4.50	0.41	95.06	98.32	97.27	92.31	97.12	93.64	4.00	0.59
Patient-2	99.37	99.50	99.43	94.72	99.00	88.14	1.33	0.26	99.34	99.40	99.42	94.72	99.03	88.49	1.33	0.26
Patient-3	88.50	95.34	91.92	78.00	92.44	74.87	6.00	0.37	88.25	93.61	90.25	76.21	92.16	73.42	7.57	0.45
Patient-4	100	100	100	100	100	100	1.00	0.21	99.63	99.63	100	95.00	97.89	88.31	1.00	0.50
Patient-5	84.20	88.82	86.51	58.52	99.08	56.88	18.00	0.23	87.72	91.19	90.45	62.96	99.20	62.16	5.00	0.22
Patient-6	98.73	99.82	99.27	97.35	98.48	90.11	2.25	0.22	98.66	99.79	99.28	96.89	99.49	95.39	2.25	0.36
Patient-7	87.33	90.10	88.72	66.63	99.35	65.49	7.33	0.14	92.31	94.61	93.20	66.63	99.69	66.64	7.33	0.27
Patient-8	81.46	97.82	89.64	92.78	97.13	84.36	4.50	0.22	78.78	98.03	88.52	94.44	97.54	86.74	4.50	0.26
Average	93.68	97.14	95.41	84.65	98.14	83.27	4.30		94.46	97.52	96.03	85.70	98.01	83.70	3.31	

Table A3: Comparison between state-of-the-art and proposed method on AUC, sensitivity (SEN), specificity (SPE) and F1-score for binary classification of seizure and non-seizure states for the unlabeled dataset. The threshold values were kept the same as being used during cross-validation. The total AUC is the AUC estimated across all the subjects.

Subject	(Hills, 2014)								Proposed method							
	$AUC_E$ (%)	$AUC_S$ (%)	AUC (%)	SEN (%)	SPE (%)	F1 (%)	Delay (s)	Thres.	$AUC_E$ (%)	$AUC_S$ (%)	AUC (%)	SEN (%)	SPE (%)	F1 (%)	Delay (s)	Thres.
Dog-1	98.80	99.63	99.22	93.08	99.47	91.64	2.75	0.30	97.70	99.12	98.41	92.45	99.57	92.16	2.75	0.29
Dog-2	97.65	96.86	97.26	100	32.27	13.63	1.00	0.28	92.98	95.45	94.22	97.37	40.67	14.89	1.50	0.26
Dog-3	94.51	98.47	96.49	93.50	97.43	85.19	1.70	0.28	92.62	97.69	95.16	89.75	97.56	83.68	1.70	0.35
Dog-4	99.79	99.61	99.70	100	67.07	20.82	1.00	0.26	99.76	98.92	99.34	100	65.75	20.18	1.00	0.20
Patient-1	98.15	99.32	98.74	98.70	98.46	91.22	1.14	0.41	97.07	99.80	98.44	92.02	99.52	93.17	1.57	0.59
Patient-2	98.93	99.73	99.33	96.51	99.07	91.32	1.50	0.26	98.98	99.72	99.35	96.07	99.05	90.91	1.50	0.26
Patient-3	73.37	95.01	84.19	90.62	88.29	61.21	2.50	0.37	85.39	96.14	90.77	85.16	95.58	75.69	3.00	0.45
Patient-4	67.50	67.50	67.50	48.00	80.73	28.40	1.00	0.21	61.84	61.84	61.84	52	84.38	33.99	1.00	0.50
Patient-5	88.10	95.75	91.93	86.90	98.33	80.89	6.50	0.23	80.60	93.71	87.16	88.10	90.92	51.75	6.00	0.22
Patient-6	98.10	99.86	98.98	93.18	99.39	92.76	1.00	0.22	98.50	99.90	99.20	88.18	99.93	93.27	3.00	0.36
Patient-7	99.83	99.99	99.91	100	98.89	95.24	1.00	0.14	99.81	99.98	99.90	98.89	99.72	98.21	1.00	0.27
Patient-8	86.48	98.15	92.32	92.78	97.93	87.21	7.50	0.22	86.59	98.08	92.34	92.78	98.22	88.36	7.50	0.26
Average	91.77	95.82	93.80	91.11	88.11	69.96	2.38		90.99	95.03	93.01	89.40	89.24	69.69	2.63	
Total		96.29								96.94						

## Chapter 6

# Hardware-friendly deep learning for seizure detection

The content presented in this chapter is published as:

- Truong, N. D., A. D. Nguyen, L. Kuhlmann, M. R. Bonyadi, J. Yang, S. Ippolito, and O. Kavehei (2018). “Integer Convolutional Neural Network for Seizure Detection.” *IEEE Journal on Emerging and Selected Topics in Circuits and Systems* 8.4, 849-857. DOI:10.1109/JETCAS.2018.2842761.

### **Statement of Contributions of Joint Authorship**

- Nhan Duy Truong (Candidate): First author, completed the analysis, writing, reviewing and editing of the manuscript
- Anh Duy Nguyen: aided in the analysis, writing, reviewing and editing of the manuscript
- Levin Kuhlmann: aided in the analysis, reviewing and editing the manuscript
- Mohammad Reza Bonyadi: aided in the analysis, reviewing and editing the manuscript
- Jiawei Yang: provided technical advice on the analysis, reviewing and editing the manuscript
- Omid Kavehei (Principal Supervisor): provided the main idea, reviewing and editing the manuscript

In addition to the statements above, in cases where I am not the corresponding author of a published item, permission to include the published material has been granted by the corresponding author.

Nhan Duy Truong

Date: 01 October 2019

As supervisor for the candidature upon which this thesis is based, I can confirm that the authorship attribution statements above are correct.

Dr. Omid Kavehei

Date: 01 October 2019

Outstanding seizure detection algorithms have been developed over the past three decades. Despite this success, their implementations as part of implantable or wearable devices are still limited. These works are mainly based on heavily handcrafted feature extraction, which is computationally expensive and is shown to be dataset specific. These issues greatly limit the applicability of such methods to hardware implementation, including in-silicon implementations such as application specific integrated circuits (ASIC). In this work, we propose an integer convolutional neural network (CNN) implementation, Integer-Net, as a memory-efficient unified hardware-friendly CNN framework. The performance of Integer-Net is evaluated with multiple time-series datasets consisting of intracranial and scalp electroencephalogram (EEG) signals. Integer-Net shows a consistent seizure detection performance across three datasets: Freiburg Hospital intracranial EEG (iEEG) dataset, Children’s Hospital of Boston-MIT scalp EEG (sEEG) dataset, and UPenn and Mayo Clinic’s seizure detection dataset. Our experimental results show that a 4-bit Integer-Net leads to only 2% drop of accuracy compared to a 32-bit real-value resolution CNN model, while offering more than 7 times improvement in memory efficiency. We discuss the structure of the integer convolution to improve computational gain and reduce inference time that are crucial for real-time application.

## 6.1 Introduction

Epileptic seizure affects nearly 1% of the world’s population but about two thirds can be treated by drugs and another 7–8% can be cured by surgery (Litt and Echauz, 2002). Therefore, epileptic seizure detection and subsequent system for warning and/or suppressing seizure become critical for the patients with refractory epilepsy. Over the past two decades many EEG based seizure detection techniques and hardware implementations have been proposed.

Most of low-power seizure detectors are based on simple methods including voltage-level threshold, line length (Raghunathan, Gupta, Ward, et al., 2009; Patel et al., 2009; Salam et al., 2011). Higher accuracy seizure detection methods employ time-frequency domain analysis that implies higher computational cost. Wavelet-based filters were utilized as a powerful tool to extract features in both frequency and time domains as well as an effective de-noising technique (Saab and Gotman, 2005; Kuhlmann, Burkitt, et al., 2009; Tieng et al., 2016). Another effective method to extract features from EEG signals in both frequency and time domains concurrently is Short-Time Fourier Transform (Samiee et al., 2015). With less computational complexity, Fast

Fourier Transform (FFT) has been shown as an effective feature engineering in many studies. However, to achieve high seizure detection performance, FFT is usually used with Support Vector Machine that is highly computational (Hills, 2014; Parvez and Paul, 2015; Verma et al., 2010). Though these methods have outstanding performance, i.e., sensitivity and specificity of 95% or above (Hills, 2014; Parvez and Paul, 2015; Tieng et al., 2016), they have limitations on implantable or portable hardware implementation because of high computation.

Deep learning and its most popular architecture, convolutional neural network, have been shown as an outstanding method for solving different tasks in computer vision and language processing (Krizhevsky et al., 2012; Sainath et al., 2013). Recently, a recurrent convolutional neural network with spectral magnitude and spatial information of electrodes as inputs can achieve performance at state-of-the-art level for seizure detection (Thodoroff et al., 2016). Particularly, the authors projected the magnitude of 3 frequency bands spanning the range of 0–49 Hz of each 1 s EEG window onto electrodes map. Their work reached 95–100% sensitivity range with patient-specific model and false positive rate less than 0.3/hour. Regarding cross patient seizure detection, the method achieved 85% sensitivity and false positive rate of 0.8/hour. In this work, we propose a convolutional neural network (CNN) structure that can perform well the seizure detection task based on both intracranial and scalp EEG but we put more focus on the applicability of CNN on a low-power device. One limitation that makes implementation of convolutional neural networks (or neural networks in general) difficult is the excessively large number of parameters, which is partially responsible for computational complexity of these algorithms. Existing techniques for reducing weight storage (memory) and computational complexity have been discussed intensively. The most common approach is to compress a pre-trained network by iteratively pruning connections and/or quantizing trained weights (Han, Pool, et al., 2015; Han, Mao, et al., 2015). Another approach is to design compact neural network by decomposing convolutional kernels into smaller ones (Iandola et al., 2016; Szegedy et al., 2017). A novel method, which is pursued in this work and is inspired by Rastegari et al. (2016), is to quantize weights during training phase. Our contributions in this work include:

- Introducing Integer-Net<sup>1</sup>, a CNN-based model with integer inputs and weights, and
- Proposing a CNN structure for seizure detection working well across multiple electroencephalogram (EEG) datasets, and evaluating performance of the

---

<sup>1</sup>Integer-Net on GitHub source code: <https://git.io/vbbul>

Integer-Net using the aforementioned datasets.

## 6.2 Dataset

In this work, we would like to determine if electrical brain activity either corresponds to epileptic seizure (ictal) activity or interictal data (the data between seizures) using three datasets: Freiburg Hospital (University of Freiburg, 2003), CHB-MIT (Shoeb, 2009) and UPenn and Mayo Clinic seizure detection (Kaggle, 2014b) datasets. The Freiburg dataset consists of intracranial EEG (iEEG) recordings at 256 Hz sampling rate from 21 patients with intractable epilepsy (University of Freiburg, 2003). Due to lack of availability of whole dataset, we were only able to use data from 13 patients with 59 seizures and 311.4 interictal hours in total. In this dataset, iEEG data is from 6 selected electrodes where three of them are from epileptogenic regions and the other three are from other remote regions. For each patient, there are 3 to 5 seizures and 24 hours of interictal (Maiwald et al., 2004).

CHB-MIT dataset contains scalp EEG (sEEG) data of 23 pediatric patients at the Children’s Hospital, Boston. The dataset consists of 844 hours of continuous sEEG recording and 163 seizures (Shoeb, 2009). Scalp EEG signals were captured using 22 electrodes for most patients and at sampling rate of 256 Hz (Shoeb, 2009). We define interictal periods that are at least 4 hours away before seizure onset and after seizure ending. In addition, patient 12 was excluded from this work because we were unable to read EEG recordings of this patient.

UPenn and Mayo Clinic’s seizure detection (Kaggle) dataset has iEEG data of 4 canines and 8 patients with epileptic seizures (Kaggle, 2014b). iEEG signals were recorded from 16 electrodes at 400 Hz for dogs, and from varying number of electrodes (from 16 to 72) for patients. This dataset consists of 48 seizures and 6.5 hours of interictal data. The data was pre-organized into 1 s epochs (S. N. Baldassano et al., 2017). We apply the same 1 s windowing to the other two datasets for consistency. Our models will be also tested with a test dataset consisting of 9.14 hours of unlabeled iEEG signals provided by Kaggle.

## 6.3 Proposed method

### 6.3.1 Pre-processing

We use Fast Fourier Transform (FFT) to translate each 1 s window of raw EEG signal into frequency domain. Most of EEG recording signals were contaminated by power line noise at 50 Hz for Freiburg dataset and 60 Hz for CHB-MIT dataset. In the frequency domain, it is convenient to effectively filter out the power line noise by excluding frequency bands of 47–53 Hz and 97–103 Hz for 50 Hz noise and frequency bands of 57–63 Hz and 117–123 Hz for 60 Hz noise. The DC component (0 Hz) was also removed for all three datasets.

Imbalanced number of instances in each class introduces a challenge in many classification tasks (Branco et al., 2016). As this issue presents also in seizure detection (e.g. in UPenn and Mayo Clinic’s dataset, interictal to ictal ratio per subject is 10 : 1 on average), we generate extra ictal segments by using overlapping technique during training phase. In particular, we slide a 1 s window along time axis at every step,  $S$ , over ictal time-series EEG signals (see Fig. 6.1).  $S$  is chosen per each subject so that we have similar number of samples per each class (ictal or interictal) in training set.

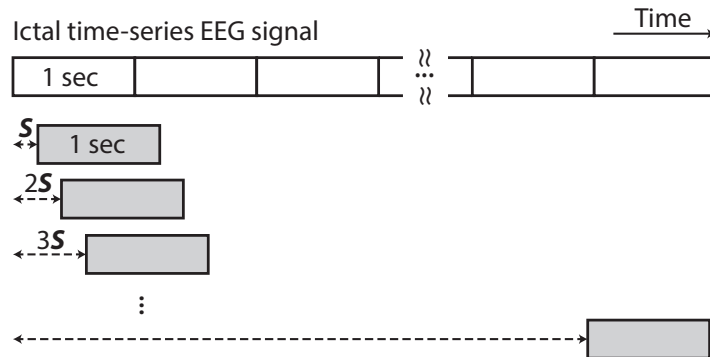


Figure 6.1: Generate extra ictal segments to balance the training dataset by sliding a 1 s window along time axis at every step  $S$  over ictal signals.  $S$  is chosen per each subject so that there are similar number of samples per each class (ictal or interictal) in training set.

### 6.3.2 Integer-Net: An integer convolutional neural network

In this section, we present an alternative implementation of convolutional neural network (CNN) that is more hardware-friendly. In the recent years, CNN has shown its

outstanding capability in recognizing patterns and extracting features in computer vision and language processing (Krizhevsky et al., 2012; Sainath et al., 2013). A typical CNN network consists of convolution layers followed by fully-connected layers (LeCun et al., 1990). A convolution layer has a set of filters, often called as kernels, each of which is convolved with input to generate a set of feature maps (output). A non-linear activation function is often introduced at the end of each convolution layer. A fully-connected layer is a regular neural network’s layer where each neuron is connected to all outputs of previous layer. Since CNN is involved with high computational complexity that limits its applicability on low-power hardware, there has been an increasing need for more hardware-friendly implementations of CNN. In general, hardware-friendly CNN structures (Courbariaux et al., 2015; Rastegari et al., 2016) aim at reducing the computational complexity and increasing memory efficiency, while maintaining the performance of the algorithm. Our Integer-Net is inspired by XNOR-Net, (Rastegari et al., 2016), and provides an additional flexibility to adjust accuracy with a cost of efficiency. Integer-Net supports integer value inputs and weights that are quantized during the training phase. Number of bits representing an integer is configurable. Integer inputs and weights are used in forward pass to speed up inference time. Real value weights are retained during training for gradient calculation and weight update. In other words, Integer-Net will not benefit the training phase. The Integer-Net is implemented in Python 2.7 with use of Tensorflow 1.4.0 and trained on an NVIDIA K80 graphics card. It is worth noting that, beyond training and in the inference phase (forward propagation), only integer weights are involved in computation and all the real value weights for training can be safely removed.

The idea behind the Integer-Net is to approximate convolution and matrix multiplication of floating matrices by performing those operations with integer values. Operation of an Integer-Net is described in Algorithm 1. Suppose we need to ”integerize” input  $I$  and weights  $W$  into  $n$ -bit integers for a matrix multiplication, i.e. dot product,  $I \cdot W$  where  $I, W \in \mathbb{R}^2$ .

$$I^i = \text{Integerize}(I) = \text{round} \left( \frac{I}{\max(|I|)} \times 2^n \right), \quad (6.1)$$

$$W^i = \text{Integerize}(W) = \text{round} \left( \frac{W}{\max(|W|)} \times 2^n \right), \quad (6.2)$$

where  $\max(|I|)$  and  $\max(|W|)$  are the maximum magnitude of input  $I$  and weights  $W$ , respectively.

Matrix multiplication,  $I \cdot W$ , can now be approximated as

$$I \cdot W \approx \alpha_I \alpha_W I^i \cdot W^i , \quad (6.3)$$

where  $\alpha_I$  and  $\alpha_W$  are floating-point scalars calculated by

$$\alpha_I = \frac{\max(|I|)}{2^n} , \quad (6.4)$$

$$\alpha_W = \frac{\max(|W|)}{2^n} . \quad (6.5)$$

Using these approximations, we integerize inputs and weights. Outputs of the fully-connected layer,  $\mathcal{O}_{FC}$ , can also be approximated by

$$\mathcal{O}_{FC} = \text{Activation} (\alpha_W \alpha_I I^i \cdot W^i) . \quad (6.6)$$

We conduct similar steps for convolution layers except that scale coefficients,  $A_{Ic}$ , of input have to be calculated according to the regions where convolution filters are applied. In the other words, input scale coefficients of convolution layers are matrices, where each element corresponds to a position of the filter being applied on the input. This can be done by convolving the input with a matrix of ones,  $M$ , with same size of convolution filter (as also used in (Ding, 2017)) divided it by  $2^n$ , as shown below

$$A_{Ic} = \frac{\max |I| * M}{2^n} . \quad (6.7)$$

Subsequently, output of a convolution layer,  $\mathcal{O}_{CONV}$ , can be approximated by integer inputs and weights as

$$\mathcal{O}_{CONV} = \text{Activation} (\alpha_W A_{Ic} \circ (I^i * W^i)) , \quad (6.8)$$

where  $\circ$  is the Hadamard product and  $*$  is the convolution operator.

The Integer-Net is fundamentally different from a quantized neural network in the training phase. In case of the quantized neural network, the cost function is calculated with the use of real value weights. Once the training is done, the weights are quantized to lower precision. The quantized weights, therefore, lack connections with the cost function that leads to a re-training step to boost the accuracy after quantization (Joulin et al., 2016). Regarding the Integer-Net, the cost function being minimized during

---

**Algorithm 1** Integer-Net training

---

**Require:** Mini-batch of inputs  $I$ , cost function  $C$ , current real-value weight  $W$  and layer output  $O$ .

- 1: **for** each layer  $l$  **do**
  - 2:     **if** convolution layer **then**
  - 3:         **if**  $l == 1$  **then** ▷ First layer
  - 4:              $A_{Ic} \leftarrow \frac{\max |I| * M}{2^n}$
  - 5:              $I^i \leftarrow \text{Integerize}(I)$
  - 6:         **else**
  - 7:              $A_{Ic} \leftarrow \frac{\max |O_{l-1}| * M}{2^n}$
  - 8:              $I_{l-1}^i \leftarrow \text{Integerize}(O_{l-1})$
  - 9:         **end if**
  - 10:        **for** each kernel  $k$  **do**
  - 11:             $\alpha_W \leftarrow \frac{\max |W_{lk}|}{2^n}$
  - 12:             $W_{lk}^i \leftarrow \text{Integerize}(W_{lk})$
  - 13:         **end for**
  - 14:        **else if** fully-connected layer **then**
  - 15:             $\alpha_W \leftarrow \frac{\max |W_l|}{2^n}$
  - 16:             $\alpha_I \leftarrow \frac{\max |O_{k-1}|}{2^n}$
  - 17:             $W^i \leftarrow \text{Integerize}(W)$
  - 18:             $I^i \leftarrow \text{Integerize}(I)$
  - 19:         **end if**
  - 20:     **end for**
  - 21: Forward propagation with  $(\alpha_K, \alpha_I, A_{Ic}, W^i, I^i)$  using Eq. (6.6) and (6.8) to calculate cost function  $C$ .
  - 22: Compute gradients w.r.t. real value weights:  $\frac{\partial C}{\partial W}$ .
  - 23: Update real value weights.
-

training is calculated using integer weights (see Algorithm 1, line 21), that ensures the integer weights result in the optimum cost value. In other words, there is no need for a re-training step with the Integer-Net.

### 6.3.3 Integet-Net for seizure detection

We use a CNN with three convolution blocks as depicted in Fig. 6.2. Each convolution block consists of a batch normalization, a convolution layer with a rectified linear unit (ReLU) activation function, and a max pooling layer. The batch normalization ensures that the inputs to convolution layer have zero mean and unit variance. The first convolution layer has sixteen  $n \times 5$  kernels, where  $n$  is the number of EEG channels, used with stride  $1 \times 2$ . The next two convolution blocks have 32 and 64 convolution kernels, respectively. The convolution blocks have kernel size of  $1 \times 3$ , stride  $1 \times 1$  and max pooling over  $1 \times 2$  region. Following the three convolution blocks are two fully-connected layers with sigmoid activation function and output sizes of 256 and 2, respectively. Drop-out layers are placed before the two fully-connected layers with dropping rate of 0.5.

Over-fitting is one of the most important challenges during training mainly due to the limited available datasets. To avoid over-fitting, we (1) keep the CNN architecture simple and shallow as described above, and (2) propose a practice to prevent over-fitting during training. A common practice is to randomly split 20% of the training set to be used as the validation set. After each training epoch, a loss and/or accuracy are calculated with respects to the validation set to check if the network starts to over-fit the training set. This practice works well with datasets where chronological ordering is not important, e.g. image classification tasks. For time-series such as seizure detection, however, we need to use samples from a different time period than those during training to monitor if the model starts to over-fit. In this work, we select 25% later samples from ictal and interictal sets for validation and the rest for training (see Fig. 6.3).

### 6.3.4 System evaluation

Area under the receiver operating characteristic curve (AUC) is used as criterion for comparing these models. Because AUC is a threshold-free metric, it is more convenient to use AUC for benchmarking with many models and multiple datasets than to use sensitivity and specificity. To have a robust evaluation, we use leave-one-out cross-validation, as illustrated by Truong, Kuhlmann, et al. (2017), and repeat it 5 times. If a subject has  $N$  seizures, one reported leave-one-out cross-validation AUC

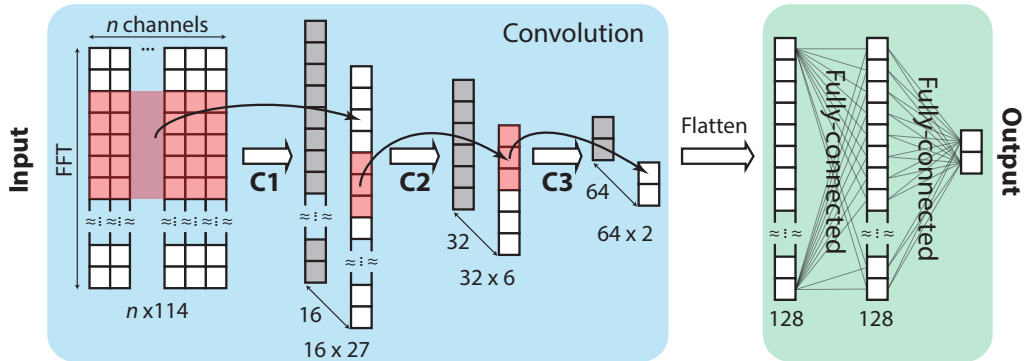


Figure 6.2: Convolutional neural network architecture. This illustration is applied for Freiburg and CHB-MIT datasets. For UPenn and Mayo Clinic’s seizure detection dataset, feature sizes are different due to different recording sampling rate. Input are FFT transforms of 1 s windows of raw EEG signals. There are three convolution blocks naming C1, C2 and C3. Each block consists of a batch normalization, a convolution layer with ReLU activation function, and a max pooling layer. For the sake of simplicity, max pooling layers are not shown and are noted as MP. For C1, sixteen  $n \times 5$  kernels, where  $n$  is number of EEG channels, are used with  $1 \times 2$  stride. ReLU activation is applied on convolution results before being sub-sampled by a max pooling layer over  $1 \times 2$  region. The same steps are applied in C2 and C3 except convolution kernel size of  $1 \times 3$ , stride  $1 \times 1$  and max pooling over  $1 \times 2$  region. Blocks C2 and C3 have 32 and 64 convolution kernels, respectively. Features extracted by the three convolution blocks are flatten and connected to 2 fully-connected layers with output sizes of 256 and 2, respectively. The former fully-connected layer uses sigmoid activation function while the latter uses soft-max activation function. Drop-out layers are placed before each of the two fully-connected layers with dropping rate of 0.5.

score is the average of  $N \times 5$  values. Regarding the UPenn and Mayo Clinic’s dataset, we also report the test results on the unlabeled dataset from Kaggle competition. Labels for this dataset, which is not publicly available, were provided by the competition organizers. The winning algorithm proposed by Hills (Hills, 2014) is also implemented for comparison. All the models were trained with the labeled dataset before being tested with the unlabeled one. Similar to the leave-one-out cross-validation, this test process was repeated 5 times and average results were reported.



Figure 6.3: Validation approach during training to prevent the convolutional neural network from over-fitting. 25% later samples (diagonal lines) from preictal and interictal sets are used for validation and the rest for training.

## 6.4 Results

We evaluate seizure detection performance on the three datasets with different models including: full precision (32-bit floating-point) CNN, binary weights (BW) CNN (Courbariaux et al., 2015), XNOR-Net (Rastegari et al., 2016), and the Integer-Net with 2- to 5-bit in use. For the BW and XNOR-Net models, the structure proposed by Ding (2017) was used.

Table 6.1: Seizure detection leave-one-out cross-validation results on Freiburg iEEG dataset.

Patient	Full	BW	XNOR	Int-2	Int-3	Int-4	Int-5
Pat1	99.9	99.4	94.9	93.3	95.4	99.2	99.6
Pat3	99.6	98.4	88.5	97.6	97.5	98.3	98.4
Pat4	100	99.9	100	99.8	100	100	100
Pat5	91.3	87.9	71.9	55.3	70.7	85.2	87.1
Pat6	88.5	82.3	75.7	66.7	80.6	86.0	87.4
Pat14	81.9	77.1	76.0	78.2	76.0	78.0	76.3
Pat15	92.6	89.1	66.2	85.6	89.7	93.5	93.5
Pat16	91.7	82.8	65.3	87.2	87.1	89.3	87.6
Pat17	99.9	99.7	97.9	99.4	99.5	99.8	99.9
Pat18	97.7	96.5	94.3	94.6	94.0	97.1	98.4
Pat19	94.8	85.8	66.5	73.6	79.2	85.0	93.3
Pat20	98.9	96.9	87.7	95.9	96.4	98.2	98.7
Pat21	94.2	93.0	87.2	92.7	93.3	93.0	91.8
<b>Average</b>	94.7	91.4	82.5	86.1	89.2	92.5	93.2

Regarding leave-one-out cross-validation, our proposed full precision CNN architecture works well across the three datasets with AUC ranging from 92.6% to 96.1% (see Fig. 6.4). Results in details are illustrated in Tables 6.1, 6.2, and 6.4. It is worth reminding that CHB-MIT dataset is scalp EEG (sEEG) while the other

two are intracranial EEG (iEEG). In other words, our CNN is generalized for seizure detection based on both scalp and intracranial EEG signals. This is important since it has been shown that only a few intracranial spikes associate with scalp ones (Tao et al., 2005), hence features for sEEG could be different from those for iEEG. Regarding hardware-friendly models, XNOR-Net delivers the worst performance. Integer-Net models perform better with larger number of bits in use. Specifically, Integer-Net with 2-bit in use (Int-2 in Fig. 6.4) has better AUC as compared to XNOR-Net which can be reasonably considered as 1-bit Integer-Net. AUC gets higher with Int-3, Int-4 and Int-5 for all three datasets. Because BW model has been tested with popular datasets (MNIST, CIFAR-10, SVHN) and achieved state-of-the-art performance (Courbariaux et al., 2015), we are interested in its performance for seizure detection task compared to Integer-Net. With 4-bit, Integer-Net surpasses BW model in seizure detection task across all three datasets with  $p$ -value of 0.0005 in Wilcoxon signed rank test.

Table 6.2: Seizure detection leave-one-out cross-validation results on CHB-MIT sEEG dataset.

Patient	Full	BW	XNOR	Int-2	Int-3	Int-4	Int-5
Pat1	99.5	99.4	80.2	98.2	99.3	99.7	99.7
Pat2	95.2	93.9	84.3	91.7	95.3	97.0	97.8
Pat3	99.4	96.1	92.6	87.7	96.7	96.6	97.8
Pat4	92.2	82.8	76.6	72.6	80.6	85.9	83.2
Pat5	99.9	99.4	92.2	97.5	99.6	99.8	99.8
Pat6	98.7	95.8	82.0	81.1	96.3	97.0	96.8
Pat7	90.8	95.4	90.2	90.0	96.1	96.2	96.3
Pat8	82.0	76.5	68.6	86.3	82.8	84.2	85.0
Pat9	99.5	98.1	88.5	93.7	98.4	98.4	98.5
Pat10	98.6	98.2	84.7	95.6	99.1	99.3	99.2
Pat11	99.4	97.3	77.7	97.8	99.3	99.5	99.6
Pat13	98.7	94.9	83.3	91.4	95.8	97.3	96.7
Pat14	97.5	97.1	91.4	87.2	96.4	97.5	97.7
Pat15	96.4	94.5	62.8	88.6	94.9	95.3	94.8
Pat16	85.7	75.0	61.9	54.9	62.5	75.0	81.2
Pat17	94.7	92.0	93.5	89.1	92.0	93.1	94.8
Pat18	96.3	91.2	76.3	87.2	93.6	98.0	96.9
Pat19	98.6	97.2	94.3	95.0	97.9	98.4	98.3
Pat20	98.3	94.4	84.7	89.7	92.8	96.4	97.8
Pat21	97.6	85.7	73.8	90.3	96.0	97.0	97.7
Pat22	94.3	94.7	87.0	93.2	97.7	95.7	97.0
Pat23	100	99.5	94.8	98.7	99.6	99.8	99.9
<b>Average</b>	96.1	93.1	82.8	89.0	93.8	95.3	95.8

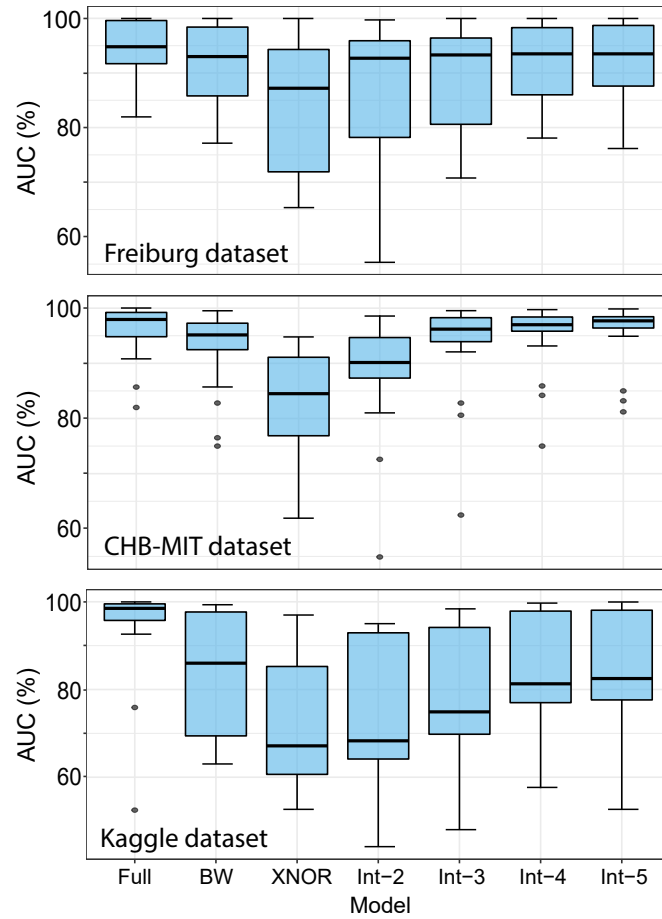


Figure 6.4: AUC scores of different seizure detection CNN models: full precision (32-bit floating-point), binary weights only (BW), XNOR-Net, and Integer-Net with 2- to 5-bit. Dots in the figure are outliers. Integer-Net with 2-bit (Int-2) has better AUC than XNOR-Net. Integer-Net with higher number of bits in use (Int-3, Int-4, Int-5) results in higher AUC.

Table 6.3: Seizure detection leave-one-out cross-validation results on UPenn and Mayo Clinic iEEG dataset.

Subj.	(Hills, Full 2014)	Full	BW	XNOR	Int-2	Int-3	Int-4	Int-5
Dog1	99.7	99.0	97.6	97.0	92.8	93.4	97.7	97.8
Dog2	99.7	99.9	99.3	92.7	94.7	96.4	99.6	99.7
Dog3	99.6	99.4	97.9	91.7	93.3	97.4	98.4	98.9
Dog4	97.2	97.9	86.2	55.9	62.2	69.8	80.5	78.9
Pat1	98.1	52.5	63.0	62.0	65.7	69.3	77.2	57.8
Pat2	99.5	98.3	96.7	83.1	75.9	92.5	95.4	95.5
Pat3	95.3	98.7	64.1	52.6	59.4	74.4	82.1	80.5
Pat4	100	99.9	64.0	56.6	44.1	48.1	57.5	52.6
Pat5	88.8	92.6	75.1	73.8	69.9	72.5	76.4	78.1
Pat6	99.8	100	99.4	64.0	94.9	98.5	99.7	99.9
Pat7	90.1	75.9	71.2	62.8	64.8	69.8	69.9	76.2
Pat8	97.8	96.8	85.8	70.3	66.7	75.4	78.2	84.5
<b>Avg.</b>	97.1	92.6	83.4	71.9	73.7	79.8	84.4	83.4

Table 6.4: Seizure detection test results on UPenn and Mayo Clinic iEEG unlabeled dataset.

Subj.	(Hills, Full 2014)	Full	BW	XNOR	Int-2	Int-3	Int-4	Int-5
Dog1	98.8	97.2	96.5	95.7	94.5	95	96.9	95.7
Dog2	97.7	95.9	86.8	85.7	79	84.4	89.5	88.6
Dog3	94.5	98	97.6	93.3	96.1	97.5	97.9	98.1
Dog4	99.8	77.9	93.9	68.7	75.2	61.6	63.5	79.5
Pat1	98.2	99	94.8	86.1	78.2	77.1	87.7	87.6
Pat2	98.9	97.7	96.9	85.1	82.9	94.6	96.3	96.9
Pat3	73.4	64.2	79.5	53.8	71.3	78.2	80.8	81.3
Pat4	67.5	64.1	55.5	48.6	49.4	48.6	48.2	46.6
Pat5	88.1	84.1	92.6	78	86.2	90.6	93.3	94
Pat6	98.1	96.5	97.9	66.5	85.8	87.3	94.6	95.9
Pat7	99.8	99.8	96.5	87.6	94.2	97.2	92.6	94.2
Pat8	86.5	98.4	93.8	69.5	72.3	73	80	82.4
<b>Avg.</b>	91.8	89.4	90.2	76.6	80.4	82.1	85.1	86.7

With respect to the unlabeled UPenn and Mayo Clinic dataset, the full precision CNN model drops by 3% in AUC, from 92.6% cross-validation AUC to 89.4% test AUC for the unlabeled dataset. The winning model (Hills, 2014) drops even more by more than 5%, from 97.1% to 91.8% which is only 6.7% better than the Int-4 model. More interestingly, all hardware-friendly models have increase in test AUC compared to the leave-one-out cross-validation results. This implies that low precision calculation could possibly help generalization of seizure detection models.

Table 6.5: Reduction rate of weight size achieved with 4-bit Integer-Net.

Layer	Freiburg dataset Input shape 6×114		CHB-MIT dataset Input shape 22×114		UPenn & Mayo dataset Input shape 16×201	
	# params	Out shape	# params	Out shape	# params	Out shape
BatchNorm*	6×4		22×4		16×4	
Conv1	6×5×16	1×55×16	22×5×16	1×55×16	16×5×16	1×99×16
MaxPool	0	1×27×16	0	1×27×16	0	1×49×16
BatchNorm*	16×4				16×4	
Conv2	16×3×32	1×13×32	16×3×32	1×13×32	16×3×32	1×24×32
MaxPool	0	1×6×32	0	1×6×32	0	1×12×32
BatchNorm*	32×4				32×4	
Conv3	32×3×64	1×4×64	32×3×64	1×4×64	32×3×64	1×10×64
MaxPool	0	1×2×64	0	1×2×64	0	1×5×64
FC1	128×128	128	128×128	128	320×128	128
FC2	128×2	2	128×2	2	128×2	2
<b>Full weight size</b>	97.7 KB		103.0 KB		198.9 KB	
<b>Int-4 weight size</b>	13.4 KB		14.3 KB		26.2 KB	
<b>Reduction rate</b>	7.3x		7.2x		7.6x	

\* Parameters in batch normalization layers are not integerized.

## 6.5 Discussion

It is shown that 4-bit Integer-Net gives the best balance between performance and computational efficiency. Comparing a 4-bit Integer-Net with a full 32-bit real-value resolution model, AUC scores only drop less than 2% for the two datasets Freiburg Hospital and CHB-MIT. There is more performance degradation with UPenn and Mayo Clinic’s dataset with roughly 8% drop in AUC. Compared to the state-of-the-art algorithm (Hills, 2014), the 4-bit Integer-Net shows less 6.7% in test AUC on the unlabeled UPenn and Mayo Clinic dataset. Note that although the state-of-the-art algorithm results in the highest score, it is involved with much more complex feature engineering and therefore inefficient for an implantable or portable device. Among

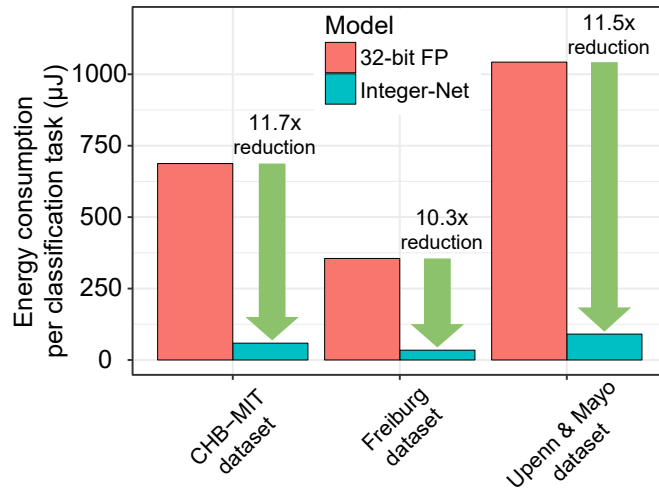
all models, XNOR has the least computational cost. However, its performance is substantially worst than other models on all three datasets. Note that in BW model, only weights are binarized, inputs are still stored as 32-bit floating-point values. Also, the 4-bit Integer-Net has been shown to be superior to BW model based on the Wilcoxon signed rank test.

Table 6.6: Energy consumption for various operations in 45nm 0.9V process (Horowitz, 2014).

Operation	Multiplication	Addition
8-bit integer	0.2 pJ	0.03 pJ
32-bit floating point	3.7 pJ	0.9 pJ

The first advantage of Integer-Net is the smaller size of weights. By reducing number of bits from 32 to 4, raw reduction rate of weight size is 8 times more or less. However, since batch normalization parameters and scale coefficients are still real values, the actual reduction rate is 7.2–7.6 times (see Table 6.5). More importantly, benefit of Integer-Net mostly comes from computational gain during inference mode. In Integer-Net, not only weights but also inputs to each convolution and fully-connected layer are binarized. In other words, all convolution and matrix multiplication operations are performed with integer numbers. Achieving appropriate level of accuracy has been the focus in this work and discussing details of power and computational gain is not discussed in this work. But with the use of much less number of bits and the use of integers instead of floating-point values, we argue that the computational gain could be significant. As a reference, 8-bit integer implementation can gain 30 and 18 times for addition and multiplication, respectively, compared to those of 32-bit floating point implementation in 45nm 0.9V process (see Table 6.6). On that basis, we estimate energy consumption per one classification task with the use of Integer-Net and 32-bit floating point implementations. Our proposed Integer-Net enables a 10x reduction in energy consumption compared to the conventional implementation (see Fig.6.5). The Integer-Net implementation consumes 34–90  $\mu$ J for each classification.

We can further achieve computational gain by reducing the number of EEG channels to be analyzed. This can be done manually by leveraging bio-medical expertise to select which channels genuinely indicate seizure onset. However, this is time-consuming and impractical if many patients are involved. Many attempts for channel reduction tasks in an automatic fashion have been introduced. In our previous work (Truong, Kuhlmann, et al., 2017), we proposed an automatic channel selection (ACS) engine that



FP: floating point.

Figure 6.5: Integer-Net implementation can reduce more than ten times in energy consumption.

was shown to be superior for the channel selection task. The ACS engine is composed of supervised classifiers in order to determine EEG channels that contribute the most to a seizure. Inputs to these classifiers are FFT transforms of 1 s windows of the raw EEG signals on all channels. The classifiers determine the importance level of each channel based on how often that feature is used to distinguish ictal windows from interictal ones (Truong, Kuhlmann, et al., 2017). In this work, we apply the ACS engine to gain more computational efficiency without compromising detection accuracy (Truong, Kuhlmann, et al., 2017). We select patients (Pat1, Pat3, Pat4, Pat5, Pat6 and Pat7) with large number of electrodes (from 30 to 72, 54 on average) from UPenn and Mayo Clinic (Kaggle) dataset (S. N. Baldassano et al., 2017) and use ACS engine to pick up top 16 electrodes. The reason of choosing 16 is merely because majority of subject in UPenn and Mayo Clinic dataset has 16 electrodes. We found that CNN and its hardware-friendly versions work well with ACS. As seen in Fig. 6.6, by using less than one third of EEG channels on average, all models, except Int-2, achieve improvement in seizure detection performance. Since the approximate operations of Integer-Net rely on dynamic range of input signals, there is potential performance degradation when testing with a prospective system. Particularly, the dynamic range of signals used for training the network may differ from the dynamic range when testing in real-time.

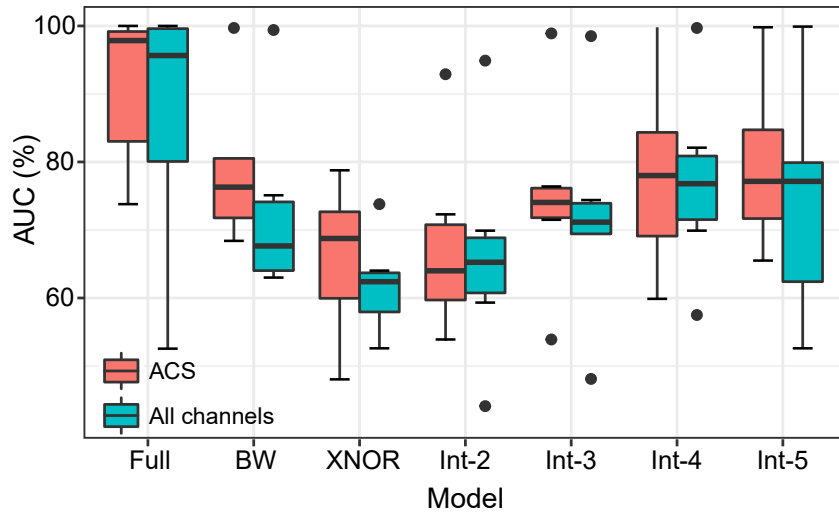


Figure 6.6: AUC scores of different seizure detection CNN models with the use of automatic channel selection for channel reduction on a subset of patients with large number of electrodes (30 to 72). Dots in the figure are outliers. All models, except Int-2, has improvement in seizure detection using less than 1/3 of channels on average.

## 6.6 Conclusion

Seizure detection is crucial for patients with intractable epilepsy. A seizure detection system needs to be not only precise but also reasonably computationally simple to be most useful as an implantable or portable device. This work proposed a generalized convolutional neural network architecture that can effectively detect seizure using either scalp or intracranial EEG and its Integer-Net version. With Integer-Net, weight storage can be reduced by 7–8 times. More importantly, convolution and matrix multiplication operations performed with integers greatly help to reduce computational cost and inference time that is critical for real-time application. Integer-Net is promising for an energy-efficient seizure detection device with high accuracy. Such device could enable a close-loop seizure detection system that can detect, give warning and potentially suppress seizures.

## Acknowledgment

This research was supported by Sydney Informatics Hub, funded by the University of Sydney. O. Kavehei and N. Truong acknowledge an Early Career Research grant from Faculty of Engineering and Information Technology, The University of Sydney. J. Yang

acknowledges National Natural Science Foundation of China for their financial support under Grant 61501332. N. Truong also acknowledges The Commonwealth Scientific and Industrial Research Organisation (CSIRO) partial financial support for a PhD Scholarship, PN 50041400.

# Chapter 7

## Low precision EEG signals for seizure detection

The content presented in this chapter is adapted from a conference proceeding published as:

- Truong, N. D. and O. Kavehei (2019). “Low Precision Electroencephalogram for Seizure Detection with Convolutional Neural Network.” *Proc. IEEE International Conference on Artificial Intelligence Circuits and Systems*. DOI:10.1109/AICAS.2019.8771569.

## Statement of Contributions of Joint Authorship

Truong, N. D. and O. Kavehei (2019). “Low Precision Electroencephalogram for Seizure Detection with Convolutional Neural Network.” *Proc. IEEE International Conference on Artificial Intelligence Circuits and Systems*. DOI:10.1109/AICAS.2019.8771569.

- Nhan Duy Truong (Candidate): First author, completed the analysis, writing, reviewing and editing of the manuscript.
- Omid Kavehei (Principal Supervisor): provided the main idea, reviewing and editing the manuscript.

In addition to the statements above, in cases where I am not the corresponding author of a published item, permission to include the published material has been granted by the corresponding author.

Nhan Duy Truong

Date: 01 October 2019

As supervisor for the candidature upon which this thesis is based, I can confirm that the authorship attribution statements above are correct.

Dr. Omid Kavehei

Date: 01 October 2019

Electroencephalogram (EEG) recording has been widely used for diagnosing and monitoring of epileptic patients. Ambulatory and reliable EEG monitoring devices that can detect or predict seizures could play an important role for patients safety, the disease management and clinical outcome for people living with pharmaco-resistant epilepsy or epilepsy monitoring units. While many EEG-based seizure detection algorithms have been proposed in the literature, their real-time and high accuracy hardware implementations are constrained by power consumption, size of the system and its real-time performance. Many commercial non-research EEG monitoring systems sample multiple electrodes at a relatively high rate and transmit the data either via a wire or wirelessly to an external signal processing unit. In this work, we studied how a reduced sampling precision in data conversion impacts the performance of our machine learning signal processing in seizure detection. To answer this question, we reduce the number of bits in an analog-to-digital converter (ADC) used in an EEG recorder. The outcome shows that the reduction of ADC precision down to 6-bit does not significantly reduce seizure detection performance. As an indication of the performance, we achieved an area under the curve (AUC) more than 92% and 96% with convolutional neural network and more than 93% and 97% with engineered feature-based approach testing on the Freiburg Hospital and the Boston Children’s Hospital-MIT seizure datasets, respectively. A possible reduction in ADC precision not only contributes to energy consumption reduction, but also offers an improved computational efficacy regarding memory requirement and circuit area.

## 7.1 Introduction

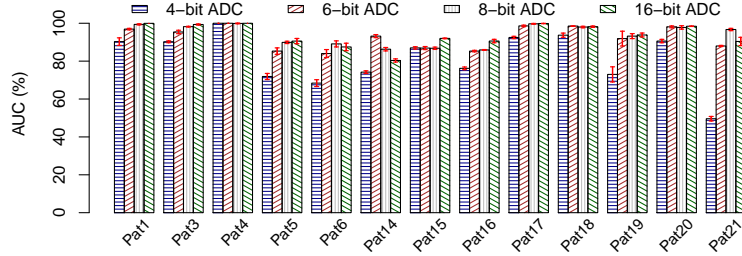
Nearly 1% of the global population has been diagnosed with epilepsy, and almost one-third of the patients have intractable epilepsy. Ambulatory systems that can detect or even forecast epileptic seizure play an important role for those patients (Echaz et al., 2007). Electroencephalogram (EEG) has been shown as critical information to enable seizure detection and prediction. Automatic seizure detection has been demonstrated to be viable by using EEG signals (Kuhlmann, Burkitt, et al., 2009; Tieng et al., 2016; Wen and Z. Zhang, 2018). Though seizure prediction is still challenging, it has been proved to be possible at least for certain groups of patients (Kuhlmann, Lehnertz, et al., 2018; Kuhlmann, P. Karoly, et al., 2018; Truong, Nguyen, et al., 2018a).

Regarding seizure detection, Parvez and Paul (2015) applied 2D-discrete cosine transformation (DCT) and extracted statistical features from the DCT coefficients as inputs for a least square support vector machine (LS-SVM) to perform seizure detection.

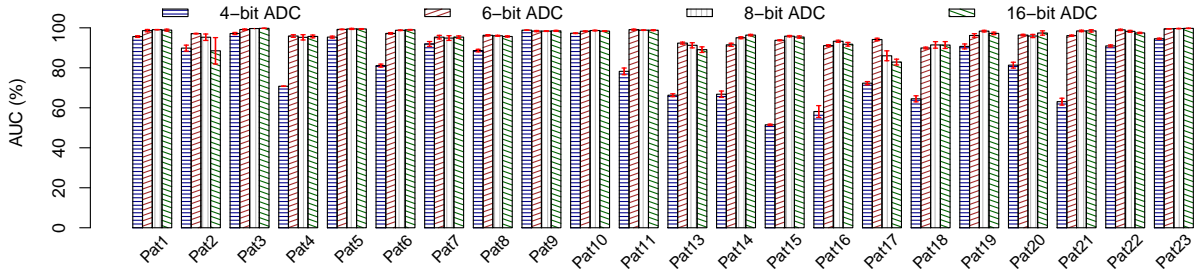
Their approach achieved sensitivity and specificity more than 96% on the Freiburg Hospital dataset. In another work, the power spectrum and the correlation between channel pairs in both frequency and time domain were used as inputs for a random forest classifier to distinguish ictal and interictal EEG signals (Truong, Kuhlmann, et al., 2017). The method achieved an area under the operating characteristics curve (AUC) of 96.94% using the Kaggle seizure detection competition dataset (Kaggle, 2014b). Wavelet transform was shown to be effective to extract useful features for seizure detection. A seizure detection method that used wavelet-based directed transfer function as feature extraction and support vector machine (SVM) as a classifier achieved a sensitivity of 95.8% and specificity of 99.5% on a private dataset consisting of 87.5 hours of EEG recordings and 44 seizure occurrences (D. Wang et al., 2018).

Recently, deep learning has been being used widely in epileptic seizure detection. Hossain et al. (2019) applied a convolutional neural network (CNN) on 2-second input window segments of time-series EEG signals from the Boston Children’s Hospital-MIT (CHB-MIT) dataset. Their patient-specific method achieved a sensitivity of 90% and specificity of 91.65%. A similar approach with CNN that was tested with a private dataset consisting of 1124.3 hours EEG recording time and 97 seizures obtained a sensitivity of 74% across patients (Emami et al., 2019). A combination of convolutional neural network and recurrent neural network that was used as a seizure detector obtained sensitivity in the range of 95–100% on the CHB-MIT dataset (Thodoroff et al., 2016). In another work, an autoencoder-based multi-view learning model used a multi-view autoencoder to learn features in a unsupervised manner, and a channel-aware seizure detection module to steer the model to the most relevant EEG channels (Yuan et al., 2019). This subject-independent seizure detection method achieved an F1-score of 85.34% using 5-fold cross-validation on the CHB-MIT dataset.

Note that the aforementioned methods are based on EEG signals with at least 16-bit resolution. The resolution of EEG signals is determined by an analog-to-digital converter (ADC) that is used by EEG recorders to digitize the signals. Typically, EEG recorders are equipped with a 16-bit ADC (University of Freiburg, 2003; Goldberger et al., 2000). In this work, we study how sensitive working seizure detection algorithms are with regards to the EEG’s resolution or the number of ADC bits. The seizure detection algorithms will be studied in this work are (1) CNN-based (Truong, Nguyen, et al., 2018b), and (2) classical engineered feature-based (Truong, Kuhlmann, et al., 2017).



(a) Freiburg Hospital dataset



(b) CHB-MIT dataset

Figure 7.1: Seizure detection performance using convolutional neural network.

## 7.2 Dataset

In this work, we evaluate the impact of ADC precision on seizure detection using two datasets: the Freiburg Hospital dataset (University of Freiburg, 2003) and the Boston Children’s Hospital (CHB)-MIT dataset (Goldberger et al., 2000). The Freiburg Hospital dataset consists of intracranial EEG (iEEG) recordings at 256 Hz sampling rate from 21 patients with intractable epilepsy (University of Freiburg, 2003). Due to the lack of availability of the dataset, we were only able to use data from 13 patients with 59 seizures and 311.4 interictal hours in total. In this dataset, iEEG signals are extracted from 6 selected electrodes where three of them are from epileptogenic regions, and the rest are from remote regions. Data of each patient contains 3 to 5 seizures and 24 hours of interictal (Maiwald et al., 2004). The CHB-MIT dataset contains scalp EEG (sEEG) recordings of 23 pediatric patients with 844 hours of continuous sEEG recording and 163 seizures in total (Shoeb, 2009). Scalp EEG signals are recorded at a sampling rate of 256 Hz from 22 non-invasive electrodes. Different from Truong, Nguyen, et al. (2018b), we define any signals that are at before seizure onset and after seizure ending

as interictal. Also, patient 12 was excluded as we were unable to load EEG signals for this patient.

### 7.3 Method

We use a convolutional neural network (CNN) (Truong, Nguyen, et al., 2018b) and a classical engineered feature-based approach (Truong and Kavehei, 2019) to evaluate the impact of ADC bit reduction on seizure detection performance. Specifically, CNN takes the Fast Fourier Transform (FFT) of 1-second time-series EEG windows as inputs. Only FFT amplitudes are considered, and all the phase information is disregarded. Moreover, components in the frequency ranges of 47–53 Hz and 97–103 Hz are removed for the Freiburg Hospital dataset. The similar step is applied for the CHBMIT dataset with components in the frequency ranges of 57–63 Hz and 117–123 Hz. The DC component was also removed. The CNN structure is comprised of three convolutional blocks, each of which contains a batch normalization, a convolutional layer, and a max-pooling layer with stride of  $(1 \times 2)$ . The three convolution layers have number of kernels of 16, 32 and 64, kernel sizes of  $(n \times 5)$ ,  $(1 \times 3)$  and  $(1 \times 3)$ , where  $n$  is the number of EEG channels, strides of  $(1 \times 2)$ ,  $(1 \times 3)$  and  $(1 \times 3)$ , respectively. Two fully-connected layers follow the convolutional blocks with sigmoid activation function and a drop out rate of 0.5 (Truong, Nguyen, et al., 2018b).

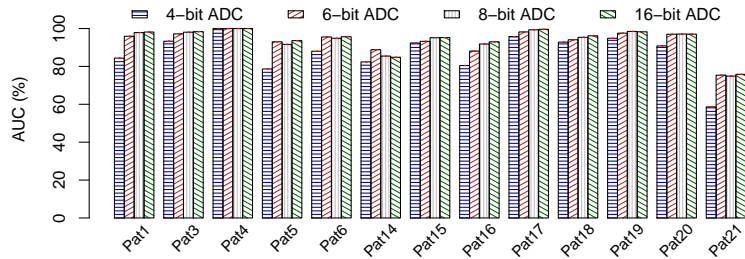
Regarding the engineered feature-based method, the features are extracted in both frequency and time domains. In the frequency domain, the features consist of spectral power in 1-Hz bins in the range of 1–47-Hz, eigenvalues of a cross-spectral matrix on all channels. In the time domain, the features are coefficients in the upper triangle and eigenvalues of the correlation matrix of EEG signals on all channels. The feature set is classified by a random forest classifier with 3000 decision trees (Truong, Kuhlmann, et al., 2017).

To simulate the ADC bit reduction, from the recorded EEG signals, we convert the 16-bit ADC readings into  $n$ -bit values using (7.1).

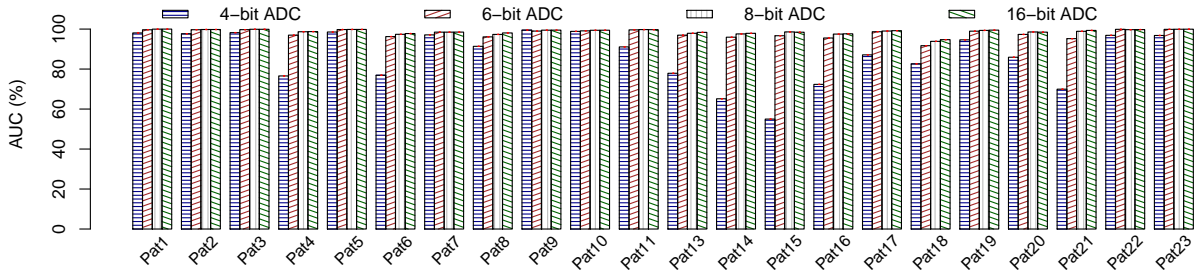
$$\text{readings}_{n\text{-bit}} = (\text{readings}_{16\text{-bit}} \gg 16) \ll n, \quad (7.1)$$

where  $\text{readings}_{16\text{-bit}}$  are the 16-bit integer outputs from ADC,  $\ll$  and  $\gg$  are left shift and right shift operators, respectively.

Original and converted readings are then applied with the CNN above for the seizure detection task. In this work, we use the area under the receiver operating characteristic curve (AUC) as a threshold-free metric for benchmarking models using different numbers of ADC bits. To have a robust evaluation, we use leave-one-seizure-out cross-validation, as illustrated by Truong, Kuhlmann, et al. (2017), and repeat the whole cross-validation 4 times. Mean values and standard deviations of AUC for each patient are reported.



(a) Freiburg Hospital dataset



(b) CHB-MIT dataset

Figure 7.2: Seizure detection performance using feature engineering and random forest classifier.

## 7.4 Results

The seizure detection performance of the CNN-based and the engineered feature-based approaches under different numbers of ADC bits is illustrated in Figs. 7.1 and 7.2, more details can be found in Tables 7.1–7.4. Regarding the CNN-based seizure detection algorithm, ADC bit reduction from 16 to 6 does not have a high impact on seizure detection performance. Particularly, for the Freiburg Hospital dataset, the average AUC

for 16- and 8-bit ADC is around 93.9%, and decreases to 92.5% 6-bit ADC. However, the 4-bit ADC does cause the AUC to degrade greatly to 81.4%. It is worth noting that six out of thirteen patients still have AUC higher than 90% in this case. Similar observations are applied to the CHB-MIT dataset. In particular, the average AUC remains above 96% when the number of ADC bits is reduced to 6, comparable with that using the original 16-bit ADC.

Table 7.1: Seizure detection performance (AUC in %) for the Freiburg Hospital dataset with convolutional neural network. Mean values and standard deviations of AUC for each patient over the course of four runs of leave-one-seizure-out cross-validation are reported.

Patient	4-bit ADC	6-bit ADC	8-bit ADC	16-bit ADC
Pat1	90.3 ± 2.0	96.9 ± 0.4	99.4 ± 0.3	99.9 ± 0.0
Pat3	90.2 ± 0.5	95.4 ± 0.9	98.2 ± 0.2	99.3 ± 0.3
Pat4	100 ± 0.0	100 ± 0.0	99.9 ± 0.2	100 ± 0.0
Pat5	71.9 ± 1.6	85.3 ± 1.7	89.9 ± 0.6	90.6 ± 1.4
Pat6	68.4 ± 1.8	84.0 ± 2.1	89.1 ± 1.6	87.5 ± 2.0
Pat14	74.2 ± 0.7	93.2 ± 0.8	86.3 ± 0.9	80.3 ± 0.8
Pat15	87.0 ± 0.6	86.9 ± 0.8	86.8 ± 0.6	92.0 ± 0.2
Pat16	76.2 ± 0.7	85.3 ± 0.4	85.9 ± 0.2	90.6 ± 0.9
Pat17	92.5 ± 0.6	98.6 ± 0.4	99.7 ± 0.2	99.9 ± 0.1
Pat18	93.7 ± 1.1	98.5 ± 0.1	98.0 ± 0.4	98.2 ± 0.4
Pat19	73.0 ± 4.0	91.9 ± 3.9	93.2 ± 1.3	93.8 ± 1.0
Pat20	90.6 ± 0.9	98.1 ± 0.5	97.8 ± 0.9	98.4 ± 0.1
Pat21	49.6 ± 1.2	88.0 ± 0.3	96.7 ± 0.6	90.4 ± 2.2
Average	81.4 ± 1.2	92.5 ± 0.9	93.9 ± 0.6	93.9 ± 0.7

Similarly, with the engineered feature-based method, seizure detection performance slightly drops when using 6-bit ADC compared with 16-bit ADC. Specifically, the average AUC decreases from 94.2% and 98.8% with 16-bit ADC to 93.3% and 97.7% with 6-bit ADC for the Freiburg Hospital dataset and the CHB-MIT dataset, respectively. The 4-bit does cause a considerable degradation in the average AUC by approximately 7% and 12% for the two datasets, although more than 50% of the patients still have AUC higher than 90%.

## 7.5 Discussion

As we use FFT transform of the time-series EEG signals as input to the CNN and power spectrum in the engineered feature-based method, we are interested in studying

Table 7.2: Seizure detection performance (AUC in %) for the CHB-MIT dataset with convolutional neural network. Mean values and standard deviations of AUC for each patient over the course of four runs of leave-one-seizure-out cross-validation are reported.

Patient	4-bit ADC	6-bit ADC	8-bit ADC	16-bit ADC
Pat1	95.6 ± 0.4	98.6 ± 0.6	99.1 ± 0.1	98.9 ± 0.5
Pat2	89.8 ± 1.5	97.1 ± 0.1	95.3 ± 1.6	88.5 ± 6.6
Pat3	97.1 ± 0.5	99.1 ± 0.3	99.6 ± 0.0	99.7 ± 0.0
Pat4	70.8 ± 0.1	95.9 ± 0.6	95.2 ± 1.3	95.7 ± 0.7
Pat5	95.3 ± 0.5	99.2 ± 0.1	99.5 ± 0.3	99.4 ± 0.2
Pat6	81.1 ± 0.7	97.2 ± 0.4	98.8 ± 0.1	99.0 ± 0.2
Pat7	91.9 ± 1.2	95.3 ± 0.9	94.9 ± 1.2	95.3 ± 0.6
Pat8	88.6 ± 0.6	96.2 ± 0.3	96.0 ± 0.2	95.7 ± 0.3
Pat9	98.8 ± 0.1	98.4 ± 0.3	98.4 ± 0.2	98.5 ± 0.3
Pat10	97.3 ± 0.2	98.3 ± 0.2	98.6 ± 0.2	98.3 ± 0.2
Pat11	78.2 ± 1.7	99.1 ± 0.3	98.8 ± 0.1	98.8 ± 0.2
Pat13	66.3 ± 0.7	92.3 ± 0.5	91.3 ± 1.3	89.1 ± 1.4
Pat14	66.8 ± 1.6	91.5 ± 0.8	95.0 ± 0.5	96.4 ± 0.4
Pat15	51.5 ± 0.3	93.8 ± 0.2	95.8 ± 0.3	95.4 ± 0.6
Pat16	58.1 ± 2.9	91.1 ± 0.4	93.3 ± 0.5	91.8 ± 0.9
Pat17	72.3 ± 0.8	94.2 ± 0.6	86.0 ± 2.5	82.9 ± 1.4
Pat18	64.5 ± 1.5	89.9 ± 0.4	91.4 ± 1.6	91.4 ± 1.7
Pat19	90.7 ± 1.2	96.2 ± 0.9	98.3 ± 0.4	97.2 ± 0.6
Pat20	81.3 ± 1.5	96.4 ± 0.4	95.9 ± 0.8	97.4 ± 1.1
Pat21	63.1 ± 1.7	96.1 ± 0.3	98.4 ± 0.4	98.5 ± 0.6
Pat22	90.9 ± 0.5	99.0 ± 0.3	98.2 ± 0.5	97.4 ± 0.3
Pat23	94.5 ± 0.3	99.5 ± 0.0	99.6 ± 0.1	99.7 ± 0.1
Average	81.1 ± 0.9	96.1 ± 0.4	96.2 ± 0.6	95.7 ± 0.9

Table 7.3: Seizure detection performance (AUC in %) for the Freiburg Hospital dataset with engineered feature-based approach. Mean values and standard deviations of AUC for each patient over the course of four runs of leave-one-seizure-out cross-validation are reported.

Patient	4-bit ADC	6-bit ADC	8-bit ADC	16-bit ADC
Pat1	84.4	95.9	97.9	98.1
Pat3	93.3	97.2	98.1	98.3
Pat4	100	100	100	100
Pat5	78.6	93	91.6	93.6
Pat6	88.0	95.5	94.8	95.7
Pat14	82.4	88.8	85.5	84.8
Pat15	92.4	93.2	95.2	95.2
Pat16	80.5	88.1	91.8	93.0
Pat17	95.7	98.2	99.3	99.6
Pat18	92.8	94.1	95.4	96.1
Pat19	94.8	97.5	98.5	98.3
Pat20	90.8	97.0	97.1	97.0
Pat21	58.6	75.4	74.9	75.8
Average	87.1	93.4	93.9	94.3

The engineered feature-based approach had virtually no variation ( $< 0.05\%$ ) in AUC among different runs.

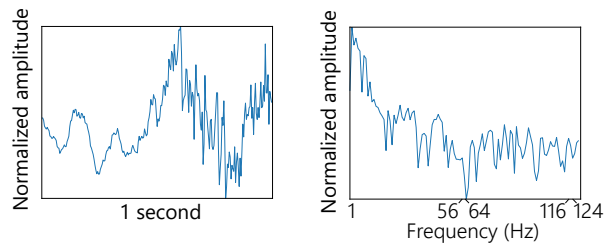
how the reduction in the number of ADC bits affects the input’s “features”. Fig. 7.3 depicts the power spectrum of a 1-second EEG with the use of different numbers of ADC bits. Reducing the number of ADC bits causes less distinguishable levels of signals captured in the EEG recording (i.e., low resolution). One may expect information at high frequencies is lost because the signals become more “pixelated” with less number of bits used in ADC. In the extreme case where only 4 bits are in use (see Fig. 7.3.e), all components above 20 Hz are depressed to zero.

Figs. 7.1 and 7.2 show that some patients have high seizure detection performance with only 4-bit ADC while the performance of others drops considerably. We select one patient with high performance and another patient with low performance of each dataset and analyze the impact of ADC bit reduction on the power spectrum of EEG signals during ictal and interictal periods. Particularly, we plot the power spectrum with DC removed of two thousand random 1-second segments for each case (see Figs. 7.4 and 7.5). For both datasets, the difference in the power spectrum of the high and low performers can be clearly observed at 4-bit ADC. Specifically, ictal and interictal groups can be visually distinguished for the patients with high seizure detection performance, but they look similar for the patients with low performance. Some patients have better performance with less number of bits, e.g., Patient 14 in the Freiburg Hospital dataset.

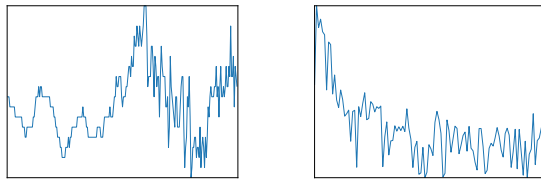
Table 7.4: Seizure detection performance (AUC in %) for the CHB-MIT dataset with engineered feature-based approach. Mean values and standard deviations of AUC for each patient over the course of four runs of leave-one-seizure-out cross-validation are reported.

Patient	4-bit ADC	6-bit ADC	8-bit ADC	16-bit ADC
Pat1	98.1	99.7	100	100
Pat2	97.7	99.7	99.8	99.8
Pat3	98.2	99.7	99.9	99.9
Pat4	76.6	97.0	98.7	98.7
Pat5	98.5	99.8	99.8	99.8
Pat6	76.9	96.2	97.4	97.8
Pat7	97.1	98.5	98.5	98.5
Pat8	91.4	96.1	97.3	98.1
Pat9	99.5	99.0	99.4	99.5
Pat10	98.8	99.1	99.4	99.4
Pat11	91.1	99.6	99.7	99.7
Pat13	77.9	97.0	97.9	98.4
Pat14	65.1	95.9	97.6	97.9
Pat15	55.0	96.7	98.6	98.4
Pat16	72.3	95.5	97.5	97.6
Pat17	87.1	98.7	99.0	99.2
Pat18	82.6	91.7	93.9	94.7
Pat19	94.6	99.0	99.3	99.5
Pat20	85.9	97.3	98.6	98.5
Pat21	69.9	95.2	98.9	99.3
Pat22	96.9	99.9	99.7	99.7
Pat23	96.8	99.9	99.9	99.9
Average	86.7	97.8	98.7	98.8

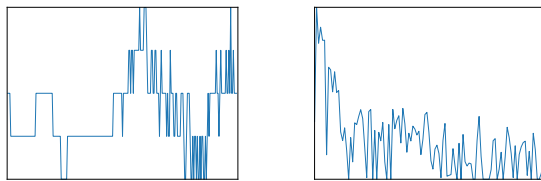
The engineered feature-based approach had virtually no variation ( $< 0.05\%$ ) in AUC among different runs.



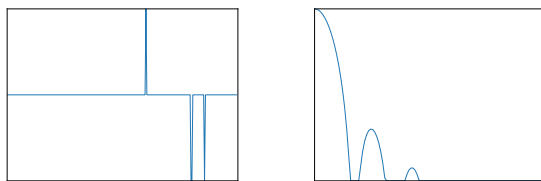
(a) 16-bit ADC



(b) 8-bit ADC



(c) 6-bit ADC



(d) 4-bit ADC

Figure 7.3: Waveform and power spectrum of a 1-second EEG segment from one channel using different numbers of ADC bits.

This can be explained that the less number of bit acts like a regularization technique that helps the model generalize better.

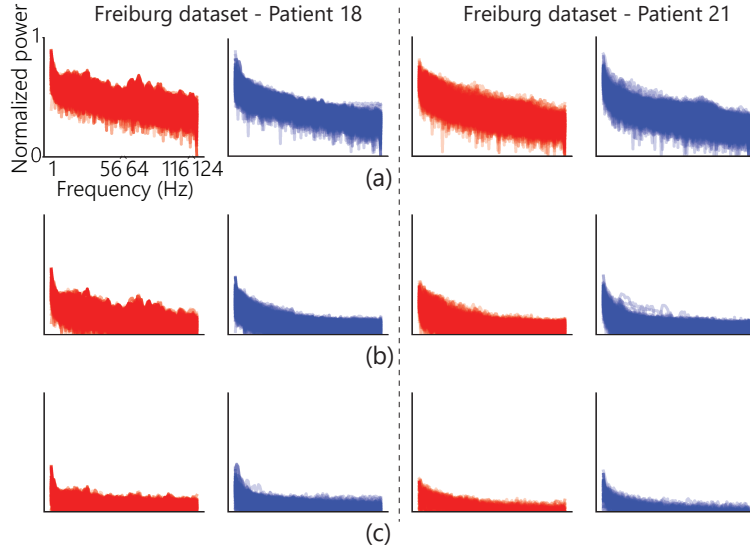


Figure 7.4: Power spectrum with DC removed of two thousand random 1-second EEG segments for patients with high (Patient 18) and low (Patient 21) seizure detection performance using different numbers of ADC bits during ictal (red) and interictal (blue) periods from the Freiburg Hospital dataset in three cases: (a) 16-bit ADC, (b) 8-bit ADC, and (c) 4-bit ADC.

We have shown that only a 6-bit (rather than 16-bit) ADC is sufficient for seizure detection. The low precision EEG signals with 6-bit ADC can be used for different seizure detection methods, namely convolutional neural network and engineered feature-based in this work. Therefore, ADC bit reduction can be applied directly to existing seizure detection system without compromising the performance. In terms of power consumption, minimum theoretical power consumption for an ADC can be reduced more than  $10\times$  for every ADC bit reduction (Kenington and Astier, 2000). The most significant consequence of this conclusion lies within the hardware design. The lack of high precision capability has been the weakest point of the most effective and efficient unconventional analog to digital conversion techniques, not to mention that even in its conventional forms, the circuitry that is used in the design of a 6-bit ADC would be way more straightforward than that of a 16-bit ADC. Hence we argue that our finding opens up a number of unexplored avenues in using unconventional, power-efficient and low-precision ADCs and therefore rethink the way we design EEG signal monitoring circuitry when it is combined with specific signal processing approaches. A fewer number of bits will also improve computational efficacy since fewer resources are required. This

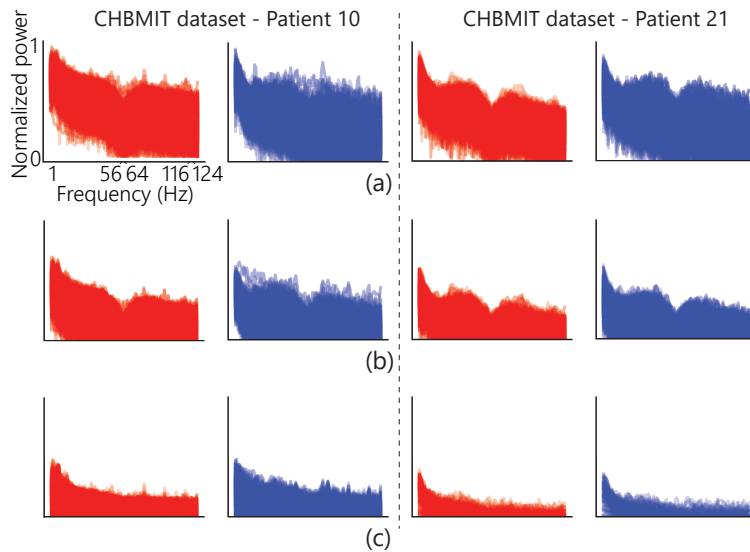


Figure 7.5: Power spectrum with DC removed of two thousand random 1-second EEG segments for patients with high (Patient 10) and low (Patient 21) seizure detection performance using different numbers of ADC bits during ictal (red) and interictal (blue) periods from the CHBMIT dataset in three cases: (a) 16-bit ADC, (b) 8-bit ADC, and (c) 4-bit ADC.

is important for a portable ambulatory seizure detection system that requires a long battery life as desired.

## 7.6 Conclusion

Reliable seizure detection plays a critical role in ambulatory epileptic seizure monitoring devices. We have shown that high seizure detection performance is achievable with considerably lower ADC precision. A 6-bit ADC, in particular, demonstrates AUCs of above 92% and 96% with a convolutional neural network and above 93% and 97% with an engineered feature-based approach for the Freiburg Hospital and the CHB-MIT seizure datasets. This enables an opportunity to not only reduce power reduction and complexity of circuits behind each electrode but also to envision a possibility for the future development of a different circuit architecture to better help patients with refractory forms of epilepsy.

## **Acknowledgment**

This research is funded by a Sydney Research Accelerator (SOAR) Fellowship at The University of Sydney. N.D.T. acknowledges partial support provided via John Makepeace Bennett Gift Scholarship funded by the Australian Institute for Nanoscale Science and Technology (AINST) and administered by The University of Sydney Nano Institute. The authors also acknowledge the support by Sydney Informatics Hub via the University of Sydney's Core Research Facilities.

# Chapter 8

## Seizure prediction on portable hardware

### 8.1 Introduction

Advances in deep machine learning in recent years have attracted significantly more attention to the application of these techniques in detective and predictive data analytics especially in health care, medical practices, and biomedical engineering (D. R. Freestone, P. J. Karoly, and Cook, 2017). While the body of available proven knowledge lacks a convincing and comprehensive understanding of sources of epileptic seizures, some early works showed the possibility of predicting, seemingly unpredictable, seizures (Rogowski et al., 1981; Salant et al., 1998). Along with continuous improvements in recording electroencephalogram (EEG) signals, there has been an increasing number of EEG-based techniques for seizure prediction (Szostak et al., 2017). In this work, we investigate a deep learning-based seizure prediction system from perspective of hardware implementation. We use an off-the-shelf deep learning accelerator, Intel Movidius Neural Computing Stick, as a proof of concept for a promising portable seizure prediction device.

### 8.2 Dataset

The Boston Children’s Hospital (CHB)-MIT dataset contains scalp EEG (sEEG) data of 23 pediatric patients with 844 h of continuous sEEG recording and 163 seizures. Scalp EEG signals were captured using 22 electrodes at sampling rate of 256 Hz (Shoeb,

2009). We define interictal periods that are at least 4 h away before seizure onset and after seizure ending. In this dataset, there are cases that multiple seizures occur close to each other. For the seizure prediction task, we are interested in predicting the leading seizures. Therefore, for seizures that are less than 30 min away from the previous one, we consider them as only one seizure and use the onset of leading seizure as the onset of the combined seizure. Besides, we only consider patients with less than 10 seizures a day for the prediction task because it is not very critical to perform the task for patients having a seizure every 2 h on average. With the above definition and consideration, there are 13 patients with sufficient data (at least 3 leading seizures and 3 interictal hours).

Table 8.1: Summary of the CHB-MIT dataset.

Patient	No. of seizures	Interictal hours
Pat1	7	17
Pat2	3	22.9
Pat3	6	21.9
Pat5	5	13
Pat9	4	12.3
Pat10	6	11.1
Pat13	5	14
Pat14	5	5
Pat18	6	23
Pat19	3	24.9
Pat20	5	20
Pat21	4	20.9
Pat23	5	3
<b>Total</b>	<b>64</b>	<b>209</b>

## 8.3 Proposed method

### 8.3.1 System overview

The seizure prediction system consists of a Raspberry Pi 3 and an Intel Movidius Neural Computing Stick (see Fig. 8.1). Time-series EEG signals are sent from a recorder to the Raspberry board where they are pre-processed to be compatible with a CNN loaded in the Neural Computing Stick. Specifically, we use Short-Time Fourier Transform (STFT)

to translate raw EEG signal into a two-dimensional matrix comprised of frequency and time axes. We use EEG window length of 28 s. Most of EEG recordings were contaminated by power line noise at 60 Hz. In frequency domain, it is convenient to effectively remove the power line noise by excluding components at the frequency range of 57–63 Hz and 117–123 Hz for power line frequency of 60 Hz. The DC component (at 0 Hz) was also removed. Though most patients have 22 EEG channels, others have less due to disruptions during recording. We, therefore, reduce the number of analyzed channels to 16 by applying technique proposed by Truong, Kuhlmann, et al. (2017) so that input shapes will be the same for all patients. After pre-processing step, input shape is  $n \times 56 \times 112$ , where  $n = 16$  is the number of analyzed EEG channels.

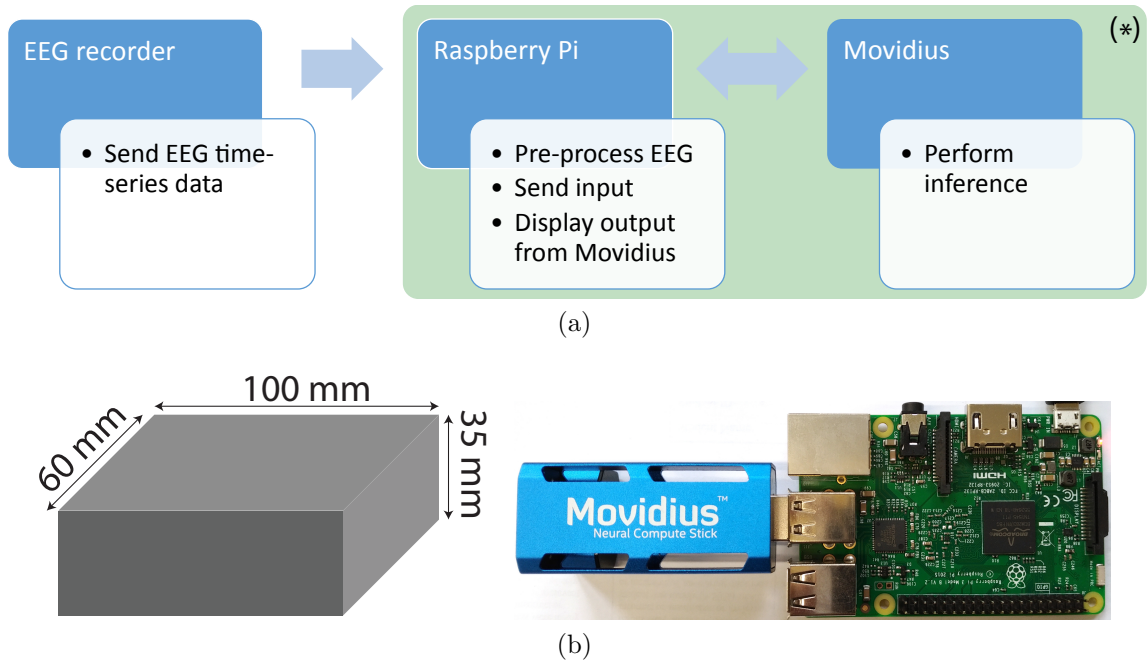
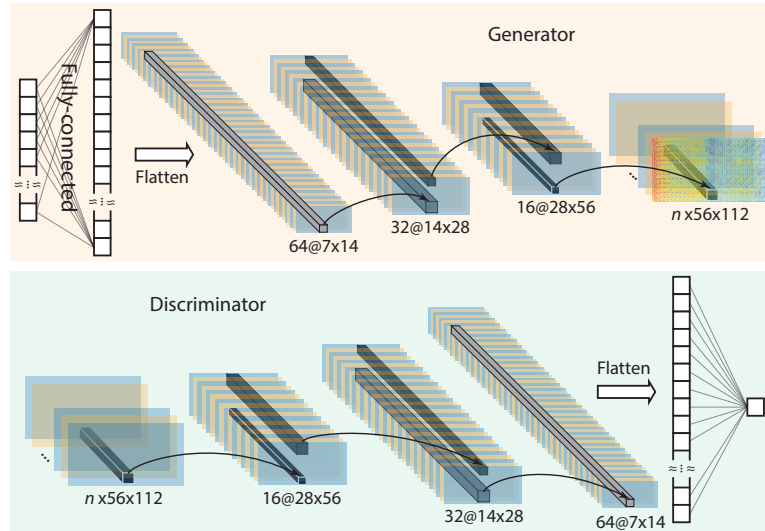
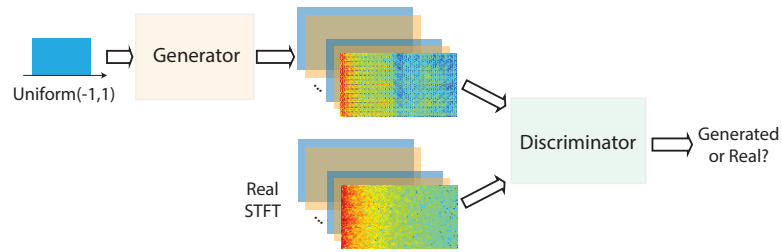


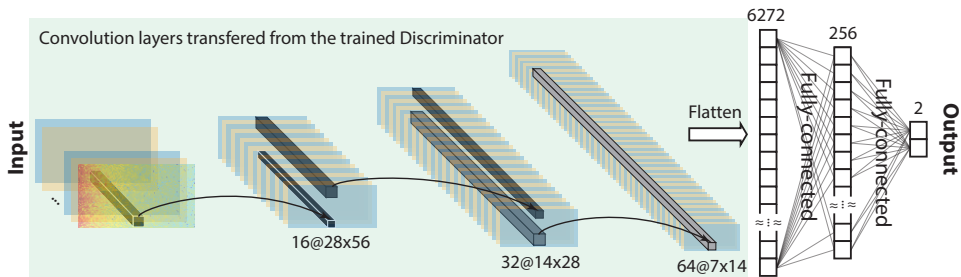
Figure 8.1: (a) Block diagram: The seizure prediction system consists of a Raspberry Pi 3 and a Movidius Neural Computing Stick (NCS). Time-series EEG signals are sent from a recorder to the Raspberry board where they are pre-processed to be compatible with a CNN loaded in the NCS. (b) Full system dimension. The NCS can sit on top of Raspberry Pi 3.

### 8.3.2 Adversarial neural network

In this work, we use a generative adversarial network (GAN) (Goodfellow et al., 2014) with three convolution layers as depicted in Fig. 8.2 as an unsupervised feature extraction



(a)



(b)

Figure 8.2: (a) The Generator takes a random sample of 100 data points from a uniform distribution  $\mathcal{U}(-1, 1)$  as input. The input is fully-connected with a hidden layer with the output size of 6272 which is then reshaped to  $64 \times 7 \times 14$ . The hidden layer is followed by three de-convolution layers with filter size  $5 \times 5$ , stride  $2 \times 2$ . Numbers of filters of the three de-convolution layers are 32, 16 and  $n$ , respectively. The Discriminator consists of three convolution layers with filter size  $5 \times 5$ , stride  $2 \times 2$ . Numbers of filters of the three convolution layers are 16, 32 and 64, respectively. (b) Seizure forecasting with features extracted by DCGAN's Discriminator. Features extracted by the three convolution blocks of the Discriminator are flattened and connected to a neural network consisting of 2 fully-connected layers with the output sizes 256 and 2, respectively. The former fully-connected layer uses sigmoid activation function while the latter uses soft-max activation function.

technique. After training the GAN, we add two fully-connected layers with sigmoid activation and output sizes of 256 and 2, respectively, after the trained convolution layers in GAN's Discriminator to form a convolutional neural network (CNN) for seizure forecasting task. The former fully-connected layer uses sigmoid activation function while the latter uses soft-max activation function. Both of the two fully-connected layers have drop-out rate of 0.5. We then train the CNN as normal except all trained convolution layers are kept unchanged. Our model training is performed on an NVIDIA K80 graphic card using Tensorflow 1.4.0 framework. Subsequently, the trained CNN is transferred to the Neural Computing Stick for inference stage.

## 8.4 Results

Seizure prediction horizon (SPH) and seizure occurrence period (SOP) need to be defined before estimating performance metrics. In this work, we follow the definition of SOP and SPH that was proposed by Maiwald et al. (2004). SOP is the interval where the seizure is expected to occur. The time period between the alarm and beginning of SOP is called SPH. For a correct prediction, a seizure onset must be after the SPH and within the SOP. Likewise, a false alarm rises when the prediction system returns a positive but there is no seizure occurring during SOP. When an alarm rises, it will last until the end of the SOP. Regarding clinical use, SPH must be long enough to allow sufficient intervention or precautions. In contrast, SOP should be not too long to reduce the patient's anxiety.

Metrics used to test the proposed approach is the area under the operating characteristic curve (AUC) with SPH of 5 min and SOP of 30 min. We use last one (for patients with less than 6 seizures) or two (for others) seizures of each patient as the test set and the rest for training. Interictal data is split according to number of seizures in the test set. Seizure prediction performance of CNN that is implemented on the K80 and the Neural Computing Stick (NCS) is shown in Fig. 8.3. Most of the patients have AUC score higher than 50% (random chance), 5 of them have high AUC, 95-100% for K80 implementation. NCS implementation has slightly lower AUC score for all patients except Pat2 and Pat10.

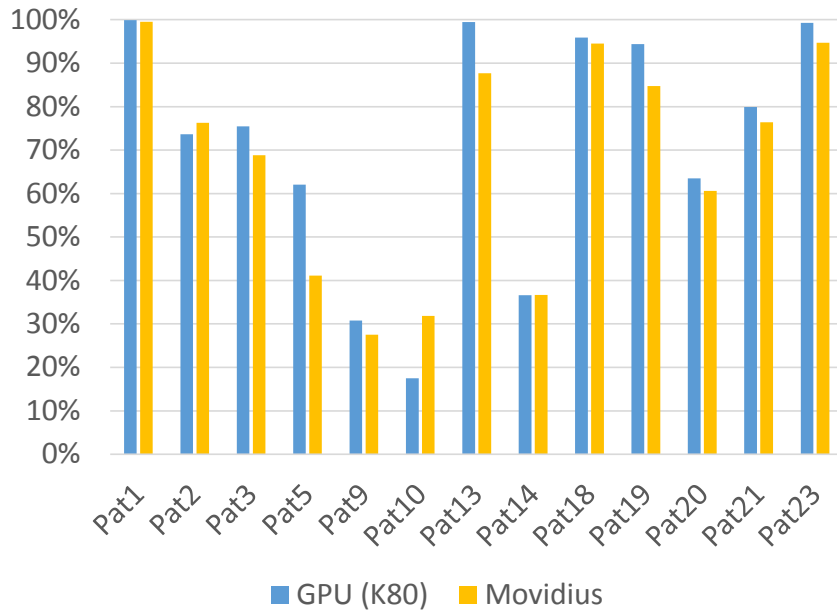


Figure 8.3: Seizure prediction AUC per patient. Prediction is within 35-5 minutes prior to seizure onset. Some patients do not have enough data.

## 8.5 Discussion

Since the K80 uses 32-bit floating-point number while the Neural Computing Stick (NCS) uses only 16-bit floating-point, it is expected to have some performance degradation. The NCS performs slightly worse than K80 with 3.7% lower on average in AUC score. This degradation is acceptable considering that the total power consumption of the seizure prediction system is only 2 Watts and the total cost is under USD 100. Importantly, it takes only 1.27 seconds for the system to process and classify a 28-second EEG segment. In other words, the system can perform a real-time seizure prediction. Furthermore, our current prototype is using a Raspberry Pi 3 and an Intel Movidius NCS, but it can be as small as the Google Voice Kit (Google, 2019) (see Fig. 8.4).

Table 8.2: Processing time for one 28-second EEG time-series data.

Task	Processing time
Movidius initiation	0.94 second
Pre-processing	0.31 second
Inference	0.02 second
<b>Total</b>	<b>1.27 seconds</b>



Figure 8.4: Google Voice Kit: A Voice Bonnet board that has the same Myriad 2 processor as in NCS is placed on top of a Raspberry Pi Zero.

## 8.6 Conclusion

We have shown that feature extraction for seizure prediction can be done using unsupervised deep learning or GAN particularly. Seizure prediction can be implemented efficiently on low-power hardware. Though our working prototype that uses off-the-shelf components does not provide impressive power consumption, it is reasonable to argue that power consumption can be greatly reduced with customized devices.

# Chapter 9

## Concluding Remarks

### 9.1 Thesis contribution

In this thesis, we have addressed several problems with epileptic seizure detection and forecasting. Regarding seizure detection, we significantly enhanced computational efficiency by employing an automatic channel selection engine as a mechanism to adequately determine most informative electroencephalogram (EEG) recordings prior to feature extraction. The engine gave rise to significant computational efficiency improvements on subjects having large number of recording channels. The overall results of the proposed method were comparable with that of the state-of-the-art while it saved 49.4% of the processing time and reduced the average number of channels requiring analysis by 71%, both critical factors for real-world applications.

Regarding seizure forecasting, we have proposed an efficient method to preprocess raw EEG data into a form suitable for a convolutional neural network (CNN), a guideline to help the CNN perform well with the seizure prediction task with minimum feature engineering and an algorithm that works well across multiple datasets; namely, the Freiburg Hospital dataset University of Freiburg, 2003, the Boston Children’s Hospital (CHB)-MIT dataset Shoeb, 2009, the American Epilepsy Society Seizure Prediction Challenge (Kaggle) dataset Kaggle, 2014a, and the EPILEPSIA data Klatt et al., 2012. A perfect prediction is not yet available, but with current prediction performance it appears possible to provide patients with a warning so they can take some precautions for their safety. This gives more patients the opportunity to possess a seizure prediction device that can help them have a more manageable life.

In another aspect of seizure forecasting, we proposed unsupervised feature learning

using generative adversarial network (GAN) for seizure forecasting that is generalizable across multiple epilepsy EEG datasets. Today the process of accurate epileptic seizure identification and data labeling is done by neurologists, which is expensive and time consuming. With unsupervised learning, we can make use of unlabelled data which is more accessible. We have shown that feature extraction for seizure forecasting can be done using unsupervised deep learning or GAN, particularly.

Relating to computational complexity and power consumption reduction, besides the automatic channel selection engine which is mentioned above, we have proposed Integer-Net, an integer convolutional neural network, to reduce computational complexity and required memory to store the algorithm. With Integer-Net, weight storage can be reduced by 7–8 times. More importantly, convolution and matrix multiplication operations performed with integers greatly help to reduce computational cost and inference time that is critical for real-time application. Integer-Net is promising for an energy-efficient seizure detection device with high accuracy. Importantly, we have also shown that high seizure detection performance is achievable with considerably lower precision EEG inputs, i.e., lower number of bits used by analog-to-digital converter (ADC) when recording EEG signals. A 6-bit ADC, in particular, demonstrates the area under the receiver operating characteristic curve (AUC) of above 92% and 96% with a convolutional neural network and above 93% and 97% with an engineered feature-based approach for the Freiburg Hospital and the CHB-MIT seizure datasets. This enables an opportunity to not only reduce power reduction and complexity of circuits behind each electrode but also to envision a possibility for the future development of a different circuit architecture to better help patients with refractory forms of epilepsy.

## 9.2 Future research directions

While we have shown seizure prediction is possible and it works well for a subset of patients tested with recorded EEG signals, we have yet to explain why some patients have substantially lower seizure forecasting performance than others. It is necessary to figure out what kind of (high-level) features appears in EEG signals of one group of patients but not others. Visualization of learned features at different layers of the convolutional neural network or other networks could be of great help.

Though we have attempted to identify groups of patients could potentially achieve high performance with seizure prediction to help with the clinical trial consideration, e.g., focus on patients who likely have high seizure prediction performance first. There

is a need of large database with data from many patients to have a meaningful statistics. The team at the University of Sydney has established a collaboration with the Royal Prince Alfred Hospital and will have access to a dataset of 500 patients. Hopefully, with the new dataset, our team will have more insights into seizure forecasting and be able to identify which groups of patients may benefit the most from seizure forecasting.

# References

Aarabi, A. and B. He (2014). “Seizure prediction in hippocampal and neocortical epilepsy using a model-based approach”. *Clinical Neurophysiology* 125.5, 930–940. DOI: 10.1016/j.clinph.2013.10.051.

— (2017). “Seizure prediction in patients with focal hippocampal epilepsy”. *Clinical Neurophysiology* 128, 1299–1307. DOI: 10.1016/j.clinph.2017.04.026.

Abdelhameed, A. and M. Bayoumi (Dec. 2018). “Semi-supervised deep learning system for epileptic seizures onset prediction”. *Proc. IEEE International Conference on Machine Learning and Applications*, 1186–1191. DOI: 10.1109/ICMLA.2018.00191.

Assenza, G. et al. (Mar. 2017). “Cathodal transcranial direct current stimulation reduces seizure frequency in adults with drug-resistant temporal lobe epilepsy: A sham controlled study”. *Brain Stimulation: Basic, Translational, and Clinical Research in Neuromodulation* 10.2, 333–335. DOI: 10.1016/j.brs.2016.12.005.

Australian Institute of Health Welfare (2016). *Australian Burden of Disease Study: impact and causes of illness and death in Australia*. URL: <https://www.aihw.gov.au/getmedia/d4df9251-c4b6-452f-a877-8370b6124219/19663.pdf> (visited on 01/30/2020).

Auvichayapat, N. et al. (2013). “Transcranial direct current stimulation for treatment of refractory childhood focal epilepsy”. *Brain Stimulation* 6.4, 696–700. DOI: 10.1016/j.brs.2013.01.009.

Axelsen, T. M. and D. P. D. Woldbye (2018). “Gene Therapy for Parkinson’s Disease, An Update”. eng. *Journal of Parkinson’s disease* 8.2, 195–215. DOI: 10.3233/JPD-181331.

Ba, J. and R. Caruana (2014). “Do deep nets really need to be deep?” *Advances in Neural Information Processing Systems*. Ed. by Z. Ghahramani et al., 2654–2662.

Babb, T. L., E. Mariani, and P. H. Crandall (1974). “An electronic circuit for detection of EEG seizures recorded with implanted electrodes”. *Electroencephalography and Clinical Neurophysiology* 37.3, 305–308. DOI: 10.1016/0013-4694(74)90036-4.

Baldassano, S. N. et al. (2017). “Crowdsourcing seizure detection: algorithm development and validation on human implanted device recordings”. *Brain* 140.6, 1680–1691. DOI: 10.1093/brain/awx098.

Bauer, S. et al. (2016). “Transcutaneous vagus nerve stimulation (tVNS) for treatment of drug-resistant epilepsy: a randomized, double-blind clinical trial (cMPsE02)”. *Brain Stimulation* 9.3, 356–363. DOI: 10.1016/j.brs.2015.11.003.

Ben-Menachem, E. (2012). “Neurostimulation - Past, Present, and Beyond”. *Epilepsy Currents* 12.5, 188–191. DOI: 10.5698/1535-7511-12.5.188.

Bizopoulos, P. A. et al. (Nov. 2013). “EEG epileptic seizure detection using k-means clustering and marginal spectrum based on ensemble empirical mode decomposition”. *Proc. IEEE International Conference on BioInformatics and BioEngineering*, 1–4. DOI: 10.1109/BIBE.2013.6701528.

Bou Assi, E. et al. (2017). “Towards accurate prediction of epileptic seizures: A review”. *Biomedical Signal Processing and Control* 34, 144–157. DOI: 10.1016/j.bspc.2017.02.001.

Branco, P., L. Torgo, and R. P. Ribeiro (2016). “A survey of predictive modeling on imbalanced domains”. *ACM Computing Surveys* 49.2, 31:1–31:50. DOI: 10.1145/2907070.

Breiman, L. (2001). “Random forests”. *Machine Learning* 45.1, 5–32. DOI: 10.1023/A:1010933404324.

Cabezas, J., M. Galleguillos, and J. Perez-Quezada (2016). “Predicting vascular plant richness in a heterogeneous wetland using spectral and textural features and a random forest algorithm”. *IEEE Geoscience and Remote Sensing Letters* 13.5, 646–650. DOI: 10.1109/LGRS.2016.2532743.

Carrette, S. et al. (2016). “Repetitive transcranial magnetic stimulation for the treatment of refractory epilepsy”. *Expert Review of Neurotherapeutics* 16.9, 1093–1110. DOI: 10.1080/14737175.2016.1197119.

Cattaneo, L. (2017). “Transcranial magnetic stimulation”. *Lateralized Brain Functions: Methods in Human and Non-Human Species*. Ed. by L. J. Rogers and G. Vallortigara. New York, NY: Springer New York, 369–406. DOI: 10.1007/978-1-4939-6725-4\_12.

Clancy, J. A. et al. (2014). “Non-invasive vagus nerve stimulation in healthy humans reduces sympathetic nerve activity”. *Brain Stimulation* 7.6, 871–877. DOI: 10.1016/j.brs.2014.07.031.

Courbariaux, M., Y. Bengio, and J.-P. David (2015). “BinaryConnect: training deep neural networks with binary weights during propagations”. *Advances in Neural Information Processing Systems*. Ed. by C. Cortes et al., 3123–3131.

- CURE (2019). *What is epilepsy?* URL: <https://www.cureepilepsy.org/what-is-epilepsy/> (visited on 04/20/2019).
- Ding, K. (2017). *XNOR-Net implementation*. URL: <https://github.com/DingKe> (visited on 01/01/2017).
- Duun-Henriksen, J. et al. (Jan. 2012). “Channel selection for automatic seizure detection”. *Clinical Neurophysiology* 123.1, 84–92. DOI: 10.1016/j.clinph.2011.06.001.
- Echauz, J. et al. (2007). “Monitoring, signal analysis, and control of epileptic seizures: A paradigm in brain research”. *Proc. Mediterranean Conference on Control & Automation*, 1–6.
- Eftekhar, A. et al. (2014). “Ngram-derived pattern recognition for the detection and prediction of epileptic seizures”. *PLoS One* 9.6, e96235. DOI: 10.1371/journal.pone.0096235.
- Elliott, R. E. et al. (2011). “Efficacy of vagus nerve stimulation over time: Review of 65 consecutive patients with treatment-resistant epilepsy treated with VNS >10 years”. *Epilepsy & Behavior* 20.3, 478–483. DOI: 10.1016/j.yebeh.2010.12.042.
- Emami, A. et al. (2019). “Seizure detection by convolutional neural network-based analysis of scalp electroencephalography plot images”. *NeuroImage: Clinical* 22, 101684. DOI: 10.1016/j.nicl.2019.101684.
- Espay, A. J. et al. (2018). “Current concepts in diagnosis and treatment of functional neurological disorders”. *JAMA Neurology* 75.9, 1132–1141. DOI: 10.1001/jamaneurol.2018.1264.
- Falco-Walter, J. J., I. E. Scheffer, and R. S. Fisher (2018). “The new definition and classification of seizures and epilepsy”. *Epilepsy Research* 139, 73–79. DOI: 10.1016/j.eplepsyres.2017.11.015.
- Fatichah, C. et al. (2014). “Principal component analysis-based neural network with fuzzy membership function for epileptic seizure detection”. *Proc. International Conference on Natural Computation*, 186–191. DOI: 10.1109/ICNC.2014.6975832.
- Fiest, K. M. et al. (2017). “Prevalence and incidence of epilepsy”. *Neurology* 88.3, 296–303. DOI: 10.1212/WNL.0000000000003509.
- Fisher, R. S. et al. (2017). “Operational classification of seizure types by the International League Against Epilepsy: Position Paper of the ILAE Commission for Classification and Terminology”. *Epilepsia* 58.4, 522–530. DOI: 10.1111/epi.13670.
- Fisher, R. et al. (2010). “Electrical stimulation of the anterior nucleus of thalamus for treatment of refractory epilepsy”. *Epilepsia* 51.5, 899–908. DOI: 10.1111/j.1528-1167.2010.02536.x.

Freestone, D. R., P. J. Karoly, and M. J. Cook (2017). “A forward-looking review of seizure prediction”. *Current opinion in neurology* 30.2, 167–173. DOI: 10.1097/WCO.0000000000000429.

Freestone, D. R., P. J. Karoly, A. D. H. Peterson, et al. (2015). “Seizure prediction: science fiction or soon to become reality?” *Current Neurology and Neuroscience Reports* 15.11, 73. DOI: 10.1007/s11910-015-0596-3.

Goldberger, A. L. et al. (2000). “PhysioBank, PhysioToolkit, and PhysioNet”. *Circulation* 101.23, e215–e220. DOI: 10.1161/01.CIR.101.23.e215.

Goodfellow, I. et al. (2014). “Generative Adversarial Nets”. *Advances in Neural Information Processing Systems*, 2672–2680.

Google (2019). *Google Voice Kit*. URL: <https://aiyprojects.withgoogle.com/voice/> (visited on 08/09/2019).

Gooneratne, I. K. et al. (2016). “Comparing neurostimulation technologies in refractory focal-onset epilepsy”. *Journal of Neurology, Neurosurgery & Psychiatry* 87, 1174–1182. DOI: 10.1136/jnnp-2016-313297.

Griffiths, G. M. and J. T. Fox (1938). “Rhythm in epilepsy”. *The Lancet* 232.5999, 409–416. DOI: 10.1016/S0140-6736(00)41614-4.

Guyon, I. and A. Elisseeff (2003). “An introduction to variable and feature selection”. *Journal of Machine Learning Research* 3, 1157–1182.

Han, S., H. Mao, and W. J. Dally (2015). “Deep Compression: compressing deep neural network with pruning, trained quantization and Huffman coding”. *arXiv preprint*. arXiv: 1510.00149.

Han, S., J. Pool, et al. (2015). “Learning both weights and connections for efficient neural network”. *Proc. International Conference on Neural Information Processing Systems*, 1135–1143.

Hanley, J. A. and B. J. McNeil (1983). “A method of comparing the areas under receiver operating characteristic curves derived from the same cases.” *Radiology* 148.3, 839–843.

Hills, M. (2014). *Seizure detection using FFT, temporal and spectral correlation coefficients, eigenvalues and Random Forest*. Tech. rep. Github.

Horowitz, M. (2014). “1.1 computing’s energy problem (and what we can do about it)”. *Proc. IEEE International Solid State Circuits Conference*, 10–14.

Hossain, M. S. et al. (Feb. 2019). “Applying deep learning for epilepsy seizure detection and brain mapping visualization”. *ACM Transactions on Multimedia Computing, Communications, and Applications* 15.1s, 10:1–10:17. DOI: 10.1145/3241056.

- Hosseini, M.-P. et al. (2017). “Optimized deep learning for EEG big data and seizure prediction BCI via internet of things”. *IEEE Transactions on Big Data* 3.4, 392–404. DOI: 10.1109/TBDATA.2017.2769670.
- Huynh, T. et al. (2016). “Estimating CT image from MRI data using structured random forest and auto-context model”. *IEEE Transactions on Medical Imaging* 35.1, 174–183. DOI: 10.1109/TMI.2015.2461533.
- Iandola, F. N. et al. (2016). “SqueezeNet: AlexNet-level accuracy with 50x fewer parameters and <1MB model size”. *arXiv preprint*. arXiv: 1602.07360.
- Joulin, A. et al. (2016). “Fasttext.zip: Compressing text classification models”. *arXiv preprint*. arXiv: 1612.03651.
- Kaggle (2014a). *American Epilepsy Society Seizure Prediction Challenge*. URL: <https://www.kaggle.com/c/seizure-prediction> (visited on 10/12/2016).
- (2014b). *UPenn and Mayo Clinic’s Seizure Detection Challenge*. URL: <https://www.kaggle.com/c/seizure-detection> (visited on 05/12/2016).
- Karoly, P. J. et al. (2017). “The circadian profile of epilepsy improves seizure forecasting”. *Brain* 140.8, 2169–2182. DOI: 10.1093/brain/awx173.
- Kassiri, H. et al. (2016). “Battery-less modular responsive neurostimulator for prediction and abortion of epileptic seizures”. *Proc. IEEE International Symposium on Circuits and Systems*. IEEE, 1298–1301. DOI: 10.1109/ISCAS.2016.7527486.
- Kenington, P. B. and L. Astier (2000). “Power consumption of A/D converters for software radio applications”. *IEEE Transactions on Vehicular Technology* 49.2, 643–650. DOI: 10.1109/25.832996.
- Khan, H. et al. (2018). “Focal onset seizure prediction using convolutional networks”. *IEEE Transactions on Biomedical Engineering* 65.9, 2109–2118. DOI: 10.1109/TBME.2017.2785401.
- Kingma, D. P. et al. (2014). “Semi-supervised Learning with Deep Generative Models”. *Advances in Neural Information Processing Systems*. Ed. by Z. Ghahramani et al. Curran Associates, Inc., 3581–3589.
- Kiral-Kornek, I. et al. (2018). “Epileptic seizure prediction using big data and deep learning: toward a mobile system”. *EBioMedicine* 27, 103–111.
- Klatt, J. et al. (2012). “The EPILEPSIAE database: An extensive electroencephalography database of epilepsy patients”. *Epilepsia* 53.9, 1669–1676. DOI: 10.1111/j.1528-1167.2012.03564.x.
- Krizhevsky, A., I. Sutskever, and G. E. Hinton (2012). “Imagenet classification with deep convolutional neural networks”. *Advances in Neural Information Processing Systems*, 1097–1105. DOI: 10.1145/3065386.

- Kuhlmann, L., A. N. Burkitt, et al. (2009). “Seizure detection using seizure probability estimation: comparison of features used to detect seizures”. *Annals of Biomedical Engineering* 37.10, 2129–2145. DOI: 10.1007/s10439-009-9755-5.
- Kuhlmann, L., D. Freestone, et al. (2010). “Patient-specific bivariate-synchrony-based seizure prediction for short prediction horizons”. *Epilepsy Research* 91.2, 214–231. DOI: 10.1016/j.eplepsyres.2010.07.014.
- Kuhlmann, L., D. B. Grayden, and M. J. Cook (2017). “Introduction”. *International Journal of Neural Systems* 27.01, 1702001. DOI: 10.1142/S0129065717020014.
- Kuhlmann, L., D. B. Grayden, F. Wendling, et al. (2015). “The role of multiple-scale modelling of epilepsy in seizure forecasting”. *Journal of Clinical Neurophysiology* 32.3, 220–226. DOI: 10.1097/WNP.0000000000000149.
- Kuhlmann, L., P. Karoly, et al. (2018). “Epilepsyecosystem.org: crowd-sourcing reproducible seizure prediction with long-term human intracranial EEG”. *Brain* 141.9, 2619–2630. DOI: 10.1093/brain/awy210.
- Kuhlmann, L., K. Lehnertz, et al. (2018). “Seizure prediction – ready for a new era”. *Nature Reviews Neurology* 14.10, 618–630. DOI: 10.1038/s41582-018-0055-2.
- Kullmann, D. M. et al. (2014). “Gene therapy in epilepsy—is it time for clinical trials?”. *Nature Reviews Neurology* 10.5, 300–304. DOI: 10.1038/nrneuro1.2014.43.
- Kwan, P., A. Arzimanoglou, et al. (2010). “Definition of drug resistant epilepsy: consensus proposal by the ad hoc Task Force of the ILAE Commission on Therapeutic Strategies”. *Epilepsia* 51.6, 1069–1077.
- Kwan, P. and M. J. Brodie (2000). “Early Identification of Refractory Epilepsy”. *New England Journal of Medicine* 342.5, 314–319. DOI: 10.1056/NEJM200002033420503.
- LeCun, Y. et al. (1990). “Handwritten digit recognition with a back-propagation network”. *Advances in Neural Information Processing Systems*. Ed. by D. S. Touretzky, 396–404.
- Lehtimäki, K. et al. (2016). “Outcome based definition of the anterior thalamic deep brain stimulation target in refractory epilepsy”. *Brain Stimulation* 9.2, 268–275. DOI: 10.1016/j.brs.2015.09.014.
- Li, S. et al. (2013). “Seizure prediction using spike rate of intracranial EEG”. *IEEE Transactions on Neural Systems and Rehabilitation Engineering* 21.6, 880–886. DOI: 10.1109/TNSRE.2013.2282153.
- Litt, B. and J. Echauz (2002). “Prediction of epileptic seizures”. *The Lancet Neurology* 1.1, 22–30. DOI: 10.1016/S1474-4422(02)00003-0.
- López González, F. J. et al. (2015). “Drug-resistant epilepsy: Definition and treatment alternatives”. *Neurología (English Edition)* 30.7, 439–446. DOI: <https://doi.org/10.1016/j.nrleng.2014.04.002>.

- Mackay, M. T. et al. (2005). “The ketogenic diet in refractory childhood epilepsy”. *Journal of Paediatrics and Child Health* 41.7, 353–357. DOI: 10.1111/j.1440-1754.2005.00630.x.
- Maiwald, T. et al. (2004). “Comparison of three nonlinear seizure prediction methods by means of the seizure prediction characteristic”. *Physica D: Nonlinear Phenomena* 194.3-4, 357–368. DOI: 10.1016/j.physd.2004.02.013.
- Martin-McGill KJ, J. C. F. B. R. L. R. G. and P. N. Cooper (2018). “Ketogenic diets for drug-resistant epilepsy”. *Cochrane Database of Systematic Reviews* 11. DOI: 10.1002/14651858.CD001903.pub4.
- Minasyan, G. R. et al. (2010). “Patient-specific early seizure detection from scalp EEG”. *Journal of Clinical Neurophysiology* 27.3, 163. DOI: 10.1097/WNP.0b013e3181e0a9b6.
- Mirowski, P. W. et al. (2008). “Comparing SVM and convolutional networks for epileptic seizure prediction from intracranial EEG”. *Proc. IEEE Workshop on Machine Learning for Signal Processing*, 244–249. DOI: 10.1109/MLSP.2008.4685487.
- Mitchell, R. J. et al. (2018). “Examining health service utilization, hospital treatment cost, and mortality of individuals with epilepsy and status epilepticus in New South Wales, Australia 2012–2016”. *Epilepsy & Behavior* 79, 9–16. DOI: <https://doi.org/10.1016/j.yebeh.2017.11.022>.
- Osorio, I. and M. Frei (2009). “Real-time detection, quantification, warning, and control of epileptic seizures: the foundations for a scientific epileptology”. *Epilepsy & Behavior* 16.3, 391–396. DOI: 10.1016/j.yebeh.2009.08.024.
- Park, Y. et al. (2011). “Seizure prediction with spectral power of EEG using cost-sensitive support vector machines”. *Epilepsia* 52.10, 1761–1770. DOI: 10.1111/j.1528-1167.2011.03138.x.
- Parvez, M. Z. and M. Paul (2015). “Epileptic Seizure Detection by Exploiting Temporal Correlation of Electroencephalogram Signals”. *IET Signal Processing* 9.6, 467–475. DOI: 10.1049/iet-spr.2013.0288.
- (2017). “Seizure prediction using undulated global and local features”. *IEEE Transactions on Biomedical Engineering* 64.1, 208–217. DOI: 10.1109/TBME.2016.2553131.
- Patel, K. et al. (2009). “Low power real-time seizure detection for ambulatory EEG”. *Proc. Pervasive Computing Technologies for Healthcare*, 1–7.
- Peterson, C. L. and C. Walker (2018). “Are medicare and pharmaceutical benefit scheme services too costly for patients? An epilepsy-based study”. *Australian Journal of Social Issues* 53.4, 386–399. DOI: 10.1002/ajs4.57.

Radford, A., L. Metz, and S. Chintala (2015). “Unsupervised representation learning with deep convolutional generative adversarial networks”. *arXiv preprint arXiv:1511.06434*.

Raghunathan, S., S. K. Gupta, H. S. Markandeya, et al. (2010). “A hardware-algorithm co-design approach to optimize seizure detection algorithms for implantable applications”. *Journal of Neuroscience Methods* 193.1, 106–117. DOI: 10.1016/j.jneumeth.2010.08.008.

Raghunathan, S., S. K. Gupta, M. P. Ward, et al. (2009). “The design and hardware implementation of a low-power real-time seizure detection algorithm”. *Journal of Neural Engineering* 6.5, 056005. DOI: 10.1088/1741-2560/6/5/056005.

Rastegari, M. et al. (2016). “XNOR-Net: ImageNet classification using binary convolutional neural networks”. *Proc. European Conference on Computer Vision*, 525–542. DOI: 10.1007/978-3-319-46493-0\_32.

Rogowski, Z., I. Gath, and E. Bental (1981). “On the prediction of epileptic seizures”. *Biological Cybernetics* 42.1, 9–15.

Saab, M. E. and J. Gotman (2005). “A system to detect the onset of epileptic seizures in scalp EEG”. *Clinical Neurophysiology* 116.2, 427–442. DOI: 10.1016/j.clinph.2004.08.004.

Sainath, T. N. et al. (2013). “Deep convolutional neural networks for LVCSR”. *Proc. Acoustics, Speech and Signal Processing*, 8614–8618. DOI: 10.1109/ICASSP.2013.6639347.

Salam, M. T., M. Sawan, and D. K. Nguyen (2011). “A novel low-power-implantable epileptic seizure-onset detector”. *IEEE Transactions on Biomedical Circuits and Systems* 5.6, 568–578. DOI: 10.1109/TBCAS.2011.2157153.

Salanova, V. et al. (2015). “Long-term efficacy and safety of thalamic stimulation for drug-resistant partial epilepsy”. *Neurology* 84.10, 1017–1025. DOI: 10.1212/WNL.0000000000001334.

Salant, Y., I. Gath, and O. Henriksen (1998). “Prediction of epileptic seizures from two-channel EEG”. *Medical and Biological Engineering and Computing* 36.5, 549–556. DOI: 10.1007/BF02524422.

Samiee, K., P. Kov, and M. Gabbouj (2015). “Epileptic seizure classification of EEG time-series using rational discrete short-time Fourier transform”. *IEEE Transactions on Biomedical Engineering* 62.2, 541–552. DOI: 10.1109/TBME.2014.2360101.

Sardouie, S. et al. (2015). “Denoising of ictal EEG data using semi-blind source separation methods based on time-frequency priors”. *IEEE Journal of Biomedical and Health Informatics* 19.3, 839–847. DOI: 10.1109/JBHI.2014.2336797.

Schelter, B. et al. (2006). “Testing statistical significance of multivariate time series analysis techniques for epileptic seizure prediction”. *Chaos: An Interdisciplinary Journal of Nonlinear Science* 16.1, 13108. DOI: 10.1063/1.2137623.

Scikit-learn (2014). *Ensemble Methods*. URL: <http://scikit-learn.org/stable/modules/ensemble.html>.

Scornet, E. (2016). “Random forests and kernel methods”. *IEEE Transactions on Information Theory* 62.3, 1485–1500. DOI: 10.1109/TIT.2016.2514489.

Sharif, B. and A. H. Jafari (2017). “Prediction of epileptic seizures from EEG using analysis of ictal rules on Poincaré plane”. *Computer Methods and Programs in Biomedicine* 145, 11–22. DOI: 10.1016/j.cmpb.2017.04.001.

Shih, E. I., A. H. Shoeb, and J. V. Guttag (2009). “Sensor selection for energy-efficient ambulatory medical monitoring”. *Proc. International Conference on Mobile Systems, Applications, and Services*, 347–358. DOI: 10.1145/1555816.1555851.

Shoeb, A. H. (2009). “Application of machine learning to epileptic seizure onset detection and treatment”. PhD thesis. Massachusetts Institute of Technology.

Sinha, N. et al. (2017). “Predicting neurosurgical outcomes in focal epilepsy patients using computational modelling”. *Brain* 140.2, 319–332. DOI: 10.1093/brain/aww299.

Smart, O. and M. Chen (Aug. 2015). “Semi-automated patient-specific scalp EEG seizure detection with unsupervised machine learning”. *Proc. IEEE Conference on Computational Intelligence in Bioinformatics and Computational Biology*, 1–7. DOI: 10.1109/CIBCB.2015.7300286.

Subasi, A. and M. Ismail Gursoy (2010). “EEG signal classification using PCA, ICA, LDA and support vector machines”. *Expert Systems with Applications* 37.12, 8659–8666. DOI: 10.1016/j.eswa.2010.06.065.

Sun, F. T. and M. J. Morrell (2014). “The RNS System: responsive cortical stimulation for the treatment of refractory partial epilepsy”. *Expert Review of Medical Devices* 11.6, 563–572. DOI: 10.1586/17434440.2014.947274.

Sun, S.-H. (2017). *Deep Convolutional Generative Adversarial Networks in Tensorflow*. URL: <https://github.com/shaohua0116/DCGAN-Tensorflow> (visited on 06/05/2018).

Supratak, A., L. Li, and Y. Guo (Aug. 2014). “Feature extraction with stacked autoencoders for epileptic seizure detection”. *Proc. IEEE Engineering in Medicine and Biology Society Conference*, 4184–4187. DOI: 10.1109/EMBC.2014.6944546.

Szegedy, C. et al. (2017). “Inception-v4, Inception-ResNet and the impact of residual connections on learning”. *Proc. AAAI Conference on Artificial Intelligence*, 4278–4284.

Szostak, K. M., L. Grand, and T. G. Constandinou (2017). “Neural interfaces for intracortical recording: Requirements, fabrication methods, and characteristics”. *Frontiers in Neuroscience* 11, 665. DOI: 10.3389/fnins.2017.00665.

- Tao, J. X. et al. (2005). “Intracranial EEG substrates of scalp EEG interictal spikes”. *Epilepsia* 46.5, 669–676. DOI: 10.1111/j.1528-1167.2005.11404.x.
- Thodoroff, P., J. Pineau, and A. Lim (2016). “Learning robust features using deep learning for automatic seizure detection”. *Proc. Machine Learning for Healthcare Conference*, 178–190.
- Tieng, Q. M. et al. (2016). “Mouse EEG Spike Detection Based on the Adapted Continuous Wavelet Transform”. *Journal of Neural Engineering* 13.2, 26018. DOI: 10.1088/1741-2560/13/2/026018.
- Truong, N. D. and O. Kavehei (2019). “Low precision electroencephalogram for seizure detection with convolutional neural network”. *Proc. IEEE International Conference on Artificial Intelligence Circuits and Systems*. DOI: 10.1109/AICAS.2019.8771569.
- Truong, N. D., L. Kuhlmann, et al. (2017). “Supervised learning in automatic channel selection for epileptic seizure detection”. *Expert Systems with Applications* 86, 199–207. DOI: 10.1016/j.eswa.2017.05.055.
- Truong, N. D., A. D. Nguyen, et al. (2018a). “Convolutional neural networks for seizure prediction using intracranial and scalp electroencephalogram”. *Neural Networks* 105, 104–111. DOI: 10.1016/j.neunet.2018.04.018.
- (2018b). “Integer convolutional neural network for seizure detection”. *IEEE Journal on Emerging and Selected Topics in Circuits and Systems* 8.4, 849–857. DOI: 10.1109/JETCAS.2018.2842761.
- Truong, N. D., L. Zhou, and O. Kavehei (2019). “Semi-supervised seizure prediction with generative adversarial networks”. *Proc. International Engineering in Medicine and Biology Conference*, 2369–2372.
- University of Freiburg (2003). *EEG Database at the Epilepsy Center of the University Hospital of Freiburg, Germany*. URL: <http://epilepsy.uni-freiburg.de>.
- Verma, N. et al. (2010). “A micro-power EEG acquisition SoC with integrated feature extraction processor for a chronic seizure detection system”. *IEEE Journal of Solid-State Circuits* 45.4, 804–816. DOI: 10.1109/JSSC.2010.2042245.
- Wang, D. et al. (Nov. 2018). “Epileptic seizure detection in long-term EEG recordings by using wavelet-based directed transfer function”. *IEEE Transactions on Biomedical Engineering* 65.11, 2591–2599. DOI: 10.1109/TBME.2018.2809798.
- Wang, G. et al. (2016). “Epileptic seizure detection based on partial directed coherence analysis”. *IEEE Journal of Biomedical and Health Informatics* 20.3, 873–879. DOI: 10.1109/JBHI.2015.2424074.
- Wassermann, E. M. (1998). “Risk and safety of repetitive transcranial magnetic stimulation: report and suggested guidelines”. *Electroencephalography and Clinical*

*Neurophysiology/Evoked Potentials Section* 108.1, 1–16. DOI: 10.1016/S0168-5597(97)00096-8.

Wen, T. and Z. Zhang (2018). “Deep convolution neural network and autoencoders-based unsupervised feature learning of EEG signals”. *IEEE Access* 6, 25399–25410. DOI: 10.1109/ACCESS.2018.2833746.

Winterhalder, M. et al. (2006). “Spatio-temporal patient–individual assessment of synchronization changes for epileptic seizure prediction”. *Clinical Neurophysiology* 117.11, 2399–2413. DOI: 10.1016/j.clinph.2006.07.312.

Xiao, C. et al. (2017). “An adaptive pattern learning framework to personalize online seizure prediction”. *IEEE Transactions on Big Data*. DOI: 10.1109/TBDATA.2017.2675982.

Yoo, J. et al. (2013). “An 8-channel scalable EEG acquisition SoC with patient-specific seizure classification and recording processor”. *IEEE Journal of Solid-State Circuits* 48.1, 214–228. DOI: 10.1109/JSSC.2012.2221220.

Yuan, Y. et al. (Jan. 2019). “A multi-view deep learning framework for EEG seizure detection”. *IEEE Journal of Biomedical and Health Informatics* 23.1, 83–94. DOI: 10.1109/JBHI.2018.2871678.

Zabihi, M. et al. (2016). “Analysis of high-dimensional phase space via Poincare section for patient-specific seizure detection”. *IEEE Transactions on Neural Systems and Rehabilitation Engineering* 24.3, 386–398. DOI: 10.1109/TNSRE.2015.2505238.

Zeng, H. and A. Song (2015). “Optimizing single-trial EEG classification by stationary matrix logistic regression in brain-computer interface”. *IEEE Transactions on Neural Networks and Learning Systems* pp.99, 1–13. DOI: 10.1109/TNNLS.2015.2475618.

Zhang, H., H. Yang, and C. Guan (2013). “Bayesian learning for spatial filtering in an EEG-based brain-computer interface”. *IEEE Transactions on Neural Networks and Learning Systems* 24.7, 1049–1060. DOI: 10.1109/TNNLS.2013.2249087.

Zhang, Z. and K. K. Parhi (2016). “Low-complexity seizure prediction from iEEG/sEEG using spectral power and ratios of spectral power”. *IEEE Transactions on Biomedical Circuits and Systems* 10.3, 693–706. DOI: 10.1109/TBCAS.2015.2477264.

Zheng, Y. et al. (2014). “Epileptic seizure prediction using phase synchronization based on bivariate empirical mode decomposition”. *Clinical Neurophysiology* 125.6, 1104–1111. DOI: 10.1016/j.clinph.2013.09.047.